OUT-OF-STEP PROTECTION USING ENERGY EQUILIBRIUM CRITERION IN THE TIME DOMAIN

A Thesis Submitted to the College of

Graduate Studies and Research

In Partial Fulfillment of the Requirements

For the Degree of Master of Science

In the Department of Electrical and Computer Engineering

University of Saskatchewan

Saskatoon

By

SUMIT PAUDYAL

Keywords: Power swing, Out-of-step, Protection, Relay, Equal area criterion, RTDS

PERMISSION TO USE

In presenting this thesis in partial fulfilment of the requirements for a Postgraduate degree from the University of Saskatchewan, I agree that the Libraries of this University may make it freely available for inspection. I further agree that permission for copying of this thesis in any manner, in whole or in part, for scholarly purposes may be granted by the professor or professors who supervised my thesis work or, in their absence, by the Head of the Department or the Dean of the College in which my thesis work was done. It is understood that any copying or publication or use of this thesis or parts thereof for financial gain shall not be allowed without my written permission. It is also understood that due recognition shall be given to me and to the University of Saskatchewan in any scholarly use which may be made of any material in my thesis.

Requests for permission to copy or to make other use of material in this thesis in whole or part should be addressed to:

Head of the Department of Electrical and Computer Engineering

University of Saskatchewan

57 Campus Drive

Saskatoon, Saskatchewan, Canada

S7N 5A9

ABSTRACT

Disturbances in power systems are common and they result in electromechanical oscillations called power swing. The power swings could be severe and it may lead to loss of synchronism among the interconnected generators. This is referred to as out-of-step condition. The voltage and current swings during an out-of-step condition damage power system equipments and also cause unwanted operations of various protective devices. The protection systems require an effective algorithm for fast and accurate detection of out-of-step condition.

This research is focused on the development of a simple and effective out-of-step relay capable of detecting out-of-step condition in a complex power system. To achieve this, the research has gone through four distinct stages: development of an algorithm, simulation, hardware implementation and its testing.

An out-of-step algorithm is proposed based on equal area criterion in time domain. The equal area criterion in time domain is obtained by modifying the traditional equal area criterion in power angle domain. A single machine infinite bus system, a two machine infinite bus system and a three machine infinite bus system and a 17-bus multiple machines system are used as case studies and are modeled using simulation tool (PSCAD™)[1].

To test the effectiveness of the proposed algorithm, various out-of-step conditions are simulated by applying disturbances at various locations in the above chosen power system configurations. For hardware implementation and testing of the algorithm, a digital signal processing board (ADSP-BF533 from Analog Devices™)[2] is used. To test the performance of the developed digital relay in a closed loop, real time power system signals are necessary and

[1] PSCAD™ is the registered trade mark of Manitoba HVDC Centre, Winnipeg, Canada.
[2] RTDS™ is the registered trade mark of RTDS Technologies Inc., Winnipeg, Canada

therefore for this purpose, a Real Time Digital Simulator (RTDS™)[3] available in the power research laboratory is used. The RTDS™ simulator mimics the actual power systems in real time. The signals required by the relays can be tapped from the RTDS™ and the signals coming from relay can be fed back into the RTDS™, which makes the closed loop testing of the digital relay possible. This research has yielded a simple out-of-step algorithm and unlike the other out-of-step detection techniques proposed in the literature does not need offline system studies to arrive at a solution. The developed digital out-of-step relay is capable of making decisions based only on the information available from its point of installation, thus it avoids the communication devices which is advantageous for the out-of-step protection of a complex power system. Finally, the simulation results show that the proposed algorithm can be applied to any power configurations and is faster compared to the conventional concentric rectangle schemes used in the literature.

[3] Analog Devices™ is the registered trade mark of Analog Devices, Inc.

ACKNOWLEDGMENTS

The author expresses his sincere gratitude to his supervisors Dr. Ramakrishna Gokaraju and Dr. M.S. Sachdev for their invaluable guidance, encouragements and supports throughout the research. Advices and assistances from them in the preparation of this thesis are thankfully acknowledged.

The author would like to thank Mr. Eli Pajuelo and Mr. Dipendra Rai for their valuable supports during the hardware implementation part of the research. Financial assistance provided by the Natural Science and Engineering Research Council and the University of Saskatchewan is gratefully acknowledged.

DEDICATION

To my parents Hom Raj Paudyal and Shanta Paudy

TABLE OF CONTENTS

page

LIST OF TABLES

LIST OF FIGURES

LIST OF SYMBOLS

δ	Power angle, Rotor angle (degree)
E_G	Generator voltage (V)
E_M	Motor voltage (V)
Z	Impedance between generator and motor (Ω)
I_R	Current at relay location (A)
V_R	Voltage at relay location (V)
r	A fraction between 0 and 1, which divides the impedance Z into two parts
Z_R	Impedance at relay location (Ω)
R_R	Resistance at relay location (Ω)
X_R	Reactance at relay location (Ω)
I	Current (A)
ΔZ	Separation of the blinders in impedance plane (Ω)
Z_L	Transmission line impedance (Ω)
Z_G	Generator's series impedance (Ω)
Z_M	Motor's series impedance (Ω)
V_M	Voltage beyond the impedance Z_M (V)
φ	Power factor angle
θ	Impedance angle (radian)
P-δ	Power versus power-angle
A_1	Positive area during the transient (in EAC)
A_2	Negative area during the transient (in EAC)

H	Inertia constant, (MJ/MVA)
ω_s	synchronous speed of generator (radian/s)
δ_0	Initial rotor angle (pre-disturbance) of the generator (degree)
δ_c	Rotor angle when disturbance is cleared (degree)
δ_{max}	Maximum swing of the rotor angle (degree)
P_m	Mechanical input power (pu)
P_e	Electrical output power (pu)
X_1, X_2	Impedances of parallel transmission lines (Ω)
X	Equivalent impedance of the transmission lines (Ω)
P_{max}	Maximum electric output power of generator (pu)
t	Time (s)
P-t	Power versus time
P_0	Pre-fault electric output power, steady-state power output (pu)
ΔP	Change in power (pu)
t_0	Time of inception of fault or time corresponding to δ_0 (s)
t_c	Fault clearing time or time corresponding to δc (s)
ω_{tc}	Rotor speed at fault clearing instance (radian/s)
t_{max}	Time corresponding to δ_{max} (s)
Δt	Simulation time step or integration time step (s)
pu	Per unit
s	Second
pu-s	Per unit-second
ns	Nanosecond

S_1	Inner Blinder Setting
S_2	Outer Blinder Setting
Hz	Hertz

LIST OF ACRONYMS

VLSI	Very Large Scale Integration
RAM	Random Access Memory
ROM	Read Only Memory
SCV	Swing Centre Voltage
EAC	Equal area criterion
PMU	Phasor measurement unit
SMIB	Single machine infinite bus
PSCAD™	A simulation tool from Manitoba HVDC Research Centre
DSP	Digital signal processing
RTDS™	Real Time Digital Simulator from RTDS Technologies Inc.
OST	Out-of-step Tripping
OSB	Out-of-step Blocking
FIS	Fuzzy inference system
RRI	Right Resistance-Inner
RRO	Right Resistance-Outer
LRI	Left Resistance-Outer
LRO	Left Resistance-Inner
TXI	Top Reactance-Inner
TXO	Top Reactance-Outer
BX	Bottom Reactance
TEF	Transient energy function

COI	Centre of inertia
COA	Centre of angle
3PC	Triple processor
GPC	Giga processor
MIPS	Million instructions per second
MFLOPs	Mega floating-point operations per second
IEEE	Institute of Electrical and Electronics Engineers, Inc.
GFLOPs	Giga floating-point operations per second
RSCAD™	A software associated with the hardware simulator RTDS
WIF	Workstation interface card
SDRAM	Synchronous dynamic random access memory
IIR	Infinite impulse response

CHAPTER 1
BACKGROUND

1.1. Introduction

This chapter briefly describes the concepts and terminologies related to an electric power system, which are used later in this thesis. The basics of power system stability, protection system and digital relays are elaborated as the conducted research deals with a technique which requires the knowledge of them. The past methods and current trends in the research area are reported in the literature review section. The objectives and main contributions that the research has made are highlighted. Organization of this thesis is explained briefly at the end of the chapter.

1.2. Introduction to a Power System

Power systems are complex networks which are designed to supply reliable, reasonably priced and quality energy to the consumers. The functional units of a power system mainly consist of generation, transmission and distribution as shown in Figure 1.1. Generation unit produces electrical energy from other forms of energy (coal, hydro etc.). The transmission unit transfers bulk amount of energy from one point to another. The distribution system finally supplies energy to the consumers. The consumer ends have various electrical loads that require energy to operate [1, 2].

The main requirements of an electric power system are: the system must meet the energy requirement of continually varying load pattern, should supply energy at minimum cost and the quality should meet the standards set (like frequency, voltage and reliability). To meet these

requirements several levels of devices are installed in generation and transmission units and are called control devices (excitation system, governor etc.). The control devices help to achieve the satisfactory operation of the power system by maintaining voltage, frequency and other system variables within standards [1].

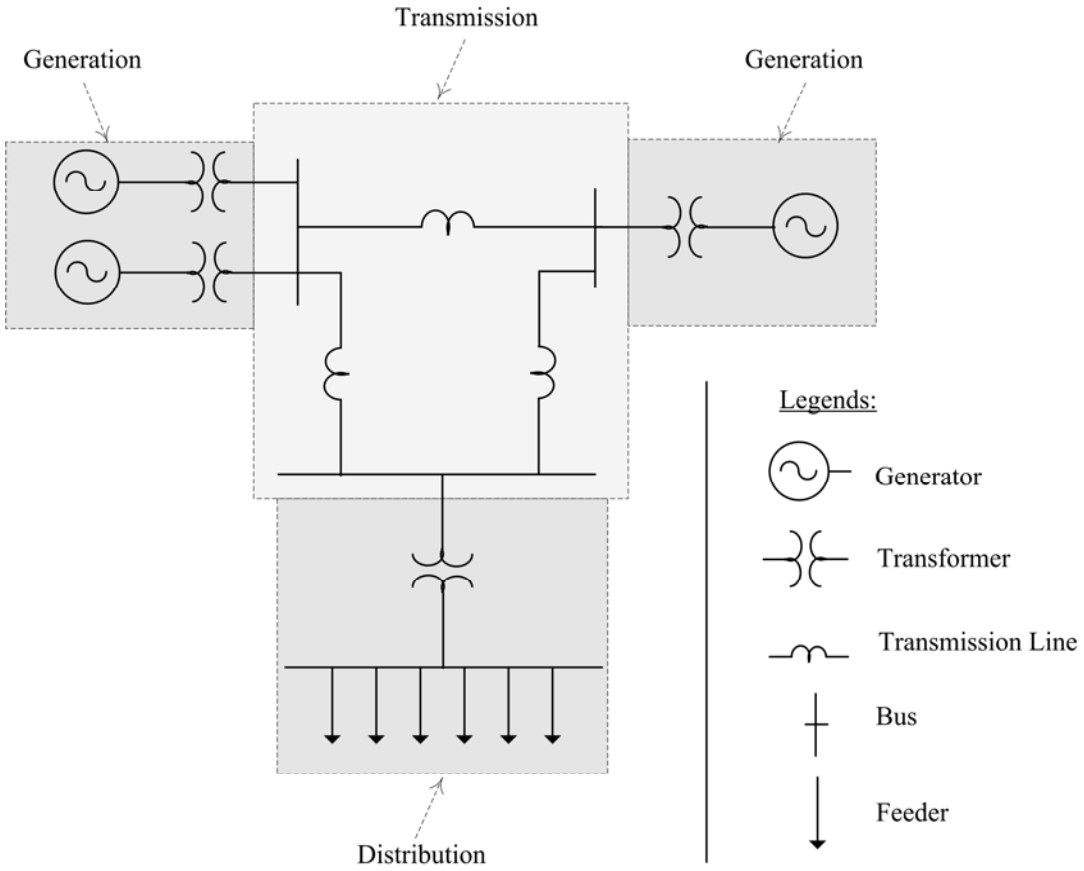

Figure 1.1 A typical power system showing its functional units

Power systems are often subjected to disturbances, which result in transients in the system. The transients introduce abnormalities in power system operation. Therefore power systems are equipped with protective devices [3, 4] which sense these abnormalities in the system and take the necessary corrective actions to isolate the abnormalities. The behavior of the power system during transients is dealt with under ***power system stability*** which is described next.

1.3. Power System Stability

Stability in general is referred to as the ability of a system to withstand disturbances and bring the system back to a new stable condition. The same definition applies for the power system but an understanding of a stable condition and a disturbance related to the power system are required. Power systems are complex systems with two or more generators interconnected through transmission lines. The steady state condition in a power system refers to the condition when the outputs of the generators are constant and all the generators are operating at the same frequency. Disturbances on the other hand are abnormal conditions that disturb the smooth operation of a power system. Disturbances could be due to changes in load/generation, loss of load/generation, loss of transmission lines etc. The disturbance results in oscillations in voltages, currents, and the frequency of the system. Thus, if the oscillatory response of a power system following a disturbance is damped and the system settles in a finite time to a new steady state operating condition, the system is stable. If the oscillations do not damp-out, the system does not restore to a steady state condition and the condition is referred to as unstable or ***out-of-step condition***. The out-of-step condition is also referred to as ***loss of synchronism*** as the interconnected generators lose synchronism and run at different speeds. If preventive measures are not taken on time, it may cause damages to power system equipments due to over-currents and over-voltages and may lead to power system blackout [5, 6].

1.4. Power System Protection

Disturbances in power systems are inevitable. So power systems are incorporated with provisions for mitigating the effects of disturbances which are called as protection systems. The function of protection system is to ensure the prompt removal of any element of a power system that might cause damage or otherwise interfere with the effective operation of the rest of the system. Power protection system mainly consists of relays, circuit breakers, instrument

transformers and communication devices. A relay is a device which senses abnormalities in a power system and makes a decision. The circuit breaker uses the relays' decisions to perform connection/disconnection actions. The relays receive information of voltage and current via the instrument transformers. Coordination of the relays is maintained by communication devices. Using the information of voltage and current, relay evaluates a composite signal (signal varies relay to relay). The computed signal is then compared with relay's threshold value to make the decision whether the system is running normally or abnormalities have occurred. The abnormalities to which a relay responds include:

- Increase in current
- Change in direction of power flow
- Under voltage condition
- Under frequency
- Increase in temperature
- Loss of synchronism (out-of-step)

The ***out-of-step relays*** sense the loss of synchronism or out-of-step condition in the power system and disconnects the asynchronous generators from the rest of the system to restore a new steady state operating condition [3, 6].

Relays are installed at various locations to protect the major components of a power system without leaving any part of the system unprotected. This is achieved by dividing the power system into segments called protection zones. A protection zone normally includes a generator, a transformer, a bus, a transmission line, a distribution feeder or a motor. Each relay has 'reach' beyond which it cannot protect. So the protection zones are overlapped to ensure the protection

of each component. Figure 1.2 shows an example of the protection zones for a sample power system.

The relay structures have gone through major transitions from electromechanical to solid-state and then to digital relays. Electromagnetic relays consist of parts which move due to the force produced by current flowing in the electromagnets. The use of moving parts requires frequent maintenance of the electromechanical relays. Solid-state relays are semiconductor devices composed of electronic components like diodes, transistors etc. These relays do not have moving parts which make them lighter and smaller than electromechanical relays [7].

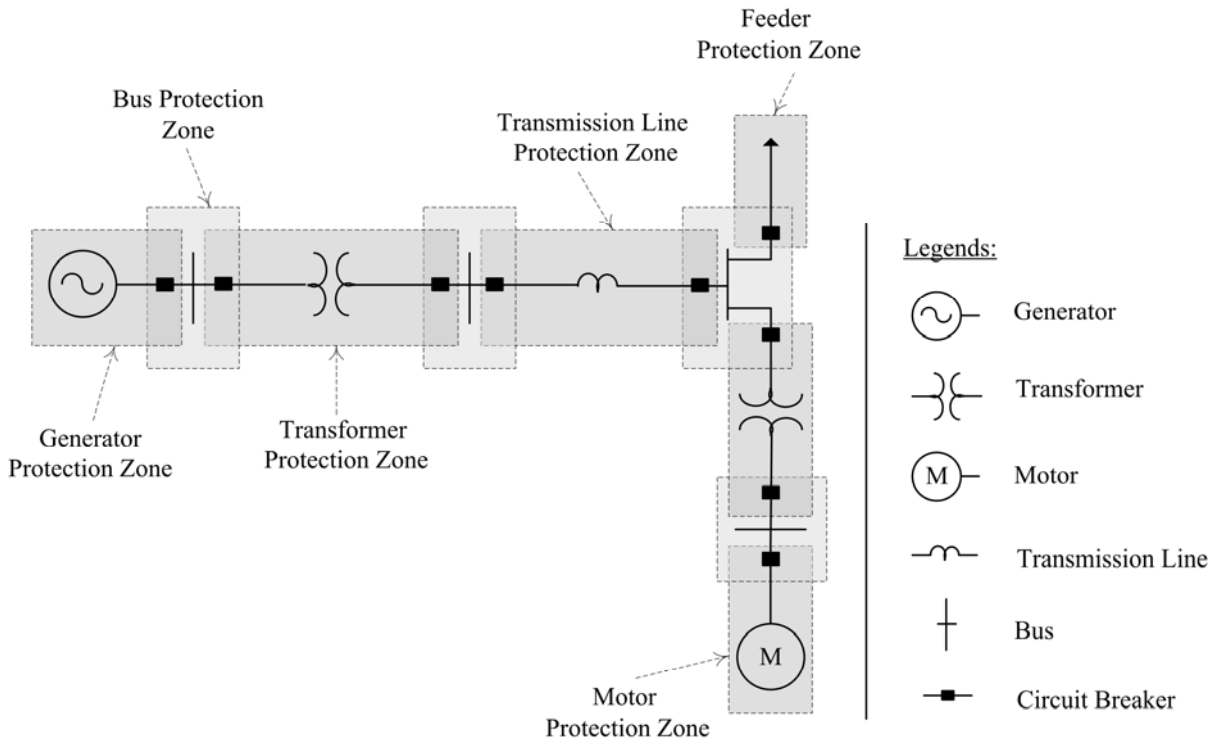

Figure 1.2 A power system showing protection zones

1.5. Digital Relays

The Very Large Scale Integrated Circuit (VLSI) technology and microprocessor technology has developed by leaps and bounds during the previous few decades. Digital relays have been implemented using this technology and are presently used widely in protection systems. These

relays use the same logics that have been used in electromechanical and solid-state relays. One or more ***microprocessors*** along with RAM and ROM and software program make the basic components of a ***digital relay***. These relays have the following advantage over electrometrical and solid-state relays [7].

- Economics: Low cost of microprocessor based system.
- Performance: The faster performance of numerical relays are due to high speed of the digital processors and absence of moving mechanical parts,
- Multiple Functions: Relays, meters, indicators and communication devices can be integrated.
- Flexibility: A general purpose hardware can be used
- Less outages, small size and easy replacements.

1.6. Literature Review

Several methods have been proposed in the literature and are in use for out-of-step detection. In this section, out-of-step detection techniques have been broadly classified into three categories based on the operating quantities and the procedures that are used inside these relays. Shortcomings of the methods are also pointed out briefly.

1.6.1. Conventional Techniques

The power angle (δ) during a power swing oscillates and results in the oscillation of electrical quantities such as frequency, voltage, current, impedance at various locations in the power system. Most of the methods for out-of-step detection are based on sensing the oscillations or the rate of change of one of the system quantities.

The Blinder technique proposed in literature uses rate of change of impedance to detect the out-of-step condition [8]. Swing Centre Voltage (SCV) technique uses rate of change of voltage

at swing centre [8] and the technique in [9] uses the rate of change of apparent resistance, respectively. The method proposed in [10] uses phase angle difference of generators and [11] uses generator's angle, angular velocities and their rate of change for out-of-step detection.

All the methods described above require an extensive system analysis for relay settings; hence creates a complex system study issue for relay settings for a multimachine power system. Besides this, the blinder scheme does not detect out-of-step condition for fast power swings, and the SCV does not perform well if the system impedance is not close to 90°. The method based on phase angle difference of generators requires extra communication devices. The method proposed in [11] requires the reduction of the multi-machine system into an equivalent two area system.

1.6.2. Technique using Equal Area Criterion (EAC) in Power Angle (δ) Domain

EAC describes the system stability based on the area under the power system curves. This concept has been employed for out-of-step detection [12]. The power curves for pre-disturbance and post-disturbance of the system are estimated and areas under them are evaluated to detect out-of-step condition. To determine the power curves, offline calculations are done using the measurements. Offline calculations are usually done for dynamic security analysis of power system, where all the possible credible contingencies are analyzed. In such analysis, plot of δ versus time for all the machines are determined. Based on δ-t curve, the machine that may become out-of-step is identified and possible remedial measures are taken. However, this kind of analysis for EAC in δ-domain is not effective to solve the out-of-step protection problem. The reason behind this is the luxury of obtaining various time domain simulations is not feasible for out-of-step protection because the decision whether the machine is going to out-of-step has to be made right at that instance (objective of any relay) and not based on hypothetical scenario.

This method is applicable for two area power system. However to apply for a multimachine system, network reduction is required to obtain an equivalent two area system. This method not only requires local information but also requires information from other buses, so additional communication devices and phasor measurement units (PMU) are required for the determination of the power curves.

1.6.3. Application of Fuzzy Logic and Neural Networks

Reference [13] proposed out-of-step detection technique based on fuzzy logic and [14] proposed the application of neural networks for out-of-step detection. Methods based on fuzzy logic and neural network required extensive offline simulations for training the algorithms. The methods perform well if adequately trained and appropriate input signals are identified but the complexity in the training process increases as the number of power system interconnections increase. The methods are cumbersome when applied to a multimachine system.

1.7. Objective of Thesis

The following two conclusions can be drawn from the above literature review: existing methods require offline calculations for relay settings, or need extra communication devices and to apply to a multi-machine require network reduction technique to reduce to an equivalent two area system. Thus the complexity of the above procedures increases as the size of the power systems increase. The objectives of this thesis are,

- Developing a simple algorithm for out-of-step detection which avoids complex system studies and extensive offline calculations. Propose an algorithm which can be applied directly to a multi-machine configuration of a power system without any network reduction.

- Developing an algorithm which is entirely based on the local electrical quantities available at the point of installation and hence avoid the need of any extra communication devices.

1.8. Contributions of Thesis (Outline)

Outline of the thesis contributions are described below. The specific contributions made in this thesis are described in more detail in Chapter 6 (Conclusions).

- Modification of EAC in δ domain to time domain. Developing an out-of-step detection algorithm based on EAC in time domain which is also referred to as energy equilibrium criterion in time domain.
- Testing the effectiveness of the proposed algorithm on a single machine infinite bus (SMIB), two machine infinite bus, three machine infinite bus and a 17-bus multimachine configurations using simulation tool (PSCAD™). The performance comparison of the proposed algorithm with a Conventional Blinder Technique.
- After successful simulation studies, hardware implementation of the proposed algorithm using a Digital Signal Processing (DSP) Board. Closed loop testing of the digital out-of-step relay to verify the results using a Real Time Digital Simulator (RTDS™).

1.9. Outline of Thesis

The thesis is organized in six chapters and six appendices. The first chapter provides a brief overview of Out-of-Step Protection, Literature Review and Outline of the Thesis. The power swing phenomenon and its impacts on the protection devices are discussed in Chapter 2. The basic functions of out-of-step relays are also described. The state-of-the-art in out-of-step

detection and protection and the strengths and the shortcomings of the techniques proposed in the literature are explained.

In Chapter 3, first the EAC in δ domain is described and its stability analysis is discussed. Next some of the difficulties associated the EAC in δ domain are described. The proposed algorithm is presented, that is, the EAC in time domain. The advantage of the proposed algorithm over the EAC in δ domain is discussed. Finally the proposed algorithm is tested on a SMIB system using PSCAD™. The performance of the proposed algorithm is compared with Conventional Blinder Technique.

In Chapter 4, the proposed algorithm is applied to multimachine configurations. A two machine infinite bus, three machine infinite bus and 17-bus multimachine system models are developed in PSCAD™ and different power swing scenarios are simulated. The proposed out-of-step algorithm is applied to detect the out-of-step conditions in the multi-machine system.

After successful simulation studies, a hardware implementation of the digital relay was done using a DSP Board and the implementation is described in Chapter 5. Basic blocks of the relay i.e. filtering, down sampling, phasor estimation and the protection algorithm are discussed. Next a SMIB system configuration is implemented on the RTDS™. The proposed relay is then tested in a closed-loop fashion using the real time electrical signals from the RTDS™. The proposed relay is tested by creating various power swing scenarios on the RTDS™ simulator.

The conclusions drawn from this research work are presented in Chapter 6. A list of possible future work is also listed.

Appendix A lists the power system parameters of a SMIB. The PSCAD™ model of SMIB is shown in Appendix B. The guidelines for setting blinders for out-of-step detection are listed in Appendix C. Appendix D lists the parameters of a two machine infinite bus system and three

machine infinite bus systems. The parameters of 17-bus multi-machine system are listed in Appendix E. PSCAD™ model of a 17-bus multi-machine system is shown in Appendix F.

CHAPTER 2
OUT-OF-STEP BASICS

2.1. Introduction

This chapter explains the fundamentals of power swings. The natures of swings are discussed and expressions are derived for swing locus. The swing locus is then used to describe the impacts of power swings in the relaying systems like distance relay and overcurrent relay. The importance of out-of-step detection is pointed out and the basic functions that an out-of-step relay has to perform during power swing are discussed. The various practices for out-of-step protection are described and the strengths and shortcomings of these techniques are identified.

2.2. Power Swing Phenomenon

During the steady state operation, all the generators connected to a power system deliver constant power at constant frequency. The interconnected generators run at synchronous speeds maintaining constant relative rotor angle with respect to its stator. There exists a balance of input mechanical and output electrical power for the individual generators and the frequency of the system remains close to the nominal frequency (50 or 60 Hz value). Figure 2.1 shows the voltage and current waveforms during the steady state operation of a power system [1, 5].

Power systems usually are subjected to various disturbances such as change in the system load, loss of transmission line, loss of generator, fault and fault clearance. The disturbance causes an imbalance of input and output powers in the system. As the input is mechanical and output is electrical, an imbalance of two powers causes electro-mechanical oscillations or transients in the system. The electro-mechanical oscillations are due to the result of relative angular velocity of

the rotors. These oscillations are electrically characterized by the fluctuation of voltages, currents and hence power flows in the system. This abnormal condition in a power system is referred to as a power swing. Figure 2.2 shows the oscillations in voltage and current waveforms during a power swing [3, 15].

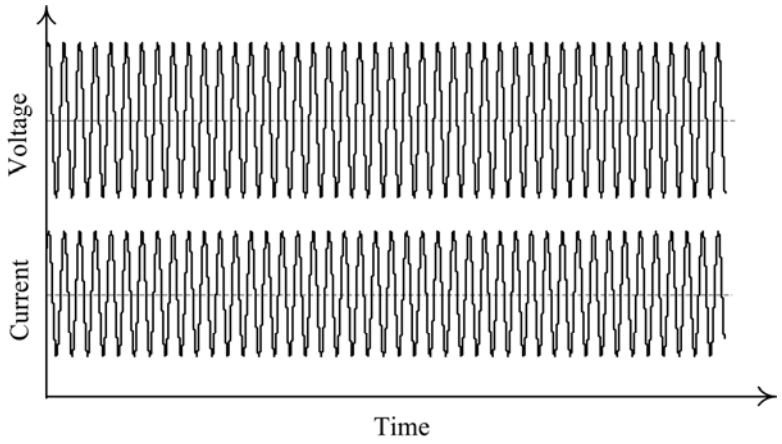

Figure 2.1 Voltage and current waveforms during steady state operation

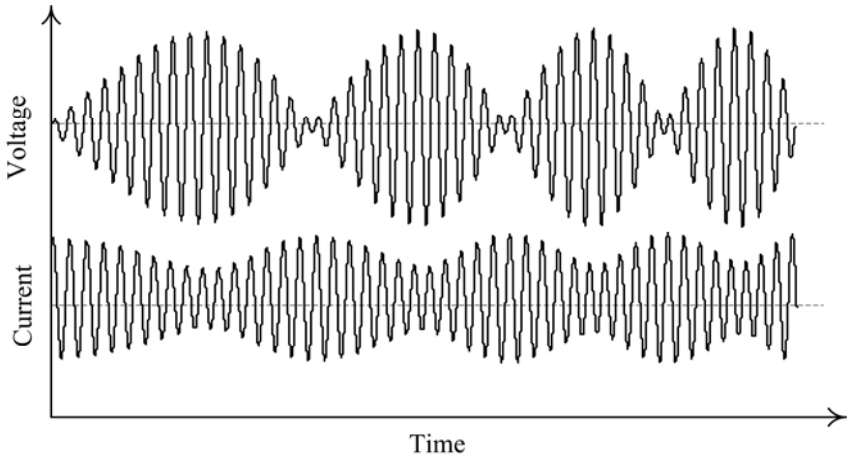

Figure 2.2 Voltage and current waveforms during power swing

As disturbances are inevitable, every power system is designed and operated such that it is capable of withstanding transients up to a certain extent beyond which the system becomes unstable (is not able to restore to a steady-state condition). The state of a power system after a disturbance depends on the initial power flow, the severity of the disturbance, action of the

control equipment and the power system itself. Depending upon the response of the system to a disturbance, the power swings can be classified as a stable swing or an out-of-step swing.

Following a disturbance, if the oscillations damp out and the system restores to a new steady state point then the power swing is referred to as a stable swing. Severe system disturbances could cause large separation of generator rotor angles, large swings of power flows, large fluctuations of voltages and currents and ultimately lead to the asynchronous operation of the generators called the out-of-step condition [6, 8].

2.3. Swing Locus in Impedance Plane

During a power swing, the two generators rotate at different speeds and cause a change in relative rotor angle of the generators. The consequence is high fluctuation of voltages and currents at different nodes of the power system (as shown before in Figure 2.2). The distance relays incorporated in a power system use the voltages and currents to calculate the impedance. This section examines the nature of the impedance locus during a power swing.

Consider a two machine system as shown in Figure 2.3. The motor voltage E_M is considered as the reference phasor. The generator voltage E_G leads E_M by δ phase angle. δ is referred to as the relative rotor angle (or the power angle) of the generator. The impedance between the generator and motor ends is Z.

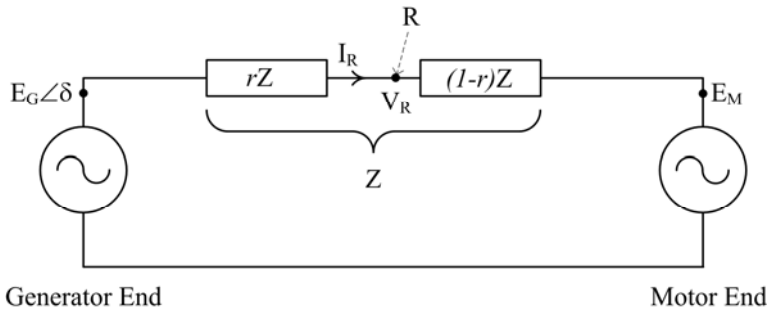

Figure 2.3 Two machine system used to illustrate power swing loci

The relay location R divides the impedance in two sections with impedances *r*Z and (1-*r*Z), where r is a fraction between 0 and 1. The current through point R and voltage at point R are,

$$I_R = \frac{E_G \angle \delta - E_M}{Z} \tag{2.1}$$

$$V_R = (1-r)E_G \angle \delta + rE_M \tag{2.2}$$

Thus, the impedance at point R, i.e. the impedance seen by relay is,

$$Z_R = \frac{V_R}{I_R} = \frac{(1-r)E_G \angle \delta + rE_M}{E_M \angle \delta - E_M} Z \tag{2.3}$$

Assume, $E_G = E_M$ then,

$$\frac{Z_R}{Z} = \frac{(1-r)\angle \delta + r}{1\angle \delta - 1}$$

$$= \frac{-r(1\angle \delta - 1) + \angle \delta}{1\angle \delta - 1}$$

$$= -r + \frac{1}{(1 - \angle - \delta)}$$

$$= -r + \frac{1 + \angle \delta}{(1 - \angle - \delta)(1 + \angle \delta)}$$

$$= -r + \frac{1 + \angle \delta}{1 + \angle \delta - \angle - \delta - 1}$$

$$= -r + \frac{1 + \cos\delta + j\sin\delta}{2j\sin\delta}$$

$$\therefore \frac{Z_R}{Z} = (\frac{1}{2} - r) - j\frac{1}{2}\cot\frac{\delta}{2} \tag{2.4}$$

Equation (2.4) represents a vertical line with offset $(\frac{1}{2} - r)$ from the horizontal axis.

$$\therefore Z_R = \left((\frac{1}{2} - r) - j\frac{1}{2}\cot\frac{\delta}{2} \right) Z \tag{2.5}$$

In equation (2.5), multiplication by Z term means the magnitude of the Z_R lines are multiplied by $|Z|$ and lines are rotated counterclockwise through $\angle Z$ [4, 6]. The impedance loci for different value of r as δ changes are shown in Figure 2.4. In the figure, R_R and X_R represent resistance and impedance at the relay location R, respectively.

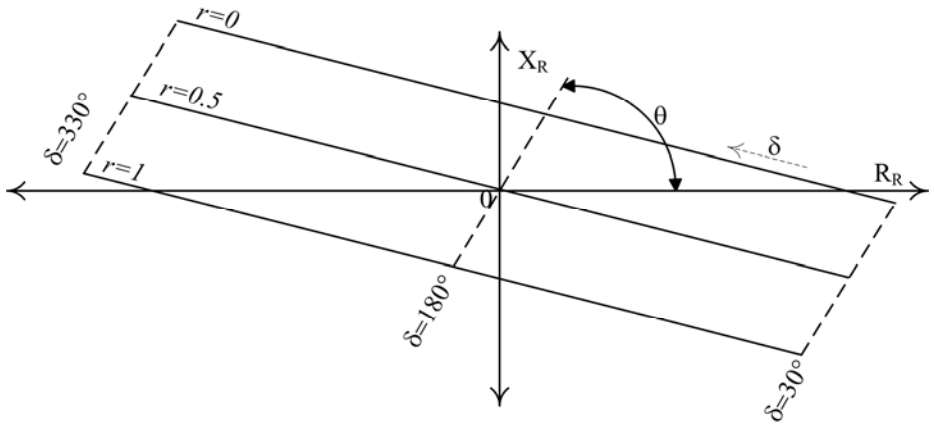

Figure 2.4 Impedance loci at point R during out-of-step condition in two machines for E_G=E_M

If $E_G \neq E_M$, the loci become circular instead of a straight line. The expression to show that the loci are circular for $E_G \neq E_M$ are given in [6]. Figure 2.5 shows the loci for different E_G and E_M .

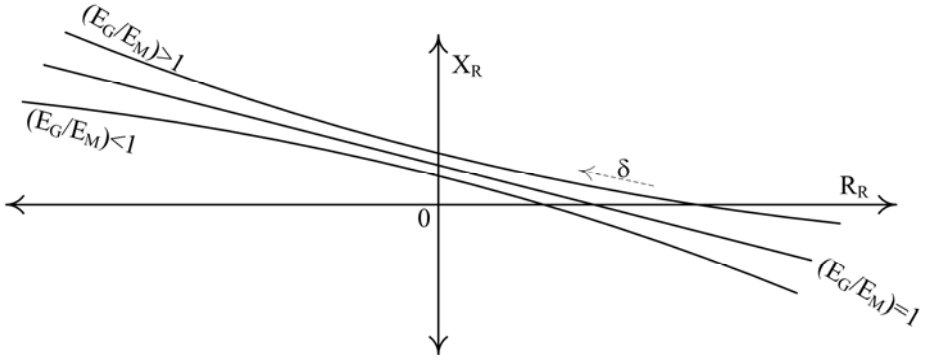

Figure 2.5 Impedance loci at point R during out-of-step condition in two machines with different E_G and E_M

2.4. Impacts of Power Swing

As stated earlier, the relative rotor angle accelerates or retards during the power swing and in the process, there may be instances when the phase angle difference between the two generator

voltages becomes 180°. During such instances, at the relay locations voltage becomes minimum and current becomes maximum. Thus, the electrical conditions are very much identical to a fault. The relays, which operate during the fault in the system, thus operate during the swing despite the nature of the swing. The protective relays prone to power swings include distance, overcurrent, directional overcurrent, undervoltage, directional comparison relays and they cause unwanted tripping of power system components.

Figure 2.6 shows an operating zone of a distance relay plotted along with the impedance loci during the swing. The distance relay will operate if the swing locus enters inside the operating zone of the distance relay. The curve 'a' shows the case where there is a stable swing but the swing locus doesn't enter the operating zone of the distance relay so it doesn't affect the operation of the relay. The curve 'b' is also stable swing but this time it crosses the operating zone of the distance relay, so it sends a trip signal to the circuit breaker associated with it. The last curve 'c' is out-of-step swing where it crosses the operating zone of the impedance relay and trips the circuit breaker [3].

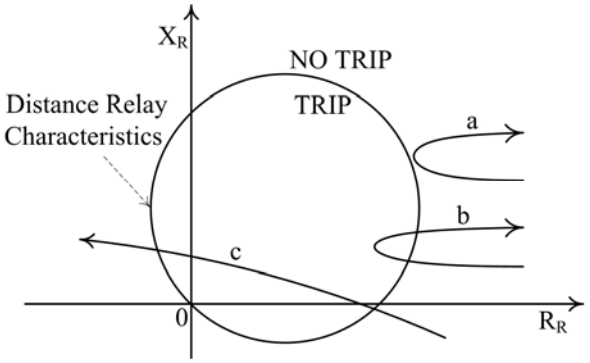

Figure 2.6 Operating characteristics of distance relay showing various power swings

The performance of overcurrent relay during the power swing can be investigated by plotting the swing loci and operating zone of the relay in the complex current plane. The equation (2.1) gives the expression of the current for a two machine system shown in Figure 2.7. It is a circle

with centre at the end of the vector $-E_M / Z$ and radius E_G / Z. The operating zone of an overcurrent relay is a circle with centre at origin as shown in Figure 2.7. So, whenever the measured current enters the operating zone of the relay, the overcurrent relay operates [6].

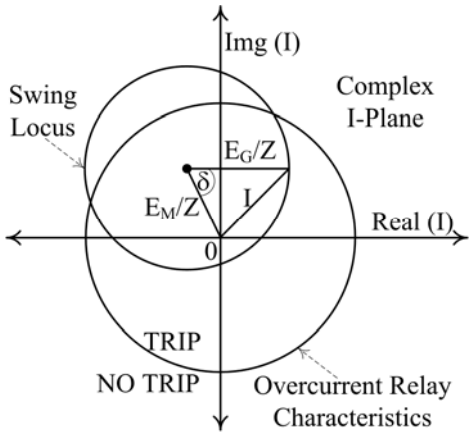

Figure 2.7 Operating characteristics of overcurrent relay showing different power swings

2.5. Out-of-Step Protection

Regardless of stable swing or out-of-step condition, the relays prone to power swing operates if the parameter sensed by the relay enters the operating zone of the relay. For example, the distance relay in Figure 2.6 operates for the cases 'b' and 'c' as the impedance seen by relay enters the operating zone. The tripping of relay during the stable swing case 'b' is not desirable. The distance relay should allow the power system to return to new steady state condition in case of a stable swing. Thus, the out-of-step relays should be coordinated with the relays prone to the power swing in order to send them signal indicating not to trip during a stable swing. In case of an out-of-step condition, the out-of-step relay sends trip signal only to the selected relays [3, 6].

From the above discussion we can see that that there are basically two functions that an out-of-step relaying system has to perform. The first is out-of-step blocking function (OSB). OSB must block relays prone to the power swing, no matter whether it is a stable or out-of-step swing. The next is out-of-step tripping function (OST) which discriminates between stable and out-of-

step swings and initiates the system separation only during the out-of-step condition. The out-of-step relaying philosophies are presented in [3] and are summarized below for completeness:

- Block trip at all locations for a stable swing.
- Protect power system components by ensuring quick separation for every out-of-step condition to avoid equipment damage and blackout of major portions of the power system.
- Separate the network effectively maintaining a load-generation balance in each area.
- Controlled tripping of certain power system components to prevent equipment damages.

2.6. Out-of-Step Detection Techniques

Many out-of-step detection techniques have been used in practice and are reported in the literature. The most popular methods include rate of change of impedance method (blinder technique), SCV technique, application of fuzzy logic, neural network, and artificial intelligence for the out-of-step detection, out-of-step detection based on wavelet transform, out-of-step detection using frequency deviation of voltage and out-of-step detection based on EAC in δ domain. The following sections elaborate some of the key methods described in the literature [8, 12-14, 16, 17].

2.6.1. Rate of Change of Impedance Method (Blinder Technique)

The most popular method is based on the measurement of positive sequence impedance at the relay location. The out-of-step relay is basically a distance relay with different shapes of relay characteristics in the impedance plane. Depending on its shape in the impedance plane, the scheme may be a blinder scheme, a concentric circle scheme, a concentric polygon scheme or a

lenticular scheme. Selection of a scheme depends on the load pattern, the power system parameters and the desired performance; however the main algorithm for their operation is the same [8, 15].

Figure 2.8 shows a rectangular (polygon) scheme for out-of-step detection. The impedance measured by relay during steady state conditions is the load impedance which lies away from the relay characteristics. The relay measures the rate of change of impedance as it travels into the protection zones of impedance relay. For discrimination, the out-of-step relay is based on the fact that the impedance seen by the relay changes slowly during the swing compared to a faulted case. To achieve this two concentric impedance characteristics 'S_1' and 'S_2' are placed in the impedance plane separated by impedance ΔZ as shown in Figure 2.8. The out-of-step relay then employs a timer to record the duration of the impedance locus as it travels between 'S_1' and 'S_2'. The relay decides the case as a system fault, if the impedance seen by relay crosses the settings 'S_1' and 'S_2' before the timer expires. But, if the timer expires before the impedance crosses 'S_1' and 'S_2'; the relay decides the case as a power swing.

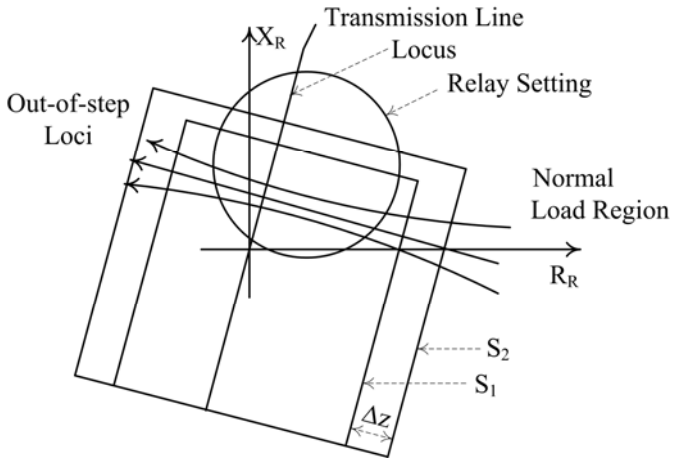

Figure 2.8 A concentric rectangular scheme for the out-of-step detection

There are number of issues and difficulties associated with this method. The inner characteristics 'S_1' must be placed outside the largest distance protection characteristic. The outer characteristics 'S_2' must be placed away from the load region to protect false tripping due to overloading. The difficulty associated with this method is the separation of the two concentric shapes (i.e. ΔZ) and the timer setting. The settings depend on the rate of slip during the transient. The rate of slip between two systems depends on the accelerating torque and system inertias. It is required to perform extensive stability studies to determine the fastest power swing. Besides, the technique also experiences difficulties in heavily loaded long transmission line. In such case, the load region lies close to operating characteristics of the relay and blinders settings may overlap the relay setting and normal load region [8, 15]. This may cause false tripping of out-of-step relay during normal operation or a fault. Reference [18] explained that this method ensured proper protection only in the worst case scenarios and [19] pointed out that scheme was not able to distinguish swing from a fault when the impedance seen by the relay changes fast.

2.6.2. Swing Centre Voltage (SCV) Technique

A two machine system as shown in Figure 2.9 is considered to illustrate the SCV technique for out-of-step detection. SCV is defined as the voltage at the location of a two-source equivalent system where the voltage becomes zero when the rotor angles difference between the two sources becomes 180° . Figure 2.10 illustrates the phasor diagram of a two machine system in which the phasor OO' represents SCV [8].

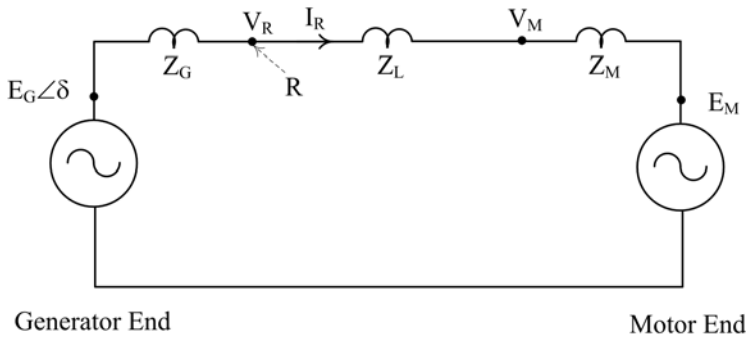

Figure 2.9 Two machine system to illustrate SCV

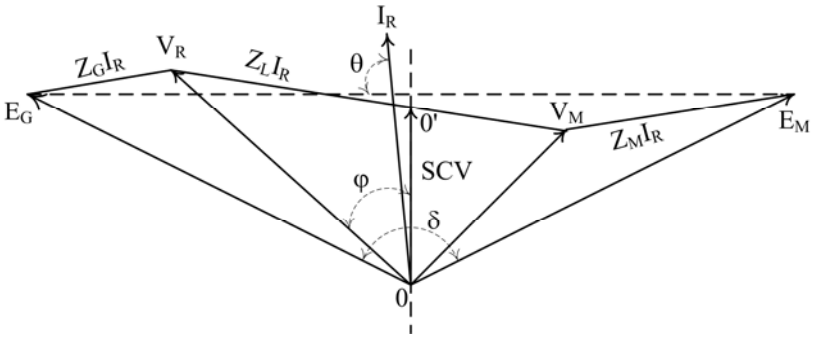

Figure 2.10 Phasors of the two machines system

The expression to evaluate the SCV is given by,

$$SCV(t) = \sqrt{2}E\sin\left(\omega t + \frac{\delta(t)}{2}\right)\cdot\cos\left(\frac{\delta(t)}{2}\right) \tag{2.6}$$

In equation (2.6), E_G and E_M are assumed to be same and equal to E.

The SCV does not exactly lie on the relay location. Relay are usually located close to the terminal of generator i.e. at point R in Figure 2.9, where the voltage phasor is V_R. SCV can be approximated from the voltage phasor V_R available at the relay location. Figure 2.11 shows the phasor diagram to approximate SCV from the measurement of voltage phasor V_R.

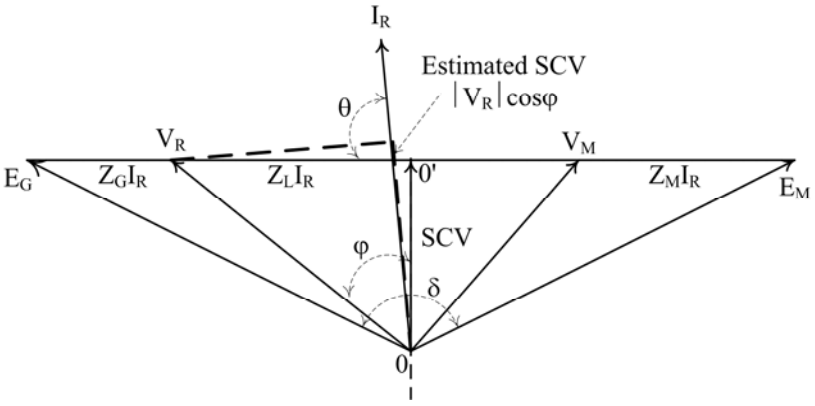

Figure 2.11 Local estimation of SCV

In Figure 2.11, the SCV is approximately equal to $|V_R| \cdot \cos\varphi$, which is also equal to

$$SCV \approx |V_R| \cdot \cos\frac{\delta}{2} \tag{2.7}$$

where φ is the phase angle difference between V_R and I_R. In Figure 2.11, phasor $|V_R| \cdot \cos\varphi$ is a projection of $|V_R|$ onto the axis of I_R. Phasor $|V_R| \cdot \cos\varphi$ approximates the magnitude of SCV for a homogeneous system with the system impedance angle (θ) close to 90°. For the purpose of power-swing detection, the rate of change of SCV information is used.

$$\frac{d(SCV)}{dt} \approx -\frac{|V_R|}{2} \cdot \frac{d\delta}{dt} \cdot \sin\frac{\delta}{2} \tag{2.8}$$

A threshold value of the rate of change of SCV is determined from system stability studies to discriminate the stable swing from out-of-step. Comparison of the measured rate of change of SCV with the threshold value gives the decision that it is either stable or out-of-step swing [8].

This technique has the advantage that SCV is independent of the power system parameters. This provides an out-of-step relay with no setting requirements. However, the estimate of swing center voltage is from locally available data from the substation, therefore the estimate is good only when the system impedance angle is close to 90°. Besides, this method also needs system

stability studies to be performed to find out the threshold value of rate of change of SVC to discriminate stable swing from out-of-step [8].

2.6.3. Techniques Based on Fuzzy Logic and Neural Network

Recent techniques such as fuzzy logic and neural network have been proposed to detect out-of-step conditions in power systems [13, 14].

The method based on fuzzy logic can be briefly described as finding the appropriate set of signals to train fuzzy inference system (FIS), developing criteria to discriminate type of power swing and making the decision based on the criterion. A block diagram of a fuzzy based out-of-step detection system is shown in Figure 2.12 [13].

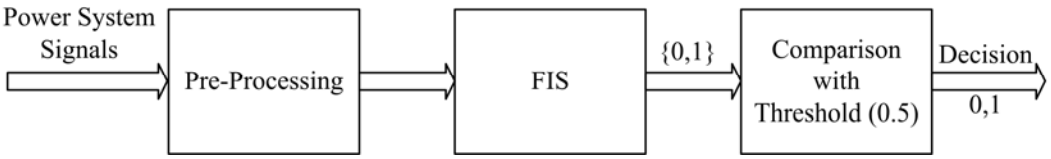

Figure 2.12 Fuzzy based out-of-step detection

Power system signals such as generators' output voltages, currents and angular speeds are recorded. Orthogonal components of phase voltages and currents are calculated and used further to derive various composite signals. In order to choose the best input signals to FIS, the statistical properties of all the available signals are determined. The most important recognition signals are machine angular frequency deviation and impedance angle measured at the machine terminals. The FIS is trained with a set of input-output patterns generated with the simulations of 108 different cases. For classification purpose, a threshold value was set to 0.5. The cases which results FIS output lower than 0.5 are classified as stable and the cases which resulted in output higher than 0.5 are classified as out-of-step. This technique needed very small time for out-of-

step detection as this method performed prediction of machine instability rather than the usual approach of waiting to detect the actual occurrence of the out-of-step condition [13].

Reference [14] proposed an out-of-step detection based on neural network which is based on the back propagation trained neural networks. The schematic diagram of out-of-step detection based on neural network is shown in Figure 2.13.

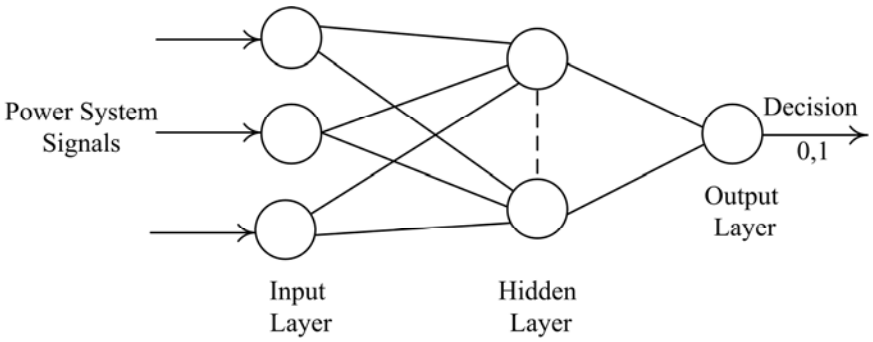

Figure 2.13 Schematic diagram of neural network based out-of-step detection

The pre-fault loading of the generator or the mechanical input power, generator kinetic energy deviation and average kinetic energy deviation are selected as input to the neural networks as they are found to be dominant in deciding stable and out-of-step conditions. The pre-fault mechanical input power is a direct outcome of the load flow results. The other two signals are determined from the transient stability study using the second order model of the machine. A nine bus power system with three generators and three loads is chosen and 162 simulations are done with faults at six different locations and three different load levels with different fault duration times. Runge-Kutta numerical integration approach is applied to find the stable and out-of-step condition. A simulation case is classified as out-of-step if the rotor angle of the generator under study reaches 180° and it is given a stability index of 0; otherwise the sample is classified as stable, and is given stability index of 1. An advantage of this method is that all the required signals can be measured locally from the machine to be protected.

The above methods had a capability to make a decision quickly for a new case which had close resemblance to a known predefined case for which the algorithm was trained for. The methods needed enormous trainings with different outage cases of the power system. Therefore it made the training process tedious. The method suffered from the pitfall that it made a quick and correct decision only if it was adequately trained.

2.6.4. Techniques Based on Equal Area Criterion (EAC) in δ Domain

EAC is an important concept which describes the stability of a two area system as shown in Figure 2.14.

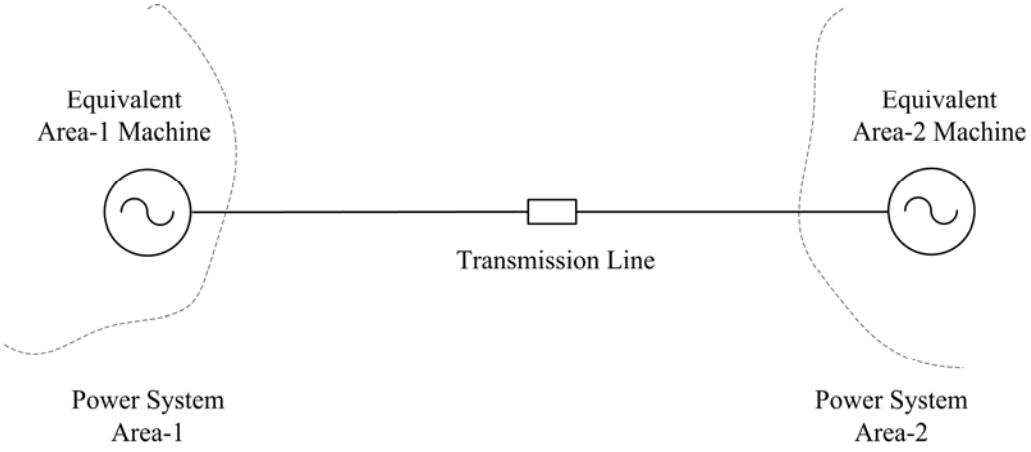

Figure 2.14 A two area power system

The EAC concept can be applied to detect out-of-step condition. Reference [12] has proposed a method which detects the out-of-step condition based on EAC in δ domain. The EAC concept requires pre-disturbance, during-disturbance and post-disturbance power versus power angle (P-δ) curves and calculates areas under them to make the decision. This concept evaluates two areas A_1 and A_2 under P-δ curves as,

$$A_1 = \int_{\delta_0}^{\delta_c} \frac{\omega_s}{H}(P_m - P_e)d\delta \tag{2.9}$$

$$A_2 = \int_{\delta_c}^{\delta_{max}} \frac{\omega_s}{H}(P_m - P_e)d\delta \tag{2.10}$$

where H is the inertia constant, ω_s is the synchronous speed, δ_0 is the initial rotor angle (pre-disturbance) of the machine, δ_c is the rotor angle when disturbance is cleared, δ_{max} is the maximum swing of the rotor angle, P_m is the mechanical input power and P_e is the electrical output power [20] .

Area A_1 is positive area as it is evaluated over $P_m \geq P_e$ and area A_2 is negative area as it is evaluated over the range $P_m \leq P_e$ in the P-δ curves. The EAC tells that for a system to be stable,

$$A_1 = A_2 \tag{2.11}$$

For out-of-step condition,

$$A_1 > A_2 \tag{2.12}$$

Based on the above equations, the EAC concept can be applied to detect out-of-step condition. However, this method not only requires local measurements but also requires the information from various locations within an area to find the equivalent machine parameters. This method requires P-δ curves for pre-disturbance and post-disturbance configuration and uses offline calculations to determine the curves. The details of this method and shortcomings associated with it are described in Sections 3.2 and 3.3. Modification of EAC from δ domain to time domain overcomes the shortcomings of this method and is the basis of my research. The modification of EAC in δ domain to time domain and a new algorithm for out-of-step detection based on modified EAC is reported in Section 3.4.

2.7. Summary

The power swing phenomenon and the variation of voltages and currents during the swing were studied. The power swing phenomenon was also studied in the complex impedance plane

which has given an insight of the swing impact on the operation of the distance relay. Also the impact of power swing on the operation of overcurrent relay was studied in the complex current plane. The basic functions that an out-of-step relay has to perform were discussed. Various techniques including rate of change of apparent impedance methods, SCV technique and technique based on fuzzy logic and neural networks were discussed and their shortcomings were pointed out.

CHAPTER 3
EQUAL AREA CRITERION (EAC) ALGORITHM

3.1. Introduction

The current practices for out-of-step detection and their shortcomings were discussed in the previous chapter. This chapter explains the EAC in power angle domain to describe the system stability. A method based on traditional EAC to detect out-of-step condition and the difficulties associated with it are also discussed. Starting from the swing equation, the expressions for EAC in time domain are derived and a new algorithm is proposed based on the expressions. The proposed algorithm is based on the power curves in the time domain, so detailed studies of the nature of the power curves are also done. The proposed algorithm is tested on a SMIB model using PSCAD™. The performance of the proposed algorithm is compared with an existing Blinder scheme for out-of-step detection.

3.2. System Stability and EAC

Power system stability refers to the ability of a power system to achieve a new steady state condition following a disturbance [20]. The new operating condition depends on the initial conditions and the nature of the disturbance [5]. Power systems undergo numerous small and large disturbances continuously. Power system stability can be classified into three broad categories: rotor angle stability, frequency stability and voltage stability. Small disturbance and transient stability comes under the rotor angle stability. The transient stability covers impacts of major disturbances such as faults, load changes, loss of generation etc [1].

The transient stability of a SMIB or a two-machine system is analyzed by solving the swing equation (Equation 3.1) [20].

$$\frac{d^2\delta}{dt^2} = \frac{\omega_s}{2H}(P_m - P_e(\delta)) = \frac{\omega_s}{2H}\Delta P \tag{3.1}$$

where H is the inertia constant, ω_s is the synchronous speed, δ is the rotor angle of the generator, P_m is the mechanical input power and P_e is the electrical output power. The solution of the equation gives the swing curve which is the plot of δ as a function of time. The analysis of the swing curve provides information about the stability of a system.

The swing equation is a non-linear second order differential equation so an analytical solution does not exist. Numerical techniques are therefore required to get the swing curves. EAC is an important concept which can be used to describe the stability of a system without solving the swing equation. EAC is described based on the areas under the power curves in P-δ plane [20]. The area under the power curve is analogous to energy so this concept is based on the energy balance in the system during the transient.

3.3. EAC in δ Domain

A two-machine or SMIB system to illustrate EAC in δ domain is shown in Figure 3.1. The generator and motor are connected by two parallel transmission lines with impedances X_1 and X_2 [1].

The generator voltage E_G is leading motor voltage E_M by phase angle δ. The power transferred from generator end to motor end is given by,

$$P_e = P_{\max} Sin\delta \tag{3.2}$$

where P_{max} is the maximum power that can be transferred between the generator and motor ends.

$$P_{\max} = \frac{E_G E_M}{X} \tag{3.3}$$

where X is the total impedance between the generator and motor ends.

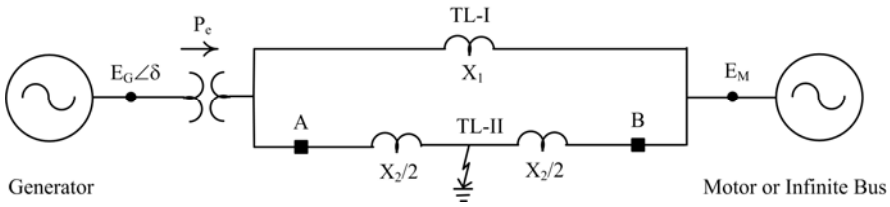

Figure 3.1 A two-machine system

The impedance between the generator and motor ends can vary for pre-fault, during fault and post-fault cases; the respective P-δ curves are shown in Figure 3.2. P_0 represents the pre-fault electrical output power corresponding to the power angle of δ_0.

3.3.1. EAC for a Stable System

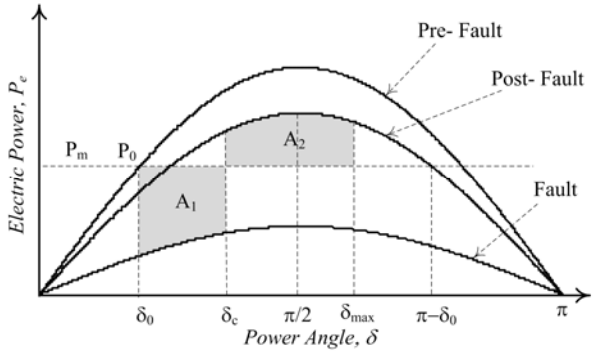

Figure 3.2 P-δ curves showing a stable condition

Figure 3.2 illustrates the application of EAC to analyze a stable case. At the pre-fault steady state, the input mechanical power is P_m and is equal to the output electrical power P_0 at power angle δ_0. When a fault is applied, the output electrical power suddenly drops and follows the P-δ curve for the fault case. After fault is cleared at δ_c, the electrical output power changes suddenly and follows the post-fault P-δ curve. The area A_1 in the Figure 3.2 represents the transient energy for $P_m \geq P_e$ and area A_2 represents transient energy for $P_m \leq P_e$. The maximum swing of power

angle (i.e. δ_{max}) can be found using the equal area concept i.e. areas A_1 and A_2 are equal. The expressions to evaluate area A_1 and A_2 are given by [20],

$$A_1 = \int_{\delta_0}^{\delta_c} \frac{\omega_s}{H}(P_m - P_e)d\delta \tag{3.4}$$

$$A_2 = \int_{\delta_c}^{\delta_{max}} \frac{\omega_s}{H}(P_m - P_e)d\delta \tag{3.5}$$

Thus for a stable system,

$$A_1 = A_2 \tag{3.6}$$

3.3.2. EAC for an Unstable System

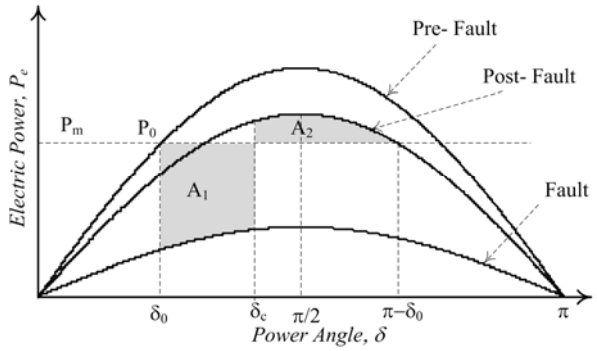

Figure 3.3 P-δ curves showing an unstable condition

Figure 3.3 shows a P-δ curve for a two-machine system to illustrate an unstable case. In an unstable case, the area A_1 is larger compared to the area A_2. The power angle δ swings up to δ_{max} where $\delta_{max}=\pi-\delta_0$. The expression for areas A_1 and A_2 are given in the following equations [20],

$$A_1 = \int_{\delta_0}^{\delta_c} \frac{\omega_s}{H}(P_m - P_e)d\delta \tag{3.7}$$

$$A_2 = \int_{\delta_c}^{\delta_{max}} \frac{\omega_s}{H}(P_m - P_e)d\delta \tag{3.8}$$

Thus for an unstable system,

$$A_1 > A_2 \tag{3.9}$$

3.3.3. Out-of-step Detection Using EAC in δ Domain

Reference [12] showed a method where EAC in δ domain is applied to detect the out-of-step condition. As already discussed in Section 3, the EAC in δ domain uses P-δ curves and Equations (3.4)-(3.9) to describe the stability of a system. Thus the method requires pre- and post-disturbance P-δ curves to be known to the out-of-step relay. The P-δ curves depend on the system configurations, and following are the key points of the above method to obtain system information.

- Outage of an important transmission line and other lines sufficiently important to affect the P-δ curves is communicated to the out-of-step relay.
- A significant outage is used to determine the post-clearing curve.
- In the case of loss of generation, the pre- and post- disturbance curves are the same and the mechanical input power changes by an unknown amount. The algorithm uses successive relative angle measurements to estimate the amount of change.
- Voltages, currents of various lines in the substation along with the status of key circuit breakers are communicated to the out-of-step relay.
- The two-machine equivalent of the power system is initialized to match the observed flow in the system.

The EAC has advantage over other techniques in that it is a graphical technique and gives more insight about the machine being stable or out-of-step. In [12], the EAC in the δ domain also needed the power system measurements from various locations along with the local

measurements at the relay location. The measurements include the parameters of various generators connected to an area and parameters of all interconnected transmission lines. These measurements are required to obtain the two-machine equivalent of the power system. The parameters of equivalent two-machine system (such as equivalent generator and equivalent transmission line parameters) are then used to obtain the P-δ curves by offline calculations. Thus the technique required many PMU and communication devices. One of the objectives of this research is to base the out-of-step protection technique only on local measurements.

As explained before, offline calculations are required for EAC in δ domain technique to evaluate P-δ curves. In power system, the offline calculations are usually done for transient stabilities studies (such as in power system security analysis). Reference [20] has shown an example of two-machine infinite bus system, where the offline studies are done to find the time domain solution of swing equation. In the example, P-t curves for two generators are determined by numerical integration technique and concluded that the one of the generator becomes out-of-step. But this kind of analysis for protection algorithm is not relevant because decision has to be made before the out-of-step condition harms the power system. The proposed algorithm has an advantage that it does not require any offline calculations.

3.4. EAC in Time Domain

The EAC concept in time domain is obtained from the swing equation. Integrating Equation (3.1) [21, 22],

$$\frac{d\delta}{dt} = \int \frac{\omega_s}{2H} \Delta P dt \tag{3.10}$$

Integrating Equation (3.10) from fault inception time t_0 to the fault clearing time t_c, we get

$$\left.\frac{d\delta}{dt}\right|_{t_c} - \left.\frac{d\delta}{dt}\right|_{t_0} = \int_{t_0}^{t_c} \frac{\omega_s}{2H} \Delta P dt \tag{3.11}$$

The speed deviation of the rotor is,

$$\omega_r = \omega(t) - \omega_s = \frac{d\delta}{dt} \tag{3.12}$$

In the region from t_0 to t_c where $P_m \geq P_e$, the expression for area A_1 using (3.11) and (3.12) is,

$$A_1 = \int_{t_0}^{t_c} \frac{\omega_s}{2H} \Delta P dt = \omega_{tc} - \omega_s \tag{3.13}$$

where ω_{tc} is the speed of the rotor at the fault clearing time. Integrating the Equation (3.10) from t_c to t_{max}, the time corresponding to the maximum swing of δ.

$$\left.\frac{d\delta}{dt}\right|_{t_{\max}} - \left.\frac{d\delta}{dt}\right|_{t_c} = \int_{t_c}^{t_{\max}} \frac{\omega_s}{2H} \Delta P dt \tag{3.14}$$

In the region from t_0 to t_{max}, where $P_m \leq P_e$, the expression for area A_2 is,

$$A_2 = \int_{t_c}^{t_{\max}} \frac{\omega_s}{2H} \Delta P dt = \omega_{\max} - \omega_{tc} \tag{3.15}$$

where ω_{max} represents the speed of the rotor at the maximum swing of δ (i.e. δ_{max}). At δ_{max}, the speed of the rotor (ω_{max}) becomes synchronous speed for a stable swing. Thus for a stable swing, the total transient energy from Equations (3.13) and (3.15) is,

$$A = A_1 + A_2 = \int_{t_0}^{t_c} \frac{\omega_s}{2H} \Delta P dt + \int_{t_c}^{t_{\max}} \frac{\omega_s}{2H} \Delta P dt = 0 \tag{3.16}$$

$$A = \int_{t_0}^{t_c} \Delta P dt + \int_{t_c}^{t_{\max}} \Delta P dt = 0 \tag{3.17}$$

For out-of-step condition, the speed ω_{max} at δ_{max} is super synchronous. From Equations (3.13) and (3.15), total transient energy is,

$$A = A_1 + A_2 = \int_{t_0}^{t_c} \frac{\omega_s}{2H} \Delta P dt + \int_{t_c}^{t_{max}} \frac{\omega_s}{2H} \Delta P dt > 0 \tag{3.18}$$

$$A = \int_{t_0}^{t_c} \Delta P dt + \int_{t_c}^{t_{max}} \Delta P dt > 0 \tag{3.19}$$

Equations (3.17) and (3.19) are the expressions for EAC in time domain which tells that during the transient, if area A_1 and A_2 are equal in a P-t curve, the system becomes stable. But if area A_1 becomes greater than area A_2, the system goes to an out-of-step condition. The area under the P-t curve represents energy, thus this concept can be referred to as the energy equilibrium criteria in time domain. A balance of transient energy results in a stable swing, whereas an unbalance of transient energy causes an out-of-step swing.

For implementing the above conditions as a relay algorithm, the integration is approximated by summation and P_m is set to P_e before the fault inception. The time limits are also expressed in terms of the conditions for P_e. Thus for a stable condition,

$$A = \sum_{t_0}^{t_{max}} (P_e\big|_{t_0 - \Delta t} - P_e(t)) \Delta t = 0 \tag{3.20}$$

For an out-of-step condition,

$$A = \sum_{t_0}^{t_{max}} (P_e\big|_{t_0 - \Delta t} - P_e(t)) \Delta t > 0 \tag{3.20}$$

where, t_0 : Time when $P_e(t)\big|_t < P_e(t)\big|_{t\ -\Delta t}$ first occurs and $t_{\max}$ is the time when $A\big|_t = 0$ (Stable) or the time when $P_e(t)\big|_{t-\Delta t} > P_e(t)\big|_{t_0 - \Delta t}$ and $P_e(t)\big|_t \le P_e(t)\big|_{t_0 - \Delta t}$ (out-of-step).

In Equations (3.20) and (3.21), Δt represents sampling interval. Equation (3.20) and the limit t_{max} for stable case need not always become exactly equal to zero because of the approximations made for the summation. To account for the inaccuracies in the summation, the

equation is modified as,

$$A = \sum_{t_0}^{t_{max}} (P_e(t)\big|_{t_0-\Delta t} - P_e(t))\Delta t \le 0 \qquad (3.22)$$

$t_{\max}$: Time when $A\big|_{t-\Delta t} > 0$ and $A\big|_t \le 0$ (Stable)

Equations (3.21), (3.22) alongwith the conditions for t_0 and t_{max} form the proposed algorithm for out-of-step detection. Based on the proposed algorithm, decision regarding stable or out-of-step condition is always made at t_{max} (time corresponding to δ_{max}) with an error of Δt or less. The algorithm depends only on P_e which can be obtained from the point where the out-of-step relay is installed. Thus, the proposed algorithm is entirely based on the local measurements. The flowchart of the proposed algorithm is shown in Figure 3.4.

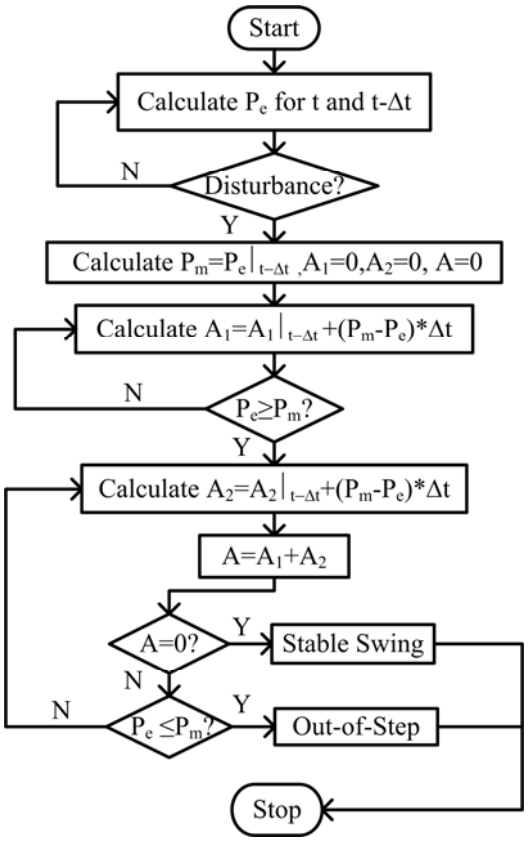

Figure 3.4 Flowchart of the proposed EAC algorithm in time domain

3.5. Power-time (P-t) Curves

This section explains the energy equilibrium criterion based on the P-t curves. The nature of P-t curve depends on the swing of δ after disturbance. For a stable system, δ can swing less than 90°, equal to 90° or more than 90°. For an unstable system, δ always swings beyond 90°. Therefore, in general three types of P-t curves are possible.

- P-t curve for a stable system with swing of $\delta \leq 90°$
- P-t curve for a stable system with swing of $\delta > 90°$
- P-t curve for an unstable system

3.5.1. P-t Curve for a Stable System with Swing of δ≤90°

A P-δ curve for a stable system with swing of $\delta < 90°$ is shown in Figure 3.5. During the transient process, the locus in P-δ plane follows the path 'a' to 'b' to 'c' to 'd' to 'e' to 'd'. Note that the swing is from 'd' to 'e' and back to'd' in the $P_m \leq P_e$ region. The point 'e' corresponds to the maximum swing of δ which is less than 90°. The maximum power during the transient occurs at δ_{max}. For this case, δ swings up to δ_{max} making area A_1 equal to the Area A_2.

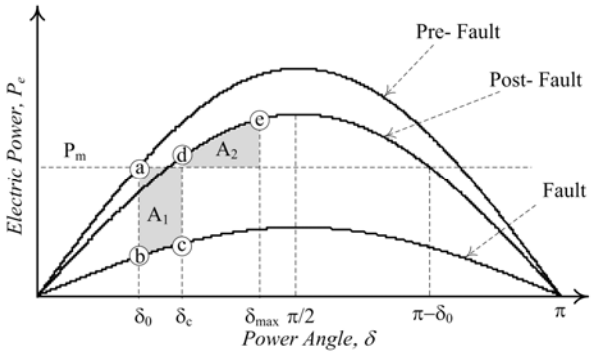

Figure 3.5 P-δ curves for a stable system with swing of $\delta < 90°$

The corresponding P-t curve for Figure 3.5 is shown in Figure 3.6. The analysis of the curve in $P_m \leq P_e$ region reveals that the P-t curve is one peaked (see point 'e') with the maximum value

of power corresponding to the maximum swing of $\delta=\delta_{max}$. The nature of P-t curve for a system with the maximum swing of $\delta=90°$ will be similar to Figure 3.6 except that the maximum power at point 'e' corresponds to the power at $\delta=90°$.

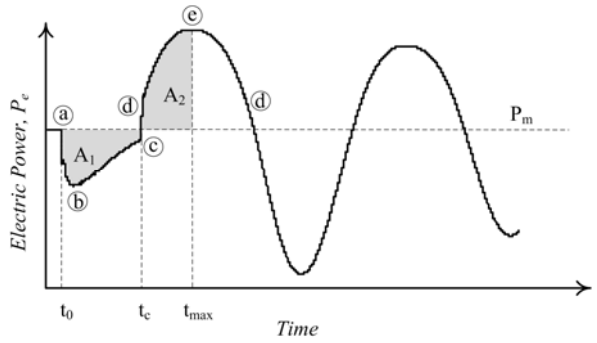

Figure 3.6 A P-t curve for a stable system with swing of $\delta \leq 90°$

3.5.2. P-t Curve for a Stable System with Swing of $\delta > 90°$

A P-δ curve for a stable system with $\delta > 90°$ is shown in Figure 3.7. After disturbance, the locus in P-δ plane follows the path 'a' to 'b' to 'c' to 'd' to 'e' to 'f' to 'e' to 'd'. Note that the locus crosses $\delta=90°$ at 'e', reaches upto 'f' and then swings backs to 'e'.

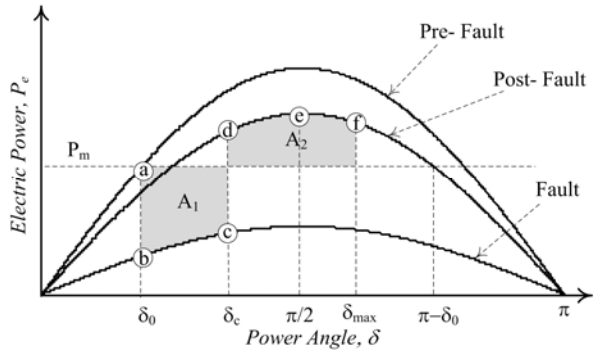

Figure 3.7 P-δ curves for a stable system with swing of $\delta > 90°$

The corresponding P-t curve for Figure 3.7 is shown in Figure 3.8. The P-t curve has two peaks in the $P_m \leq P_e$ region corresponding to the power at $\delta=90°$. The minimum power between the two peaks corresponds to the power at $\delta=\delta_{max}$.

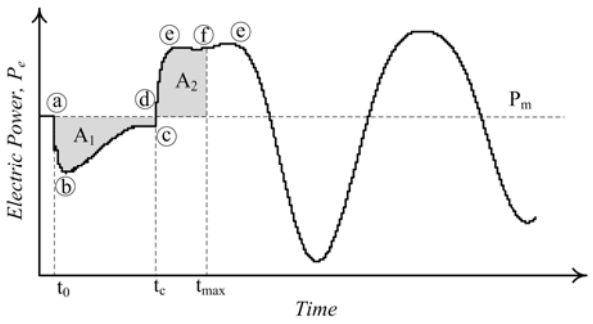

Figure 3.8 A P-t curve for a stable system with swing of $\delta > 90°$

3.5.3. P-t Curve for an Unstable System

A P-δ curve for an unstable system is shown in Figure 3.9. After a disturbance, the locus in P-δ plane follows the path 'a' to 'b' to 'c' to 'd' to 'e' to 'f' to 'g'. Note that the locus crosses $\delta=90°$ at 'e' and never swings back. For an unstable system, the A_2 is always less than the area A_1 [20] .

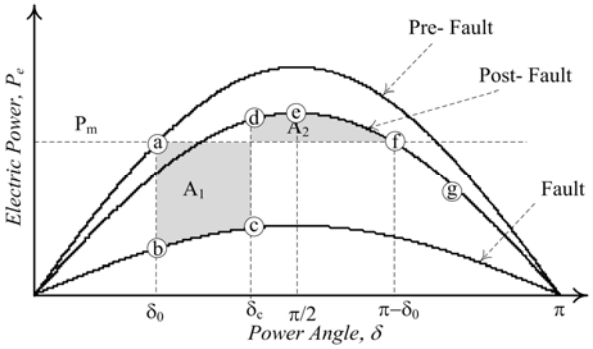

Figure 3.9 P-δ curves for an unstable system.

The corresponding P-t curve for the unstable system is shown in Figure 3.10. The maximum power corresponds to the power at $\delta=90°$. As mention earlier δ never swings back after it crosses $\delta=90°$.

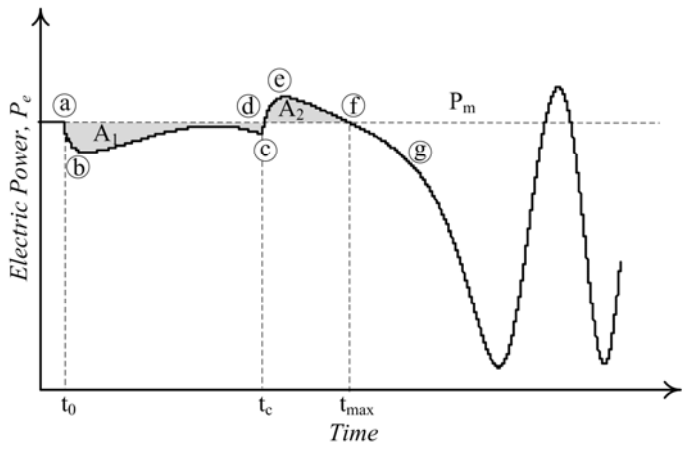

Figure 3.10 P-t curve for an unstable system.

In summary, a stable system can have one or two peaked power curves in the $P_m \leq P_e$ region. An unstable system always has one peaked P-t curve in $P_m \leq P_e$.

3.6. Case Studies-SMIB Simulations

A power system as shown in Figure 3.1 is used first to test the proposed algorithm for a SMIB system [1]. The system parameters are given in Appendix A. Different power swings are obtained by applying three phase fault at the middle of a transmission line (TL-II) and clearing the fault by opening the breakers A and B simultaneously at two ends of the transmission line. Stable and out-of-step swings are obtained by operating the power system at different pre-fault conditions and varying the fault duration time. PSCAD™ is chosen for the simulation and the PSCAD™ model of SMIB system is shown in Appendix B [23].

3.6.1. Stable Swings

Five different scenarios were used for the stable case studies. In the first case, small pre-fault load and small fault clearing time was used. In the successive cases, pre- fault load and fault clearing time were increased to obtain various stable swing scenarios. Figure 3.11 shows a case

with pre-fault δ=25° and the fault cleared after 10 cycles (0.167 s). The area A_1 is 0.035 pu-s. After 0.5 s, the total area A becomes zero. Thus this case is concluded as a stable swing.

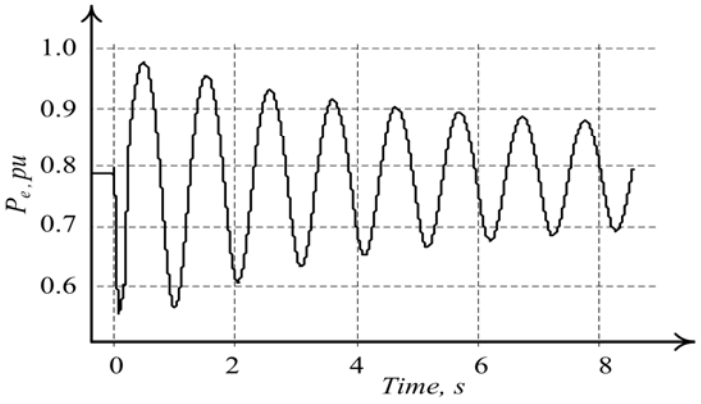

Figure 3.11 P-t curve for pre-fault δ=25° and cleared after 10 cycles

Figure 3.12 shows another simulation case in which the pre-fault δ is kept constant and the fault clearing time is increased to 12 cycles (0.2 s). As fault clearing time is more compared to the previous case, area A_1 (0.040 pu-s) is also more. So it takes 0.51 s to decide that it is a stable swing.

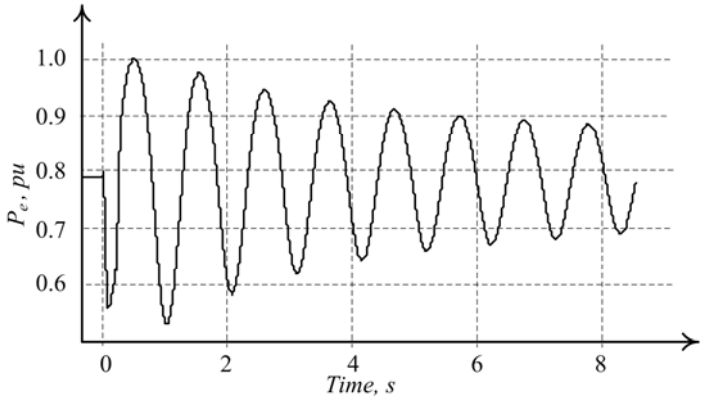

Figure 3.12 P-t curve for pre-fault δ=25° and cleared after 12 cycles

Next the pre-fault δ is increased to 30° and the fault is cleared after 8 cycles (0.133 s). The P-t curve is shown in Figure 3.13. Decision is made at 0.59 s that it is a stable swing.

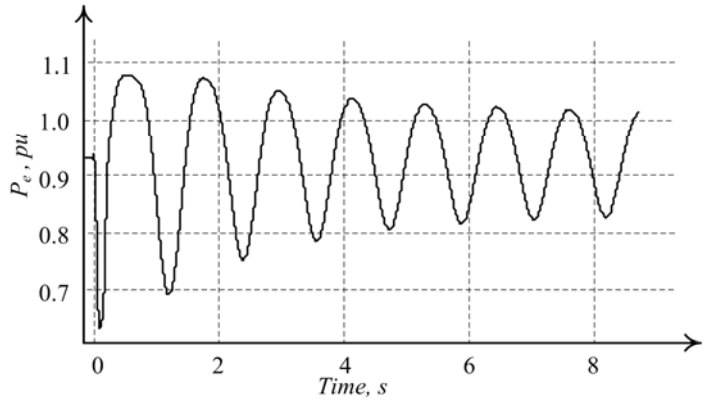

Figure 3.13 P-t curve for pre-fault δ=30° and cleared after 8 cycles

Keeping the pre-fault δ the same, next the fault clearing time is increased to 12 cycles (0.167 s). The area A_1 is more compared to the previous case, so it takes more time to make the decision. Figure 3.14 shows the P-t curve for this case. Decision is made that it is a stable swing at 0.64 s.

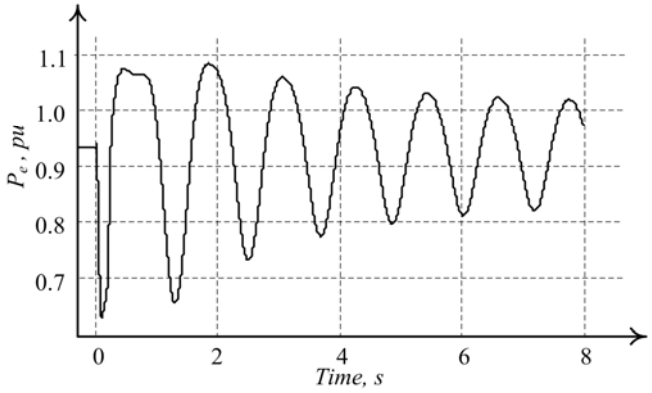

Figure 3.14 P-t curve for pre-fault δ=30° and cleared after 10 cycles

By further increasing the fault clearing time to 12 cycles (0.2 s), large oscillations in swing are observed as shown in Figure 3.15. It takes 0.85 s to decide the swing as a stable swing. The time taken is larger than the previous case because the area A_1 is increased. The results of the above five simulation cases are summarized in Table 3.1.

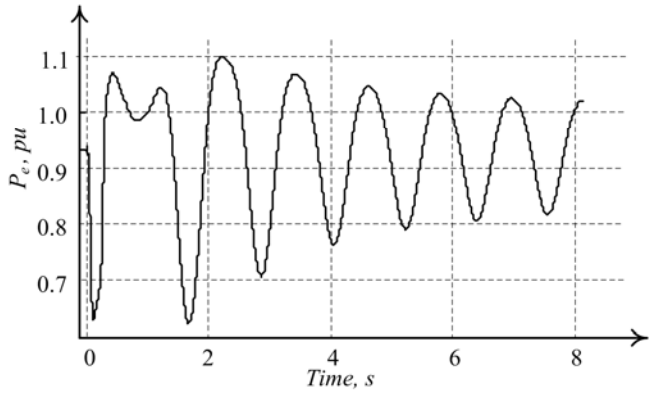

Figure 3.15 P-t curve for pre-fault δ=30° and cleared after 12 cycles

Table 3.1 Summary of simulation results for stable swings

Case	**1**	**2**	**3**	**4**	**5**
Power Angle(δ)	25°	25°	30°	30°	30°
Fault Duration Cycles	10	12	8	10	12
Fault Duration Time, s	0.167	0.20	0.133	0.167	0.20
Area A_1, pu-s	0.035	0.040	0.041	0.048	0.054
Area A_2, pu-s	-0.035	-0.040	-0.041	-0.048	-0.054
$A=A_1+A_2$	0	0	0	0	0
Decision Time, s	0.5	0.51	0.59	0.64	0.85
Swing Frequency, Hz	0.8-1.0				

Among the five stable cases, the P-t curves of the first three cases are one peaked in the $P_m \le P_e$ region. The P-t curves for the rest of the three cases are two peaked in $P_m \le P_e$ region. A P-t curve having two peaks in $P_m \le P_e$ region is always stable. The frequencies of the swings encountered during the simulation are in the range of 0.8 to 1 Hz.

3.6.2. Out-of-step Swings

Five different simulations are reported here to demonstrate the out-of-step detection using the proposed algorithm. Starting with the stable simulation cases, fault clearing time is increased to obtain out-of-step conditions. Figure 3.16 shows a P-t curve with pre-fault δ=30° and the fault is

cleared after 14 cycles (0.233 s).The area A_1 is 0.061 pu-s and the area A_2 is 0.027 pu-s. In the first swing, the total area calculated is not zero. So this is an out-of-step condition and decision is made in 0.598 s.

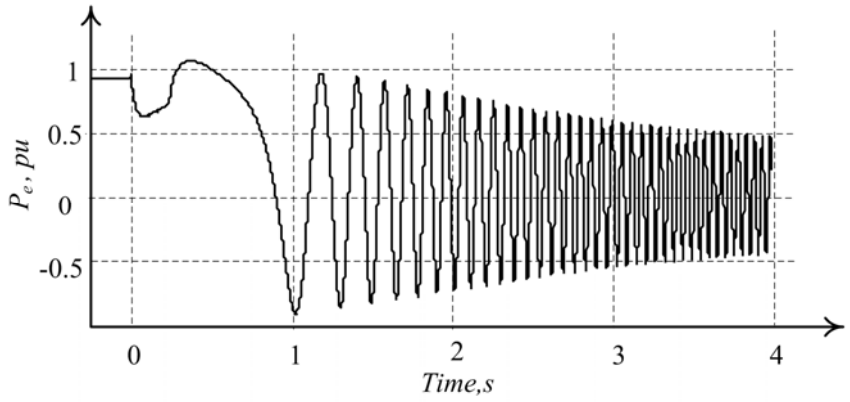

Figure 3.16 P-t curve for pre-fault δ=30° and cleared after 14 cycles

Figure 3.17 shows the P-t curve for a fault clearing time of 16 cycles (0.267 s). The area A_1 increases to 0.067 pu-s and out-of-step condition is detected at 0.504 s. Note that the decision made is faster compared to the previous case because area A_2 has reduced to 0.016 pu-s.

Figure 3.18 shows the P-t curve for another case with fault duration time of 18 cycles (0.3 s). The area A_1 increases to 0.073 pu-s and the area A_2 drops to 0.008 pu-s. The out-of-step decision is made at 0.466 s.

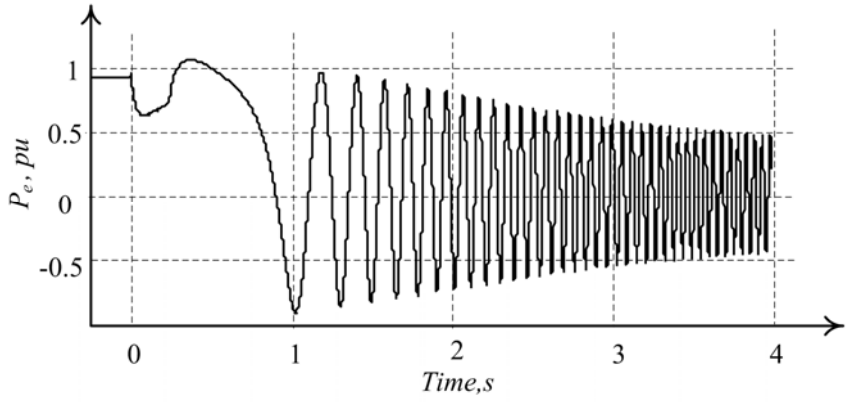

Figure 3.17 P-t curve for pre-fault δ=30° and cleared after 16 cycles

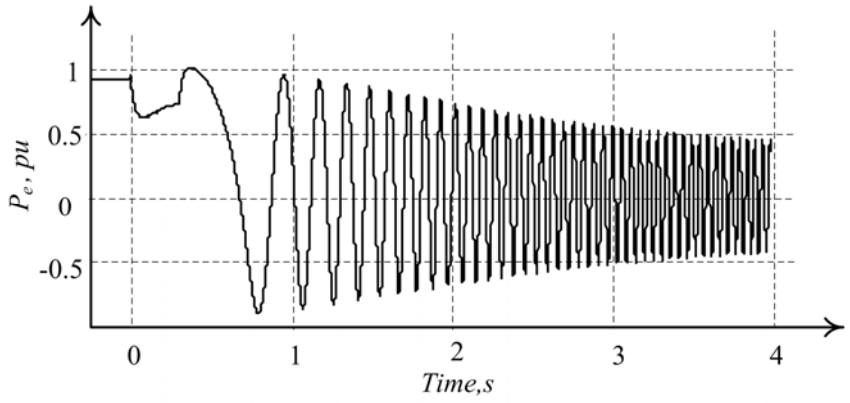

Figure 3.18 P-t curve for pre-fault at δ=30° and cleared after 18 cycles

In another study, the pre-fault δ is increased to 35° and the two simulations are carried out with fault duration times of 8 and 10 cycles. When the fault duration time is 8 cycles (0.133 s), the area A_1 is 0.050 pu-s and the area A_2 is 0.031 pu-s. The out-of-step is detected at 0.76 s and the total area is 0.019 pu-s. The P-t for this case is shown in Figure 3.19.

In the second case, fault duration time is 10 cycles (0.167 s) which results on larger area A_1 of 0.057 pu-s. The area A_2 is 0.019 pu-s, which is smaller compared to the previous case. It takes 0.554 s to make the decision that it is out-of-step. The decision is made faster compared to previous case. The P-t for this case is shown in Figure 3.19. The simulation results are summarized in Table 3.2.

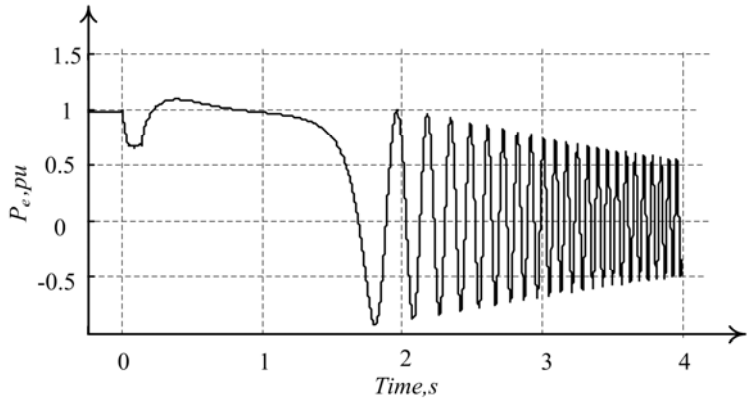

Figure 3.19 P-t curve for pre-fault δ=35° and cleared after 8 cycles

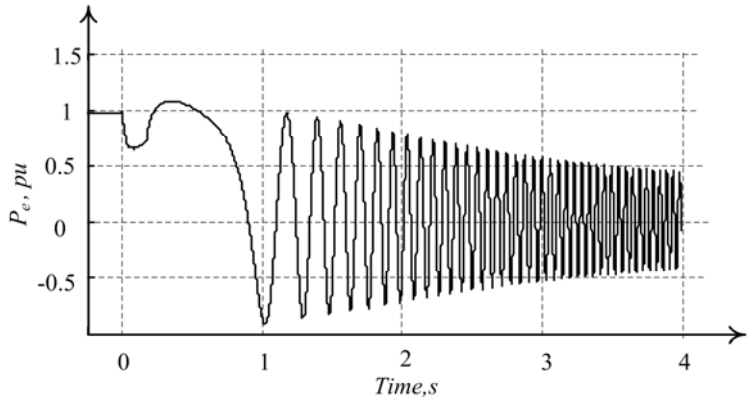

Figure 3.20 P-t curve for fault applied δ=35° and cleared after 10 cycles

Table 3.2 Summary of simulation results for out-of-step condition

Case	**6**	**7**	**8**	**9**	**10**
Power Angle(δ)	30°	30°	30°	35°	35°
Fault Duration Cycles	14	16	18	8	10
Fault Duration Time, s	0.233	0.267	0.30	0.133	0.167
Area A_1, pu-s	0.061	0.067	0.073	0.050	0.057
Area A_2, pu-s	-0.027	-0.016	-0.008	-0.031	-0.019
$A=A_1+A_2$	0.033	0.051	0.065	0.019	0.038
Decision Time, s	0.598	0.504	0.466	0.760	0.554
Swing Frequency, Hz	4-6				

Overall the analysis of the P-t curves shows that the out-of-step curves are one peaked curves in the $P_m \leq P_e$ region. The frequency of swing measured in these simulations is in the range of 4-6 Hz. For the kind of synchronous machine that is used in the simulation it is not possible to get swing frequencies larger than 6 Hz. As the proposed algorithm is based on only the areas, the swing frequency should not affect the accuracy of the algorithm. Therefore this algorithm will work for larger frequency of swings as well.

3.6.3. Comment on the Decision Time

This section explains the effect of disturbance on areas A_1 and A_2 of P-t curve and in decision making. Comparison is done based on the simulations carried out in the previous sections for pre-fault $\delta = 30°$. Decision times for various faults clearing cycles are listed in Table 3.3.

Table 3.3 Summary of simulation results to compare the decision time

Case	**3**	**4**	**5**	**6**	**7**	**8**
Power Angle (δ)	30°	30°	30°	30°	30°	30°
Fault Duration Cycles	8	10	12	14	16	18
Fault Duration Time, s	0.133	0.167	0.20	0.23	0.26	0.30
Area A_1, pu-s	0.041	0.048	0.054	0.061	0.067	0.073
Area A_2, pu-s	-0.041	-0.048	-0.054	-0.027	-0.016	-0.008
Decision Time, s	0.59	0.64	0.85	0.598	0.504	0.466
Decision	Stable	Stable	Stable	Out-of-step	Out-of-step	Out-of-step

In Table 3.3, Cases 1 through 3 are for stable swing and Cases 4 through 6 are for out-of-step condition. For stable cases, when the fault duration time is increased from 8 to 12 cycles, the area A_1 increases from 0.041 to 0.054 pu-s. Larger the area A_1, the larger will be the area A_2 required to make the total area to zero. So the time taken to make a decision increases from 0.6 s to 0.85 s. For out-of-step condition, the area A_1 increases from 0.061 to 0.073 pu-s. But the area A_2 decreases from 0.027 to 0.008 pu-s. It requires less time to calculate the area A_2. This reduces the decision time from 0.6 s to 0.47 s.

Stable swings with smaller oscillations are obtained when pre-fault δ is small and the fault is cleared as quickly as possible. The area A_1 for such stable swings becomes less (see Figure 3.11). It is not necessary to wait longer in the $P_m \leq P_e$ region to obtain the total area equal to zero. Thus the algorithm is able to make the decisions quickly. For out-of-step condition with larger pre-fault load and larger fault duration, the area A_1 becomes large but the area A_2 becomes

very small. So the decision still can be made quickly. But when the swing is marginally stable or marginally unstable, the area A_1 as well as area A_2 becomes comparable so it takes more time to make the decision.

3.6.4. Comparison with a Blinder Scheme

It is very useful while proposing a new relaying algorithm for protection to compare it with a standard practice available in literature for relaying. The performance of proposed out-of-step detection algorithm is compared with the Blinder scheme (concentric rectangle scheme) discussed in Section 2.4. Figure 3.21 shows a concentric rectangle scheme in which time taken by impedance seen by the relay to traverse inner and outer rectangles is compared with the pre-set time to discriminate between fault and the swing. If the swing locus traverses inner and outer rectangles in less than the pre-set time, the disturbance is a fault. If the locus enters the outer rectangle and takes more than pre-set time to cross inner rectangle, then it is an out-of-step condition. If the swing locus crosses outer rectangle but does not cross the inner rectangle, the swing is a stable swing [15].

For performance comparison an impedance relay with concentric rectangle schemes is located at one end of the TL-I (Figure 3.1) which protects 80% of the line. Power swing in TL-I is achieved by applying fault at the middle of TL-II and opening breakers A and B simultaneously with time delay. Detailed guidelines used for relay settings are described in [15]. A brief explanation of the procedure is provided in Appendix C.

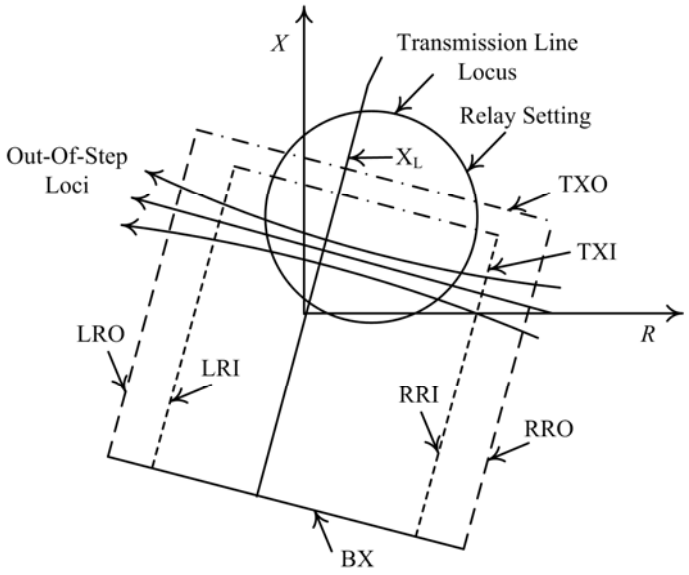

Figure 3.21 Blinder settings for out-of-step detection

In Fig. 3.21,

Right Resistance-Inner (RRI) =0.3 p.u

Right Resistance-Outer (RRO) =0.4p.u

Left Resistance-Outer (LRI) =-0.3 p.u

Left Resistance-Inner (LRO) =-0.4 p.u

Top Reactance-Inner (TXI) =0.2 p.u

Top Reactance-Outer (TXO) =0.3 p.u

Bottom Reactance (BX) =-1.94 p.u

Using the above settings, different simulations are carried out for comparing the proposed algorithm with concentric rectangle scheme just described.

In first simulation pre-fault power angle is set $\delta=30°$ and the fault clearing time is set to 14 cycles (0.233 s). To detect that the system is out-of-step, concentric rectangular scheme takes 4.93 s. The locus of swing is shown in Figure 3.22. The swing alone takes 27.5 cycles (0.458 s)

to traverse the two concentric rectangles. For this case, the proposed algorithm takes 0.6 s to detect that it is out-of-step.

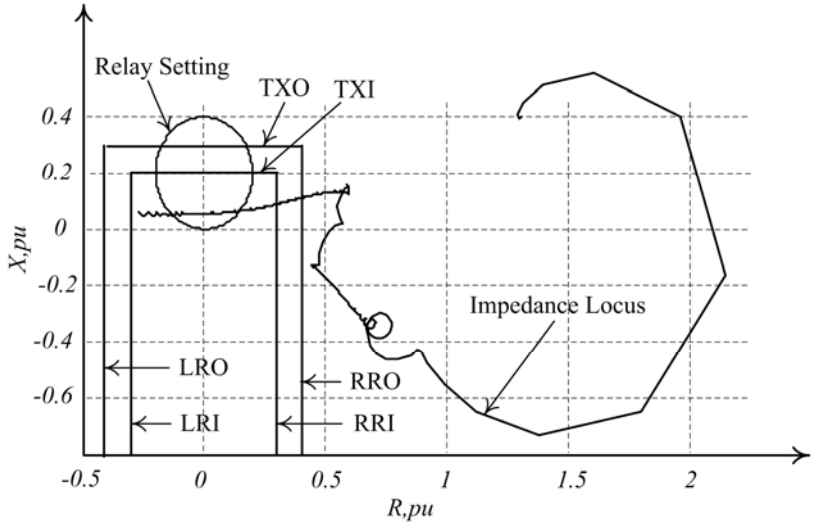

Figure 3.22 Out-of-step locus for fault duration 12 cycles and δ=30°

In the next case, fault clearing time is increased to 16 cycles (0.26 s). The swing locus takes 20.98 cycles (0.349 s) to completely traverse the two concentric rectangles and the decision that it is out-of-step is obtained at 4.70 s, whereas the proposed algorithm only takes 0.5 s to make the decision. Increasing the fault clearing time makes the swing more severe, thus the swing locus traverses the two rectangles in 17.37 cycles (0.289 s). The concentric rectangle scheme takes 4.58 s whereas the proposed algorithm takes 0.47 s to make the decision. The results are summarized in Table 3.4.

Table 3.4 Comparison of EAC algorithm and concentric rectangle schemes

Case	**6**	**7**	**8**
Pre-fault power Angle (δ)	30°	30°	30°
Fault Duration Cycles	14	16	18
Fault Duration Time, s	0.23	0.26	0.30
Decision Time (Rectangles), s	4.93	4.70	4.58
Decision Time (Proposed Algorithm),s	0.60	0.50	0.47

The simulations show that the proposed algorithm is accurate and much faster than the standard concentric rectangular scheme. Note that the decision time for a concentric rectangular scheme depends on the guidelines used for the relay settings. Besides, finding the required settings for concentric rectangular method is not straightforward. It depends on the system parameters whereas the proposed algorithm is independent of the system parameters, which is quite a useful advantage.

3.7. Summary

The modification of EAC from power angle domain to time domain makes the out-of-step algorithm simpler and easier. It avoids the need for system studies as it just needs the information of active power flowing in the system. The simulations showed accurate results to detect stable and out-of-step condition in a SMIB power system. Comparisons made with the existing blinder technique showed that the proposed algorithm is faster. The algorithm took more time to decide marginally stable and unstable cases. The simulation result showed that the algorithm is applicable to all swing frequencies.

CHAPTER 4
EAC IN TIME DOMAIN APPLIED TO MULTIMACHINE SYSTEM

4.1. Introduction

In this chapter, first the current practices for out-of-step detection in a multi-machine system and the difficulties associated with those techniques are discussed. Next the proposed EAC algorithm in time domain is presented for a multimachine configuration. A two machine infinite bus, three machine infinite bus, and a 17-bus multimachine system are modeled in PSCAD™ for testing the proposed algorithm. The algorithm is tested for various transient scenarios and the simulation results and the analyses are presented.

4.2. Multimachine Out-of-step Detection

As the number of interconnected systems increase, the modeling sophistication increases as well. Numerical integration techniques are useful to analyze the stability of a larger system but as the size of the systems increase, the number of computations needed become very large [5]. A number of techniques currently exist in practice which analyze the stability of a multimachine system and give the critical clearing time without numerical computation. The Transient Energy Function (TEF) method is one of the methods which gives the critical clearing time directly [5, 24]. However this technique requires reduction of the system to an equivalent two machine system and therefore the implementation of this technique as an out-of-step algorithm is not straightforward. The out-of-step detection practices were discussed in Section 2.6. In literature [8, 15], the Blinder schemes and SCV technique are explained basically for a two machine equivalent system. Reference [15] listed the guidelines for relay settings using the Blinder

scheme for a two area system. The SCV technique discussed in [8] tracked the swing centre of a two source equivalent system. A multimachine system can be reduced to an equivalent two area system using Centre of Inertia (COI) or Centre of Angle (COA) technique [5, 24, 25], and the algorithms proposed for two area system can be implemented. However, for a multimachine configuration, implementation of the above techniques is not clear-cut as a two area system.

Reference [12] described an EAC in δ domain which can be applied to a multimachine configuration but this method also required COI or COA reduction technique to obtain the equivalent two area system. To obtain an equivalent two area system, this method needed many communication and PMU devices to gather information from other buses of the system.

The algorithm based on Fuzzy Logic is also explained for a two area system [13]. To extend this method to a multimachine system, an enormous amount of offline calculations and simulations will be required. Reference [14] proposed a technique based on Neural Networks for out-of-step detection on a 9-bus multimachine system. This technique required extensive offline simulations for training.

The proposed EAC algorithm in time domain only requires calculation of the electric power of the machines during the transients. The concept is similar to a SMIB configuration, thus it does not require the system to be reduced to a two area system. It can be applied directly to any multimachine configuration.

4.3. Proposed Algorithm for Multimachine System

The same equations (Equations 3.21 and 3.22) as obtained in the Section 3.4 are used for the multimachine out-of-step detection. The P-t curves of all the interconnected machines are monitored. The flowchart of the algorithm is similar to a SMIB system as shown in Figure 3.4 except that in the multimachine system, the algorithm is applied to all the connected machines.

4.4. Case Studies- A Two Machine Infinite Bus System

The effectiveness of the proposed algorithm is first tested on a two machine infinite bus system. Figure 4.1 shows the network configuration of the system and its parameters are listed in Appendix D. The out-of-step relay is installed to detect the out-of-step condition of generator (Gen2) as shown in Figure 4.1. The proposed algorithm is applied to the P-t curve of Gen2.

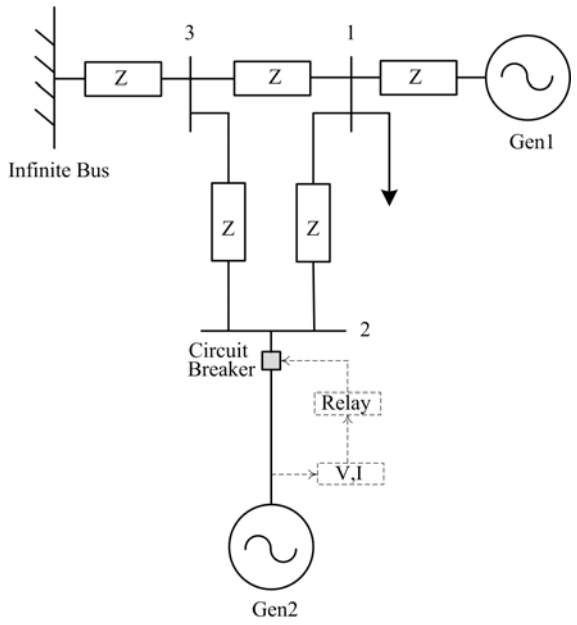

Figure 4.1 A two machine infinite bus system

4.4.1. Stable Cases

Two simulation cases are described for the stable case studies. In the first case, the total load in the system is 0.892 pu. A three phase fault is applied at Bus 1 and cleared after 0.1 s. The P-t curves of both the generators are shown in Figure 4.2. From the P-t curve of Gen2, the area A_1 is 0.0601 pu-s. After 0.281 s, the total area A becomes zero. Thus this case is concluded as a stable swing.

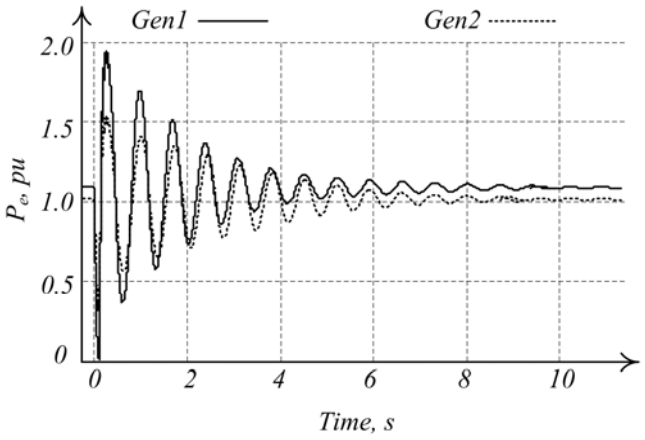

Figure 4.2 P-t curves for pre-fault load of 0.892 pu and fault cleared after 0.1 s

In the next simulation, the total load in the system is set at 1.761 pu and the fault is cleared after 0.1 s. The P-t curves for both generators are shown in Figure 4.3. From the Gen2's P-t curve, the area A_1 is found to be 0.0778 pu-s. The case is decided as stable case at 0.303 s when the total area becomes zero.

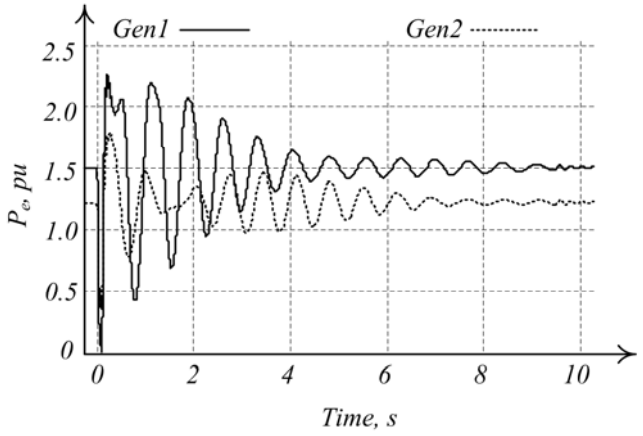

Figure 4.3 P-t curves for pre-fault load of 1.761 pu and fault cleared after 0.1 s

4.4.2. Out-of-step Cases

Two simulations are presented for the out-of-step condition. In the first simulation case, the total load in the system is set to 0.892 pu. A three phase fault is applied at Bus 1 and cleared after 0.25 s. The P-t curves for this simulation case are shown in Figure 4.4. In Gen2's P-t curve, the

area A_1 is 0.1511 pu-s and the area A_2 is 0.0231 pu-s. In the first swing, the total area calculated is 0.1280 pu-s. So this is an out-of-step condition and the decision is made at 0.368 s.

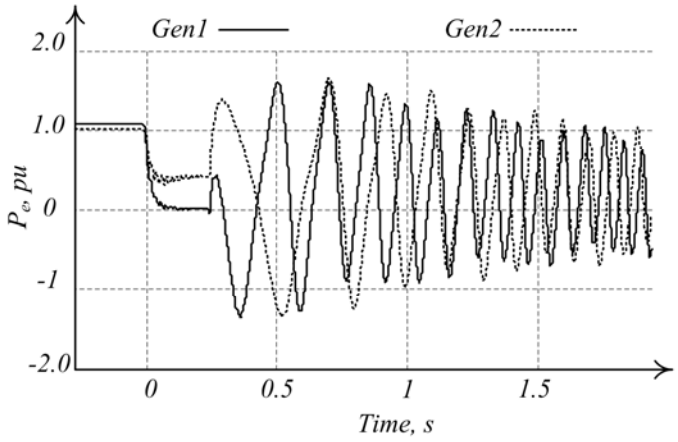

Figure 4.4 P-t curves for pre-fault load of 0.892 pu and fault cleared after 0.25 s

Figure 4.5 shows the P-t curve for another out-of-step simulation case. The total load is 1.761 pu and the fault is cleared after 0.25 s. In the Gen2's P-t curve, the area A_1 is 0.1404 pu-s and out-of-step condition is detected at 0.339 s when the area A_2 is 0.0338 pu-s. Summary of stable and out-of-step condition simulation results for the two machine infinite bus system are listed in Table 4.1.

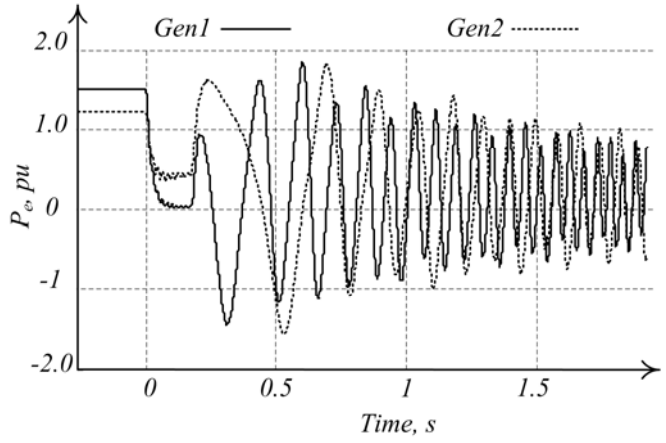

Figure 4.5 P-t curves for pre-fault load of 1.761 pu and fault cleared after 0.25 s

Table 4.1 Summary of simulation results for two machine infinite bus system.

Case	1	2	3	4
Pre-fault Load, pu	0.892	1.761	0.892	1.761
Fault Duration Time, s	0.1	0.1	0.25	0.25
Area (A_1), pu-s	0.0601	0.0778	0.1511	0.1404
Area (A_2), pu-s	-0.0601	-0.0778	-0.0231	-0.0338
$A=A_1+A_2$	0	0	0.1280	0.1066
Decision Time, s	0.281	0.303	0.368	0.339
Decision	Stable	Stable	Out-of-step	Out-of-step

4.5. Case Studies- A Three Machine Infinite Bus System

A three machine infinite bus system as shown in Figure 4.6 is considered to illustrate the effectiveness of the algorithm in a more complex power system. The parameters of the system are given in Appendix D. The out-of-step relay is installed to detect the out-of-step condition of generator (Gen2) as shown in Figure 4.6. The proposed algorithm is applied to the P-t curve of Gen2.

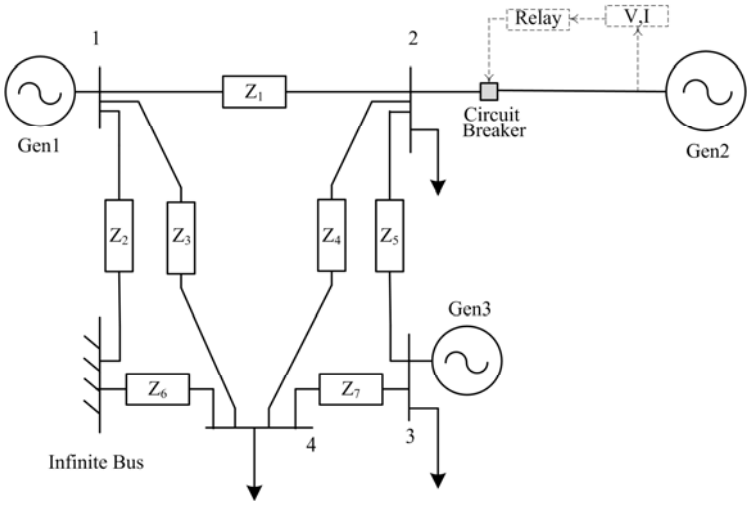

Figure 4.6 A three machine infinite bus system

4.5.1. Stable Cases

For the first simulation, three phase fault is applied at Bus 1. The pre-fault load is 1.569 pu and fault duration is 0.1 s. The P-t curves for the three generators are shown in Figure 4.7. From

the P-t curve of Gen2, the area A_1 is found to be 0.0895 pu-s. At 0.346 s, the total area becomes zero and a stable swing is decided.

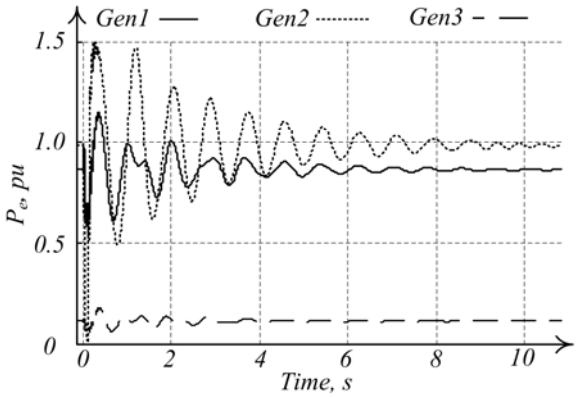

Figure 4.7 P-t curves for pre-fault load of 1.596 pu and fault cleared after 0.1 s

The pre-fault load in the system is set at 1.2189 pu. Three phase fault is applied at Bus 1 and the fault is cleared after 0.25 s. The P-t curves for this case are shown in Figure 4.8. From the P-t curve of Gen2, the area A_1 is found to be 0.2127 pu-s and the total area is zero at 0.519 s. This case is decided as a stable swing.

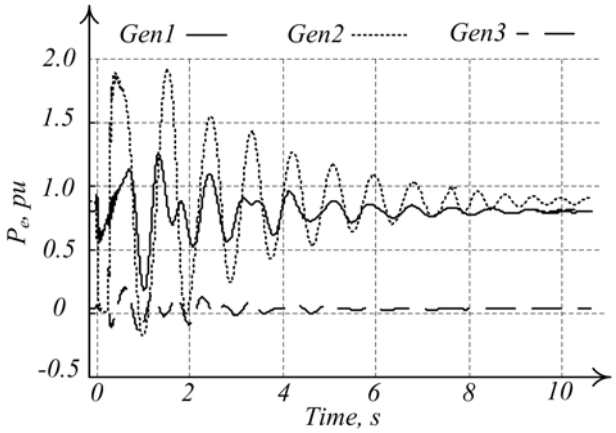

Figure 4.8 P-t curves for pre-fault load of 1.2189 pu and fault cleared after 0.25 s

4.5.2. Out-of-step Cases

Two simulations are shown here to detect the out-of-step condition using the proposed technique. In the first simulation, the pre-fault load in the system is set at 1.569 pu, a three phase

fault is applied at Bus 1 and cleared after 0.25 s. The P-t curves for this simulation are shown in Figure 4.9. From the P-t curve of Gen2, the area A_1 is 0.2391 pu-s and the A_2 area is 0.1204 pu-s. This case is decided as an out-of-step condition at 0.536 s when the total area is 0.1187 pu-s.

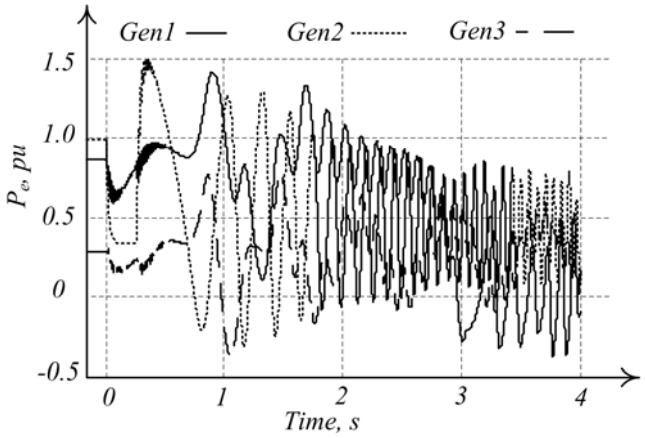

Figure 4.9 P-t curves for pre-fault load of 1.596 pu and fault cleared after 0.25 s

In the next simulation, the pre-fault total load is set at 1.2189 pu. Three phase fault is applied at the Bus 1 and cleared after 0.30 s. Figure 4.10 shows the P-t curves for this case. From the P-t curve of Gen2, the area A_1 is 0.2531 pu-s and the area A_2 is 0.0774 pu-s. This case is decided as an out-of-step condition at 0.50 s when the total area is 0.1789 pu-s. Summary of stable and out-of-step condition simulations for a three machine infinite bus system are listed in Table 4.2.

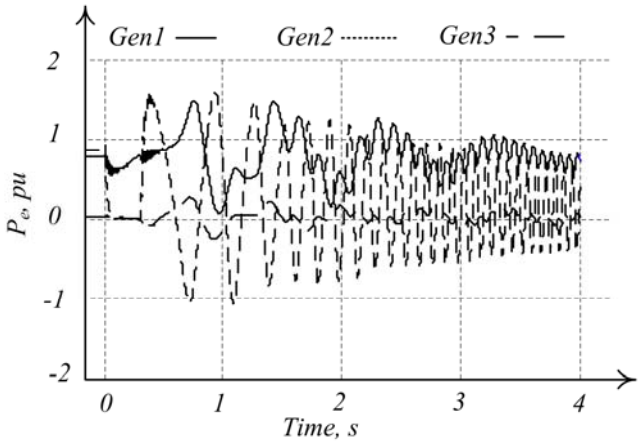

Figure 4.10 P-t curves for pre-fault load of 1.2189 pu and fault cleared after 0.30 s

Table 4.2 Summary of simulation results for three machine infinite bus system.

Case	**5**	**6**	**7**	**8**
Pre-fault Load, pu	1.569	1.2189	1.569	1.2189
Fault Duration Time, s	0.1	0.25	0.25	0.30
Area (A_1), pu-s	0.0895	0.2127	0.2391	0.2531
Area (A_2), pu-s	-0.0895	-0.2127	-0.1204	-0.0774
$A=A_1+A_2$	0	0	0.1187	0.1789
Decision Time, s	0.346	0.519	0.536	0.500
Decision	Stable	Stable	Out-of-step	Out-of-step

4.6. Case Studies- A 17 Bus Multimachine System

A power system as shown in Figure 4.11 is considered for testing the proposed algorithm in a multimachine system. The power system has 17 buses (B1-B17), 8 transformers (Tr1-Tr8) and 14 transmission lines (T1-T13). The system has two synchronous generators (Gen1 and Gen2), two motor loads (M1 and M2) and four static loads (L1-L4). The details of the power system parameters are given in Appendix E. The PSCAD™ model is given in Appendix F.

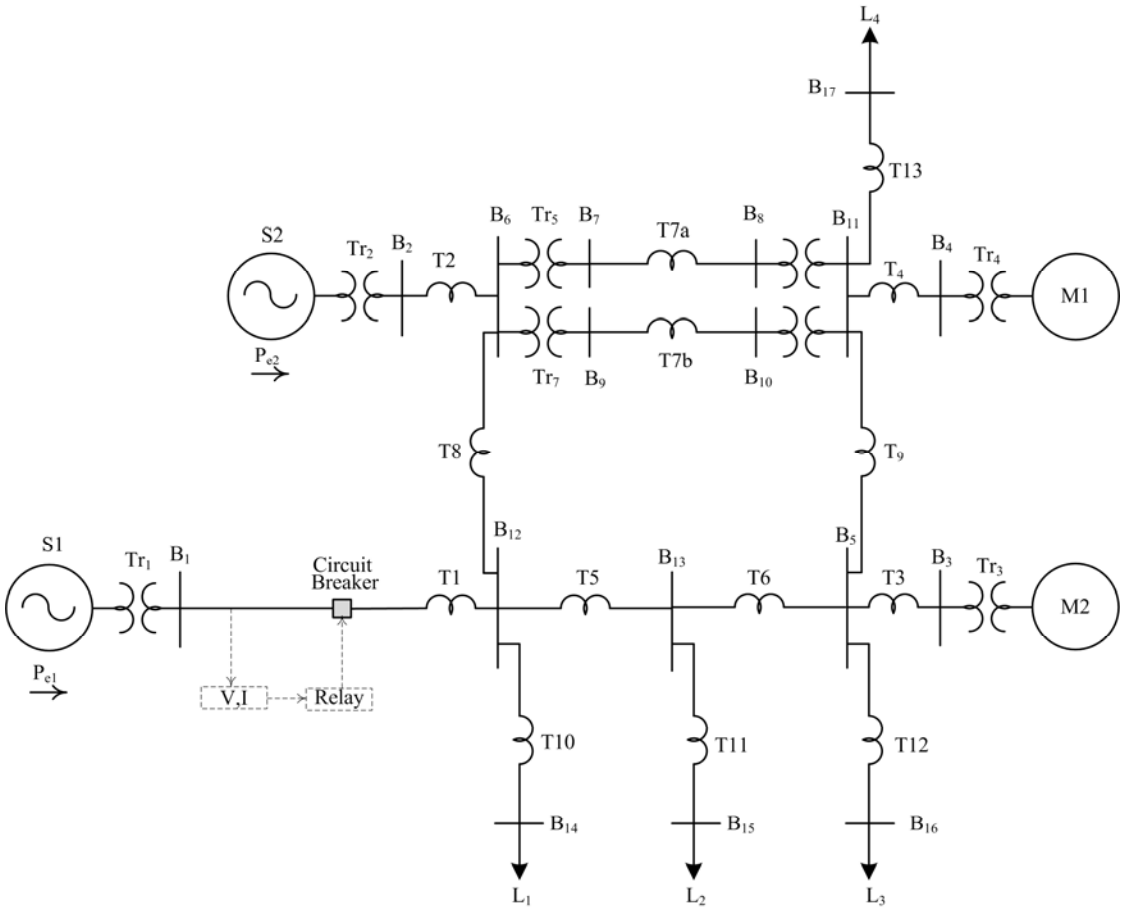

Figure 4.11 A 17-bus multimachine power system

Various simulations are carried out with three phase fault applied at the middle of the transmission lines T5, T7a, T9. Fault clearing times and the total system load are varied to obtain various natures of stable and out-of-step swings. Figure 4.12 through Figure 4.47 shows the P-t curves of generators Gen1 and Gen2 for different swing conditions. In all Figures, Pe_1 and Pe_2 represent the power output (i.e. P-t curve) of generator Gen1 and Gen2, respectively. An out-of-step relay is located to protect the system from out-of-step condition in Gen1 as shown in Figure 4.11. The proposed algorithm is applied to the P-t curve of Gen1. The simulation results are presented in the following sub-sections.

4.6.1. Multimachine Simulations with No Motor Impact

In the first set of simulations, the electric power output of the generators Gen1 and Gen2 are set at 0.977 and 0.46 pu respectively, which supply the total system load of 1.437 pu. The two motors M1 and M2 are replaced by equivalent static loads. Three phase fault is applied at the middle of the transmission line (T5). Figure 4.12 shows a stable case where the fault duration time is set at 0.06 s.

Area (A_1) = 0.0581 pu-s

Area (A_2) =-0.0581 pu-s

Total area (A) =A_1+A_2 = 0 at 0.582 s

Decision = Stable

Decision time = 0.582 s

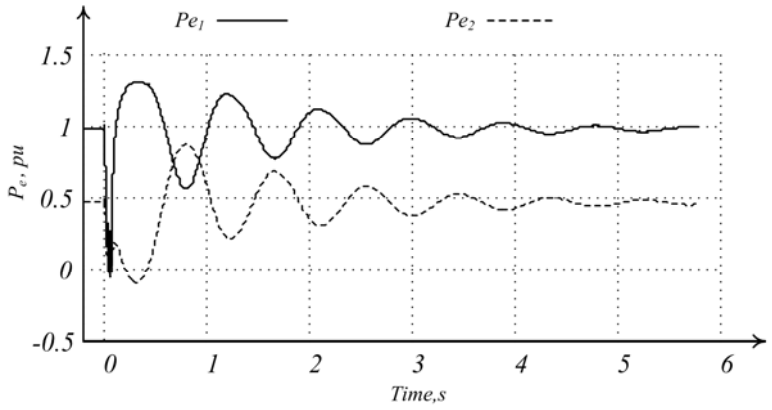

Figure 4.12 P-t curves for fault applied at the middle of T5 and cleared after 0.06 s

Figure 4.13 shows P-t curves for another stable case where the total system load and fault location is kept the same as before but the fault duration time is increased to 0.105 s. The areas calculated, the decisions made and the decision times are summarized in Table 4.3.

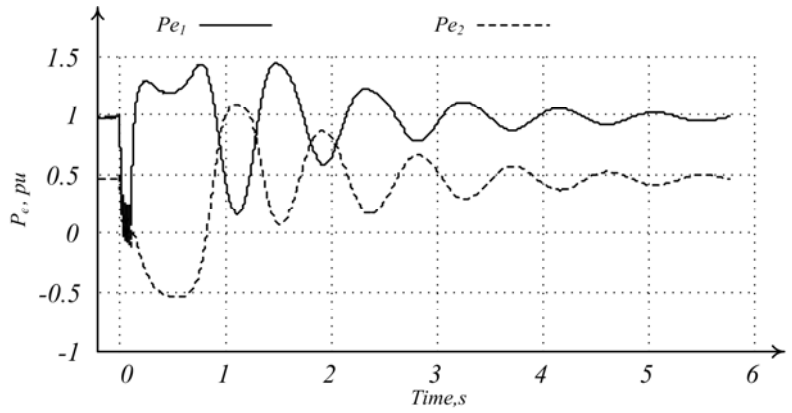

Figure 4.13 P-t curves for fault applied at the middle of T5 and cleared after 0.105 s

When the fault duration time is increased to 0.106 s, the system goes to an out-of-step condition. The P-t curves are shown in Figure 4.14. The areas and the decision times obtained in this case are as follows,

Area (A_1) = 0.0975 pu-s

Area (A_2) =-0.0827 pu-s

Total area (A) =A_1+A_2 =0.0148 at 1.1331 s

Decision = Out-of-step

Decision time = 1.1331 s

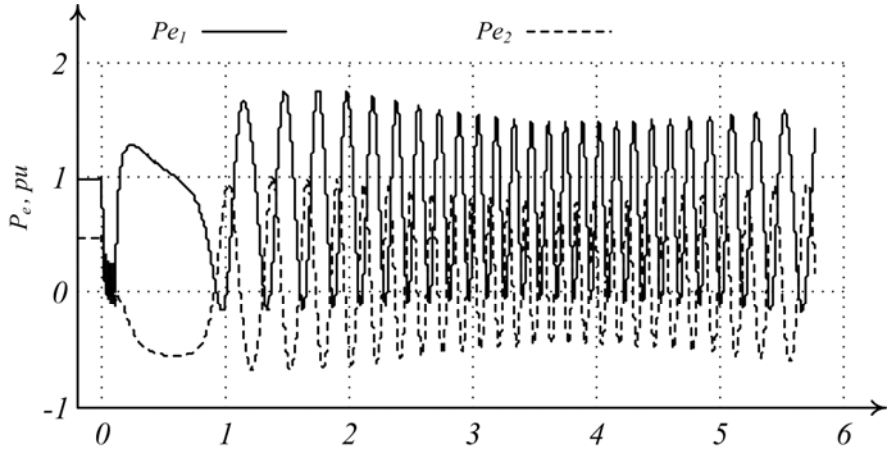

Figure 4.14 P-t curves for fault applied at the middle of T5 and cleared after 0.106 s

Next, the fault duration time is increased to 0.12 s to simulate a more severe out-of-step case. The P-t curves are shown in Figure 4.15 and the simulation results are listed in Table 4.3.

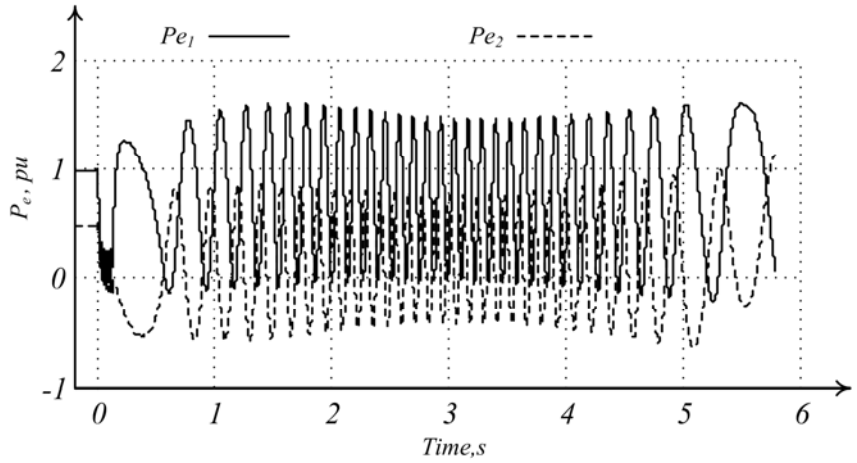

Figure 4.15 P-t curves for fault applied at the middle of T5 and cleared after 0.12 s

Table 4.3 Summary of simulation results for fault applied at the middle of the transmission line T5, total system load of 1.437 pu and considering no motor impact.

Case	**9**	**10**	**11**	**12**
Fault duration time, s	0.0600	0.1050	0.1060	0.1200
Area (A_1), pu-s	0.0581	0.0941	0.0975	0.1070
Area (A_2), pu-s	-0.0581	-0.0941	-0.0827	-0.0438
Area A_1+A_2, pu-s	0	0	0.0148	0.0632
Decision time, s	0.582	1.0366	1.1331	0.8951
Decision	Stable	Stable	Out-of-step	Out-of-step

The location of the fault is changed to the middle of the transmission line (T7a) and the output of Gen1 and Gen2 are set at 0.9528 and 0.4464 pu, respectively. The two generators are supplying total system load of 1.3992 pu. Fault duration time is set at four different values to obtain different natures of stable and out-of-step swings. Figure 4.16 and 4.17 shows stable swings with fault duration times of 0.08 and 0.131 s, respectively. In the next case, the fault duration time is increased to 0.132 s and an out-of-step swing is observed. The P-t curve for this case is shown in Figure 4.18. A more severe out-of-step case is shown in Figure 4.19 with the

fault duration time of 0.14 s. The areas calculated and the decision times and the decisions are listed in Table 4.4.

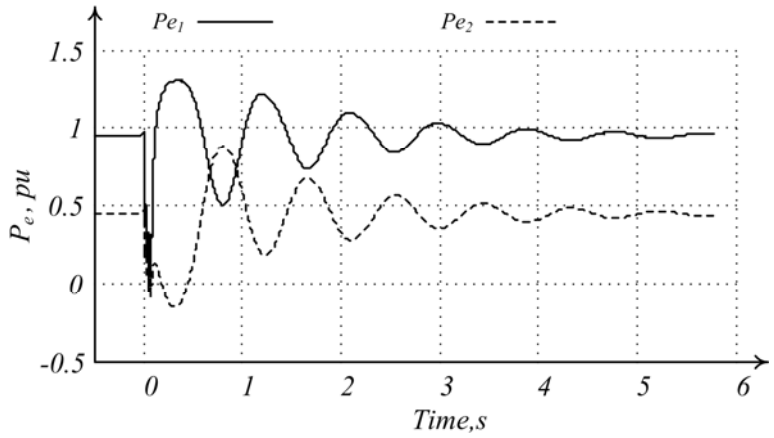

Figure 4.16 P-t curves for fault applied at the middle of T7a and cleared after 0.08 s

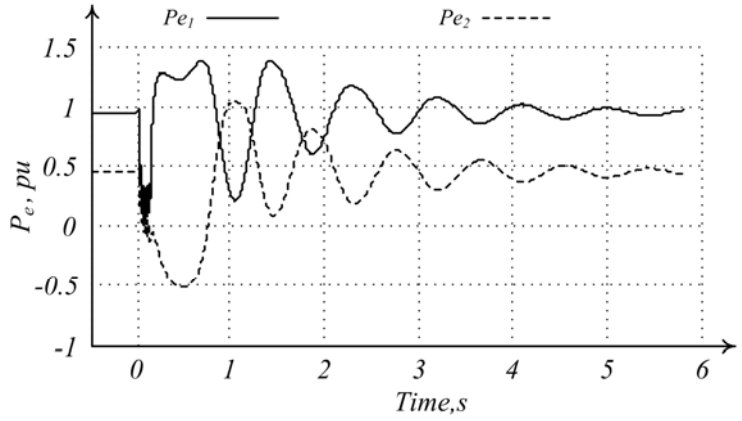

Figure 4.17 P-t curves for fault applied at the middle of T7a and cleared after 0.131 s

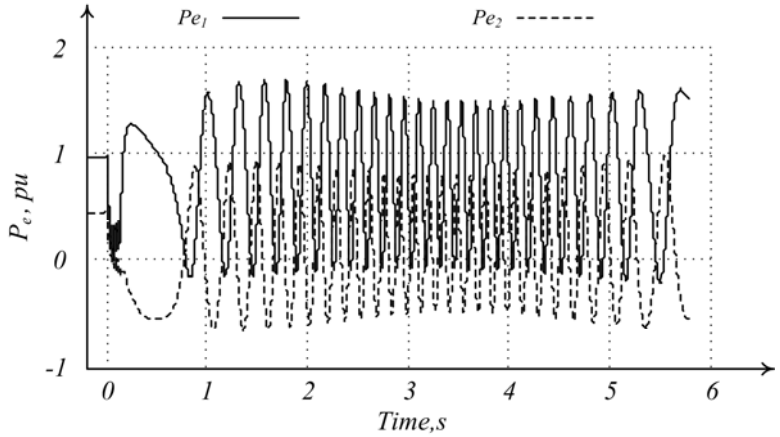

Figure 4.18 P-t curves for fault applied at the middle of T7a and cleared after 0.132 s

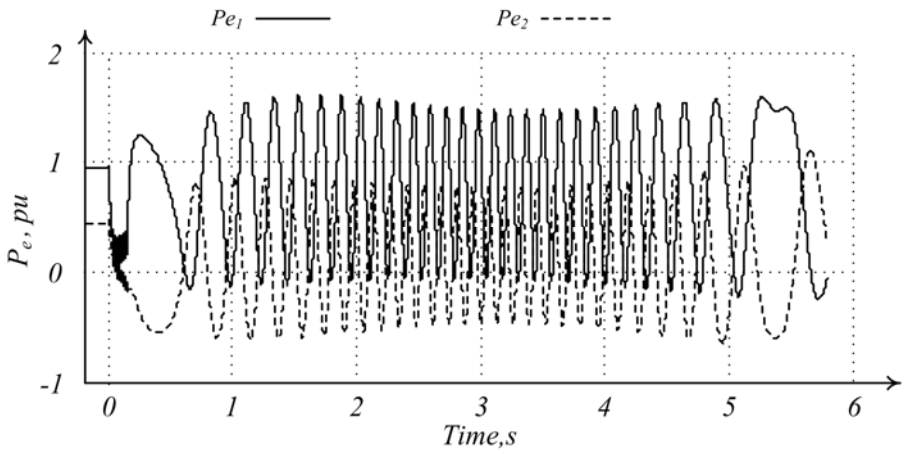

Figure 4.19 P-t curves for fault applied at the middle of T7a and cleared after 0.14 s

Table 4.4 Summary of simulation results for fault applied at the middle of the transmission line T7a, total system load of 1.3992 pu and considering no motor impact.

Case	**13**	**14**	**15**	**16**
Fault duration time, s	0.0800	0.1310	0.1320	0.1400
Area (A_1), pu-s	0.0618	0.0956	0.0985	0.1044
Area (A_2), pu-s	-0.0618	-0.0956	-0.0720	-0.0502
Area A_1+A_2, pu-s	0	0	0.0265	0.0542
Decision time, s	0.8478	1.0720	1.0410	0.9275
Decision	Stable	Stable	Out-of-step	Out-of-step

Next, the generators Gen1 and Gen2's output are set at 0.8345 and 0.4091 pu respectively, which supplies the total system load of 1.2436 pu. A three phase fault is applied at the middle of the transmission line (T9) and duration of fault is set at four different values 0.14, 0.147, 0.148 and 0.160 s, respectively. The first two fault duration time results in stable swings and the respective P-t curves are shown in Figure 4.20 and 4.21. The next two fault duration times make the system go out-of-step and the corresponding P-t curves are shown in Figures 4.22 and 4.23. The results obtained from the simulations are listed in Table 4.5.

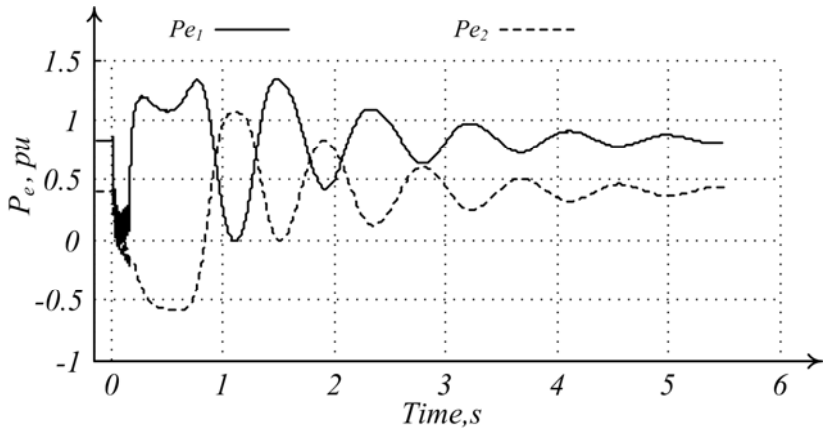

Figure 4.20 P-t curves for fault applied at the middle of T9 and cleared after 0.14 s

Table 4.5 Summary of simulation results for fault applied at the middle of the transmission line T9, total system load of 1.2436 pu and considering no motor impact.

Case	**17**	**18**	**19**	**20**
Fault duration time, s	0.1400	0.1470	0.1480	0.1600
Area (A_1), pu-s	0.1009	0.1024	0.1051	0.1103
Area (A_2), pu-s	-0.1009	-0.1024	-0.0753	-0.0548
Area A_1+A_2, pu-s	0	0	0.0298	0.0555
Decision time, s	1.0265	1.0881	1.0249	0.9329
Decision	Stable	Stable	Out-of-step	Out-of-step

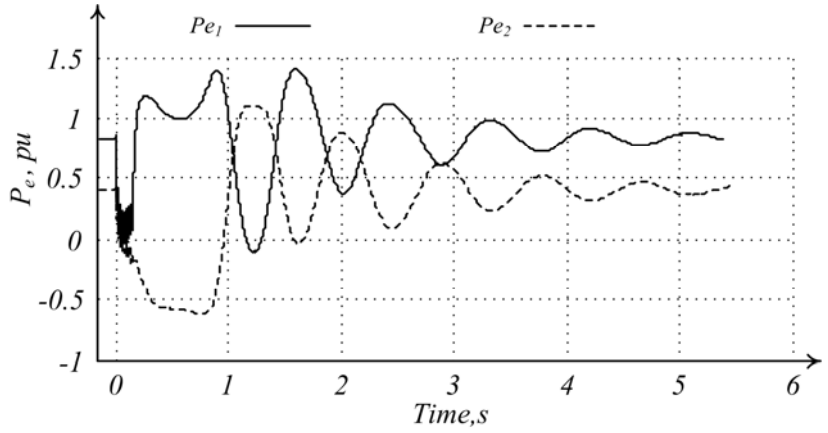

Figure 4.21 P-t curves for fault applied at the middle of T9 and cleared after 0.147 s

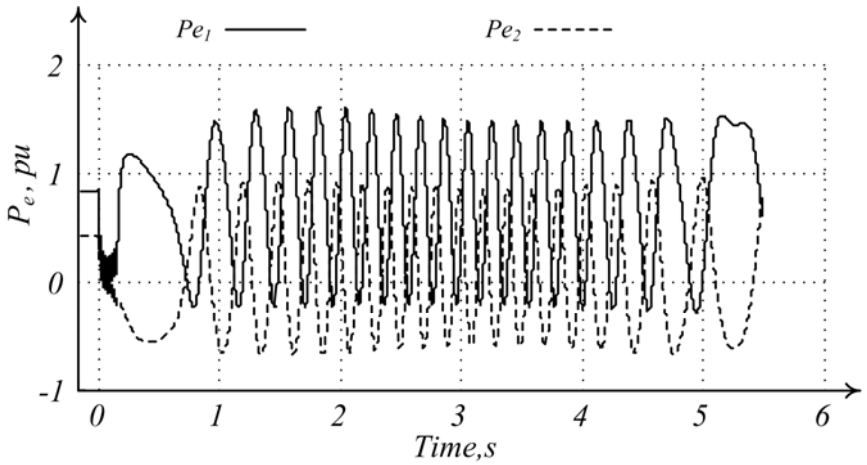

Figure 4.22 P-t curves for fault applied at the middle of T9 and cleared after 0.148 s

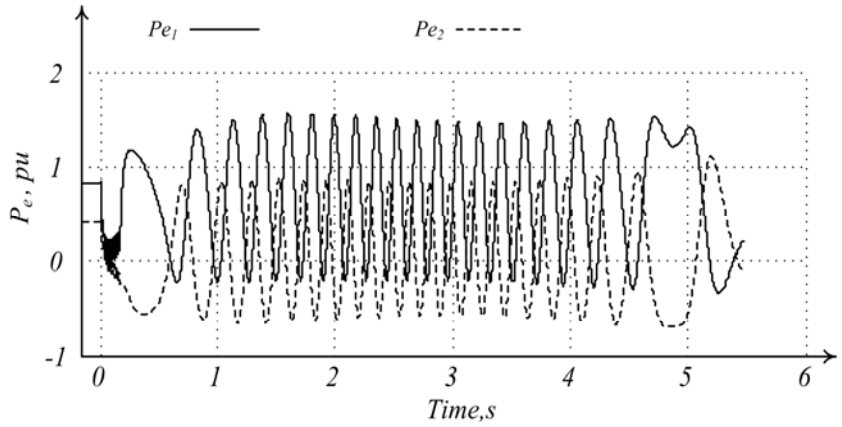

Figure 4.23 P-t curves for fault applied at the middle of T9 and cleared after 0.16 s

4.6.2. Multimachine Simulations with One Motor Impact

In the multimachine system shown in Figure 4.11, only the impact of motor M2 is considered and the other motor M1 is replaced by an equivalent static load. Twelve different simulation cases are reported here with different loading conditions, different locations of fault and fault duration times.

A three phase fault is applied at the middle of the transmission line (T5). The total system load is set at 1.3199 pu, out of which Gen1 is supplying 0.8091 pu whereas Gen2 is supplying 0.5108 pu. Fault duration times are set at 0.08, 0.10, 0.101 and 0.11 s, respectively. The P-t curves for these cases are shown in Figure 4.24 through 4.27. When the fault duration is

increased from 0.10 to 0.101 s, the swing becomes an out-of-step from a stable case. The areas, the decisions and the decision times found using the proposed algorithm are listed in Table 4.6.

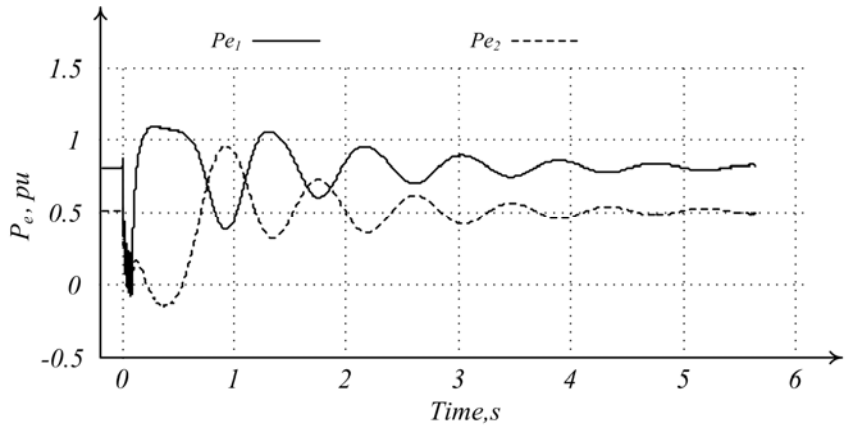

Figure 4.24 P-t curves for fault applied at the middle of T5 and cleared after 0.08 s

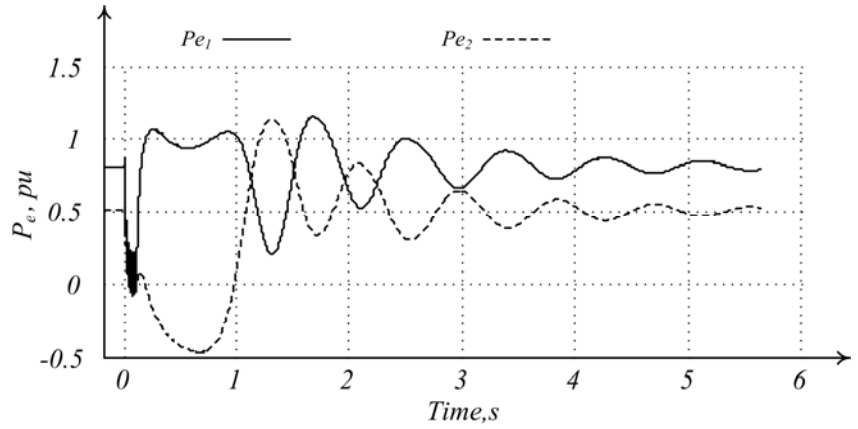

Figure 4.25 P-t curves for fault applied at the middle of T5 and cleared after 0.1 s

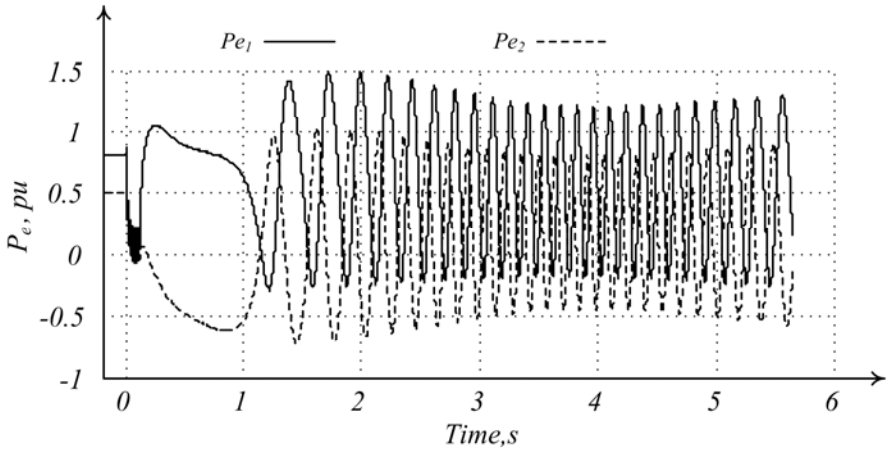

Figure 4.26 P-t curves for fault applied at the middle of TL5 and cleared after 0.101 s

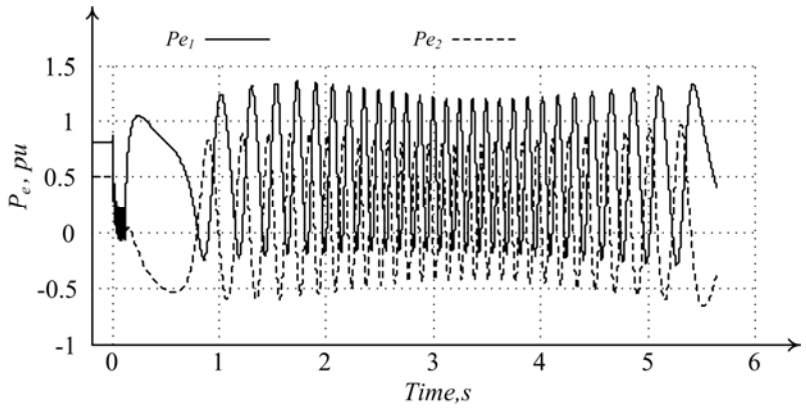

Figure 4.27 P-t curves for fault applied at the middle of T5 and cleared after 0.11 s

Table 4.6 Summary of simulation results for fault applied at the middle of the transmission line T5, total system load of 1.3199 pu and considering one motor impact.

Case	**21**	**22**	**23**	**24**
Fault duration time, s	0.0800	0.1000	0.1010	0.1100
Area (A_1), pu-s	0.0616	0.0765	0.0794	0.0833
Area (A_2), pu-s	-0.0616	-0.1639	-0.0663	-0.0483
Area A_1+A_2, pu-s	0	0	0.0131	0.0350
Decision time, s	0.8963	1.0914	1.2458	1.0039
Decision	Stable	Stable	Out-of-step	Out-of-step

The system load is set at 1.13 pu, out of which Gen1 is supplying 0.6667 pu whereas Gen2 is supplying 0.4633 pu. Three phase fault is applied at the middle of the transmission line T7a and fault duration time is set at 0.14, 0.165, 0.175 and 0.18 s, respectively. Figure 4.28 through 4.31 shows the corresponding P-t curves and the simulation results are listed in Table 4.7.

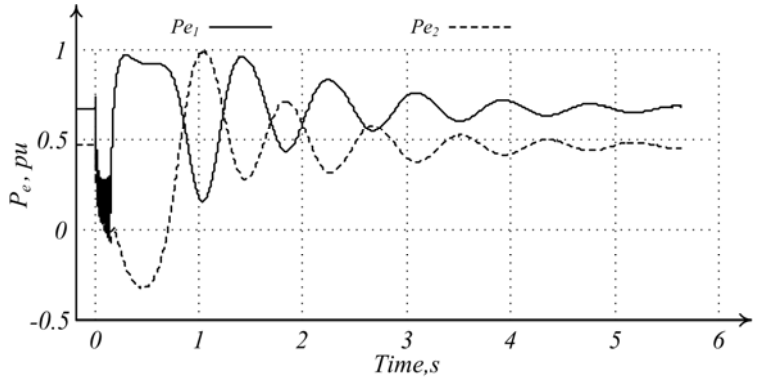

Figure 4.28 P-t curves for fault applied at the middle of T7a and cleared after 0.14 s

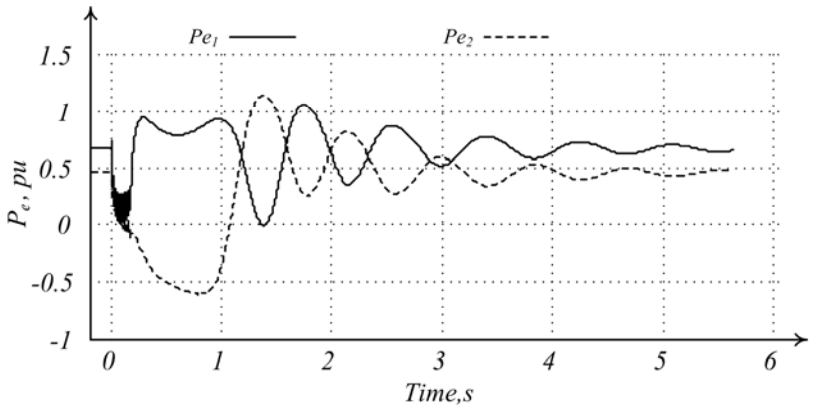

Figure 4.29 P-t curves for fault applied at the middle of T7a and cleared after 0.165 s

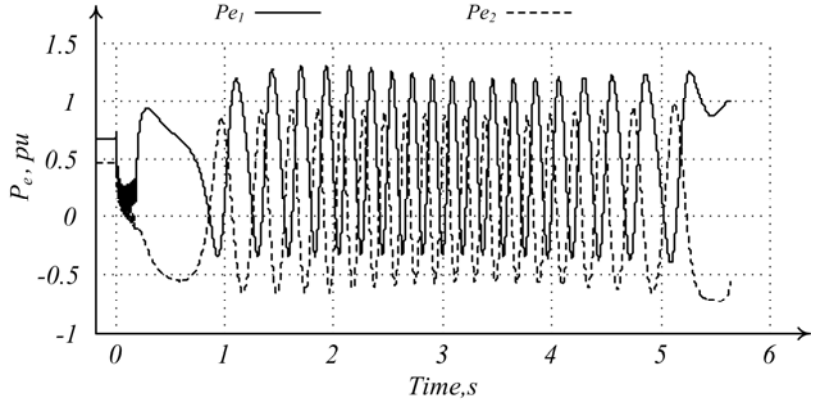

Figure 4.30 P-t curves for fault applied at the middle of T7a and cleared after 0.175 s

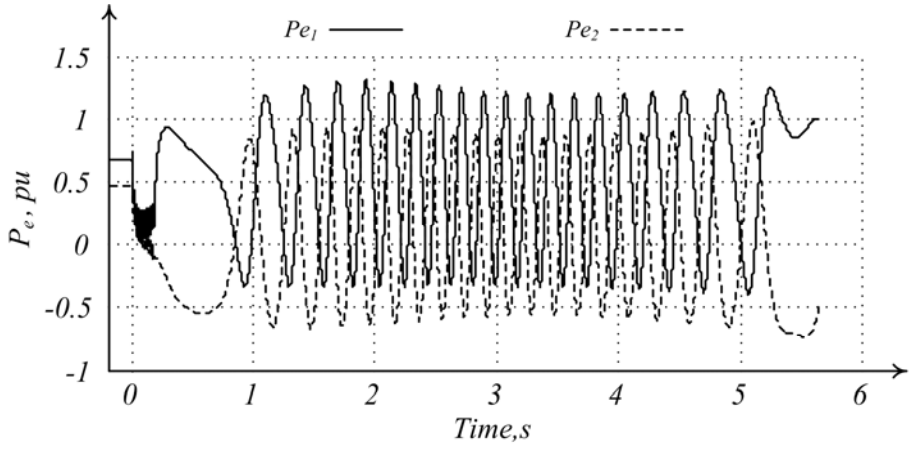

Figure 4.31 P-t curves for fault applied at the middle of T7a and cleared after 0.18 s

Table 4.7 Summary of simulation results for fault applied at the middle of the transmission line T7a, total system load of 1.13 pu and considering one motor impact.

Case	**25**	**26**	**27**	**28**
Fault duration time, s	0.1400	0.1650	0.1750	0.1800
Area (A_1), pu-s	0.0722	0.0818	0.0858	0.0859
Area (A_2), pu-s	-0.0722	-0.0818	-0.0580	-0.0575
Area A_1+A_2, pu-s	0	0	0.0278	0.0248
Decision time, s	0.9623	1.1394	1.0930	1.0889
Decision	Stable	Stable	Out-of-step	Out-of-step

Next the fault location is changed to the middle of the transmission line T9. The Gen1 and Gen2's outputs are set to 0.9578 pu and 0.5643 pu, respectively. The total load in the system is 1.5221 pu. The fault duration time is set at 0.055, 0.081, 0.082, and 0.085 s to simulate four different swing cases. The P-t curves are show in Figure 4.32 through 4.35 and the simulation results are summarized in Table 4.8.

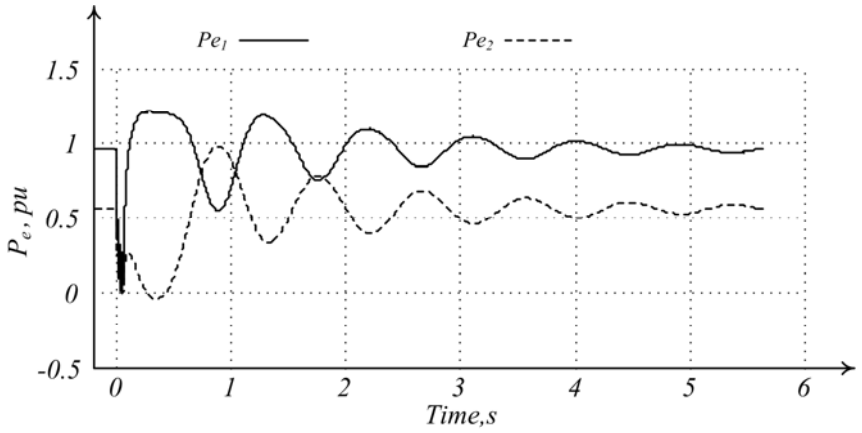

Figure 4.32 P-t curves for fault applied at the middle of T9 and cleared after 0.055 s

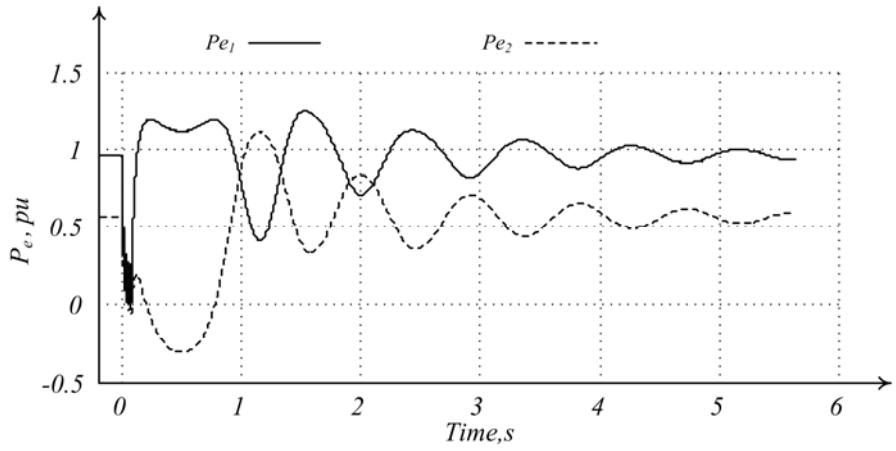

Figure 4.33 P-t curves for fault applied at the middle of T9 and cleared after 0.081 s

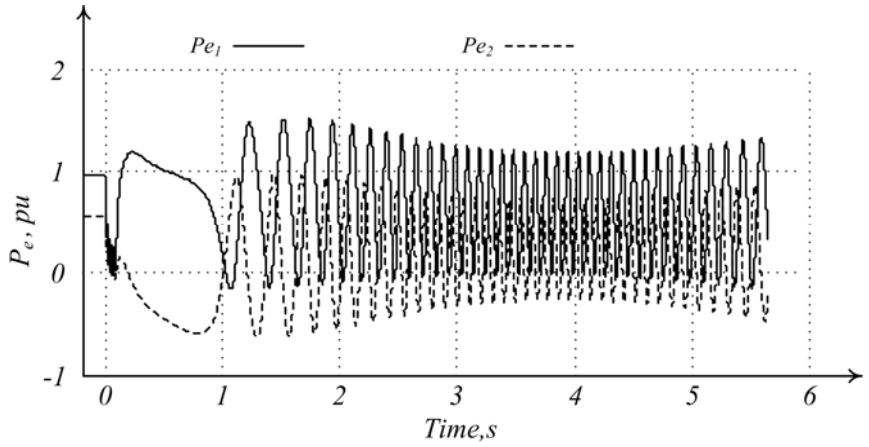

Figure 4.34 P-t curves for fault applied at the middle of T9 and cleared after 0.082 s

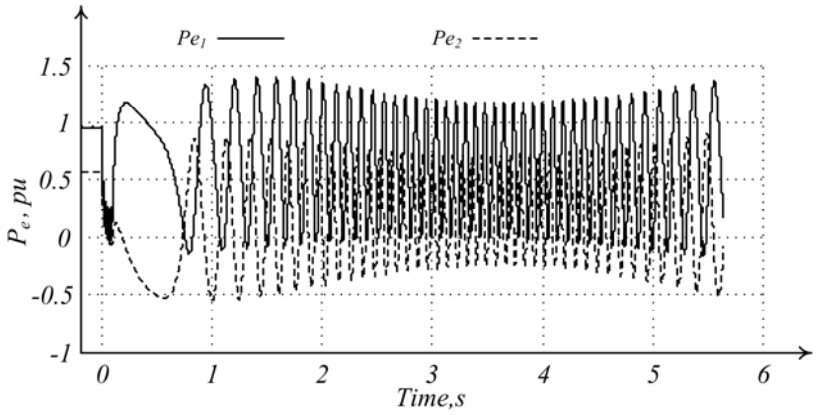

Figure 4.35 P-t curves for fault applied at the middle of T9 and cleared after 0.085 s

Table 4.8 Summary of simulation results for fault applied at the middle of the transmission line T9, total system load of 1.5221 pu and considering one motor impact.

Case	29	30	31	32
Fault duration time, s	0.0550	0.0810	0.0820	0.0850
Area (A_1), pu-s	0.0540	0.0687	0.0745	0.0789
Area (A_2), pu-s	-0.0540	-0.0687	-0.0571	-0.0408
Area A_1+A_2, pu-s	0	0	0.0174	0.0381
Decision time, s	0.8723	1.0026	1.1212	0.9525
Decision	Stable	Stable	Out-of-step	Out-of-step

4.6.3. Multimachine Simulations with Two Motor Impact

In the final sets of simulation, impacts of both the motors M1 and M2 are considered. Like the previous simulations, fault is applied at the middle of the transmission lines T5, T7a and T9 and different fault duration times are set to obtain various natures of swings.

The total pre-fault load in the system is set at 1.2162 pu. Gen1 and Gen2 supply 0.6607 and 0.5555 pu respectively to the system. A three phase fault is applied at the middle of the transmission line (T5) and four different simulations are carried out with the fault duration times of 0.08, 0.09, 0.115 and 0.116 s. The P-t curves from the simulations are shown in Figure 4.36 through 4.39 and the simulation results are listed in Table 4.9.

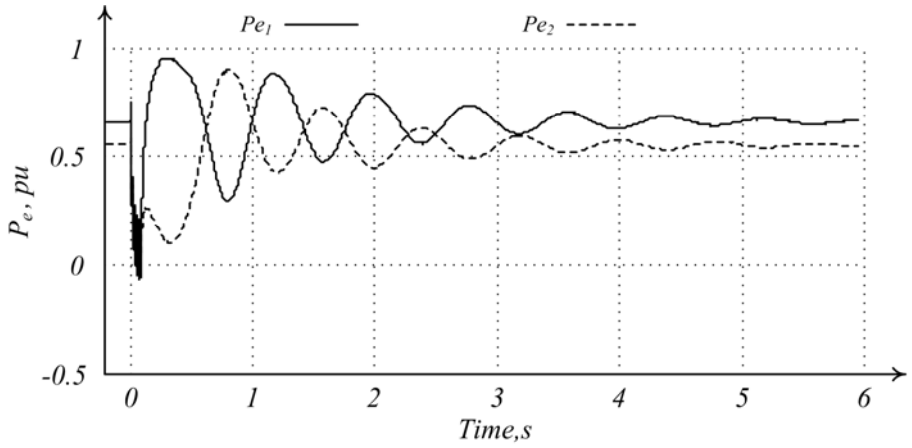

Figure 4.36 P-t curves for fault applied at the middle of T5 and cleared after 0.08 s

Table 4.9 Summary of simulation results for fault applied at the middle of the transmission line T5, total system load of 1.2162 pu and considering two motor impact.

Case	**33**	**34**	**35**	**36**
Fault duration time, s	0.0800	0.0900	0.1150	0.1160
Area (A_1), pu-s	0.0491	0.0544	0.0697	0.0720
Area (A_2), pu-s	-0.0491	-0.0544	-0.0697	-0.0566
Area A_1+A_2, pu-s	0	0	0	0.0154
Decision time, s	0.8444	0.8711	1.1201	1.0786
Decision	Stable	Stable	Stable	Out-of-step

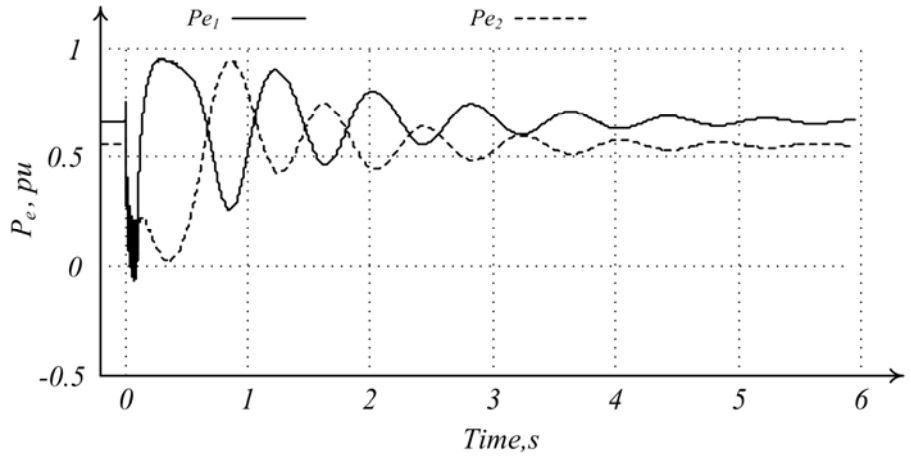

Figure 4.37 P-t curves for fault applied at the middle of T5 and cleared after 0.09 s

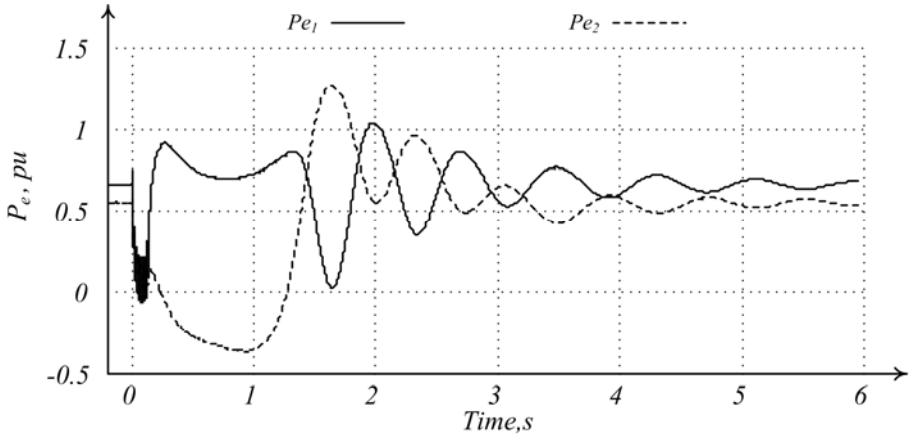

Figure 4.38 P-t curves for fault applied at the middle of T5 and cleared after 0.115 s

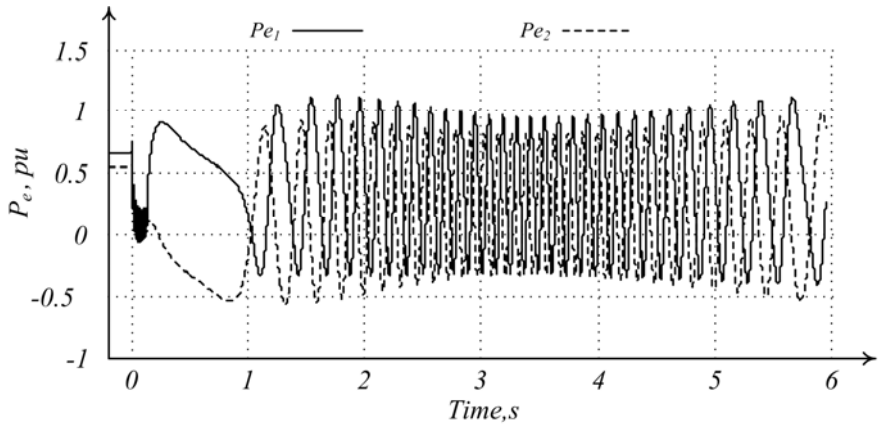

Figure 4.39 P-t curves for fault applied at the middle of T5 and cleared after 0.116 s

Next the fault location is changed to the middle of the transmission line (T7a) and the total system load is set at 1.4289 pu. Gen1 is supplying 0.8219 pu , whereas Gen2 is supplying 0.6070 pu to the system. Fault duration time is set at 0.075, 0.095, 0.099 and 0.11 s to obtain four different nature of the P-t curves. The P-t curves are shown below in Figure 4.40 through 4.43 and the simulation results are summarized in Table 4.10.

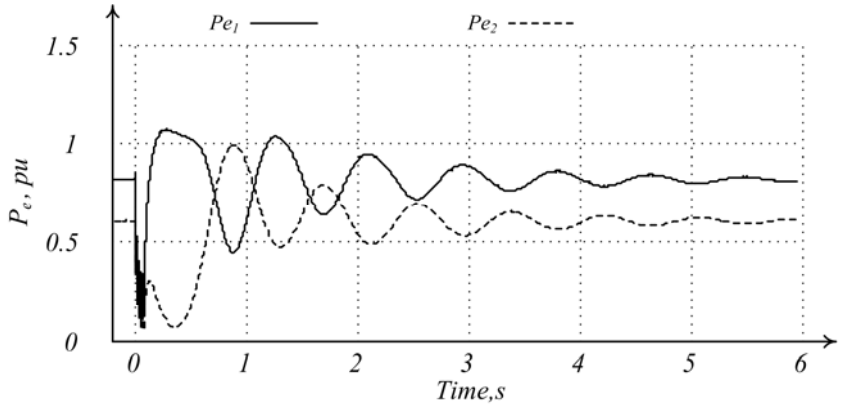

Figure 4.40 P-t curves for fault applied at the middle of T7a and cleared after 0.075 s

Table 4.10 Summary of simulation results for fault applied at the middle of the transmission line T7a, total system load of 1.4289 pu and considering two motor impact.

Case	**37**	**38**	**39**	**40**
Fault duration time, s	0.0750	0.0950	0.0990	0.1100
Area (A_1), pu-s	0.0503	0.0594	0.0632	0.0683
Area (A_2), pu-s	-0.0503	-0.0594	-0.0577	-0.0375
Area A_1+A_2, pu-s	0	0	0.0055	0.0308
Decision time, s	0.8793	0.9758	1.1705	0.9546
Decision	Stable	Stable	Out-of-step	Out-of-step

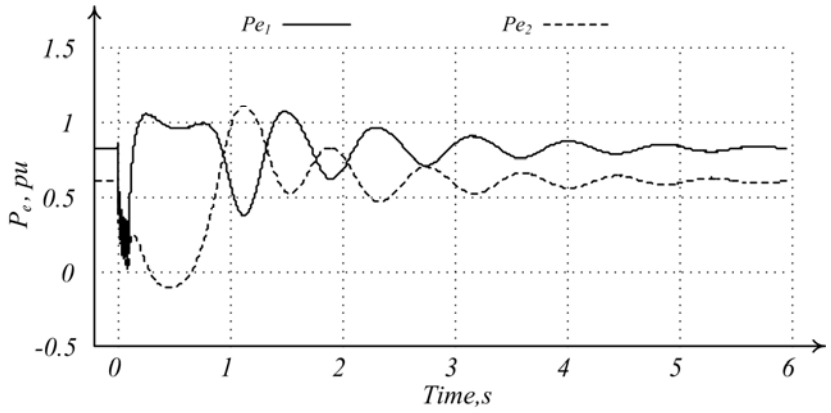

Figure 4.41 P-t curves for fault applied at the middle of T7a and cleared after 0.095 s

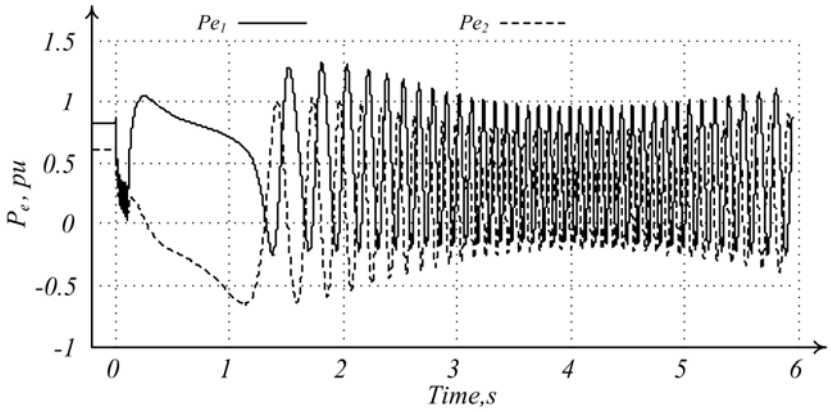

Figure 4.42 P-t curves for fault applied at the middle of T7a and cleared after 0.099 s

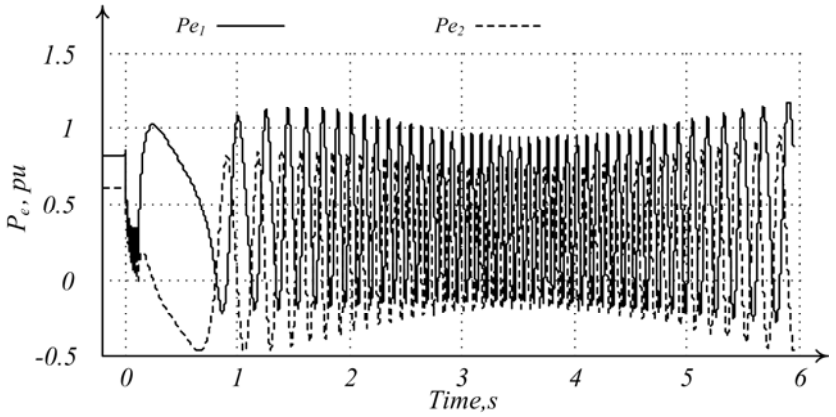

Figure 4.43 P-t curves for fault applied at the middle of T7a and cleared after 0.11 s

Next the total system load is set at 1.325 pu, out of which Gen1 is supplying 0.7425 pu whereas Gen2 is supplying 0.5825 pu. Three phase fault is applied at the middle of the transmission line (T9). Four different fault duration times 0.8, 0.09, 0.091 and 0.100 s are set to obtain different nature of P-t curves. The P-t curves obtained form the simulations are shown in Figure 4.44 through 4.47 and the results are summarized in Table 4.11.

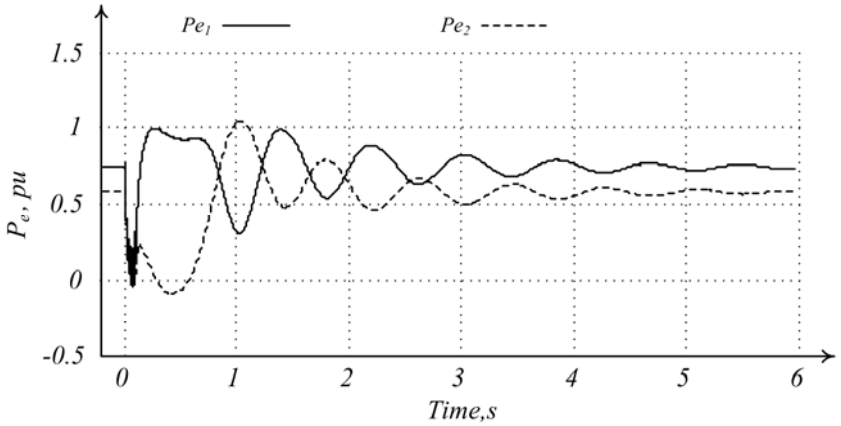

Figure 4.44 P-t curves for fault applied at the middle of T9 and cleared after 0.08 s

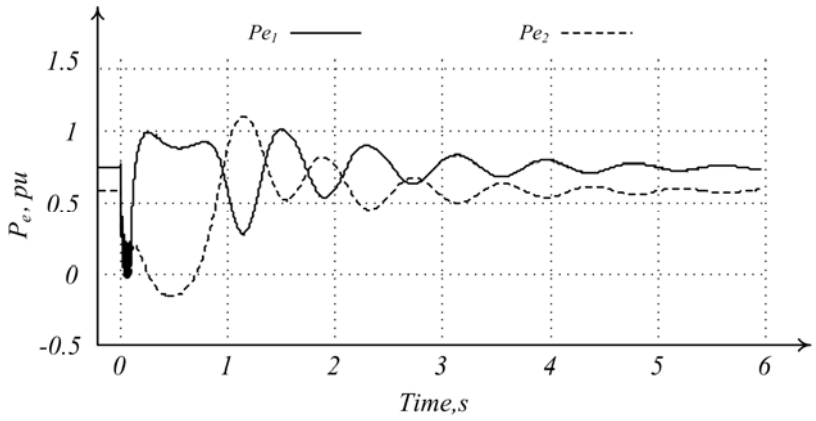

Figure 4.45 P-t curves for fault applied at the middle of T9 and cleared after 0.09 s

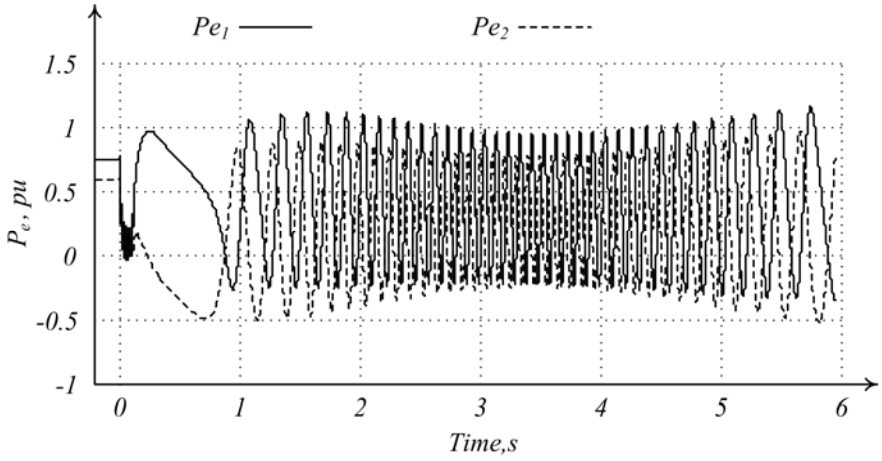

Figure 4.46 P-t curves for fault applied at the middle of T9 and cleared after 0.091 s

Table 4.11 Summary of simulation results for fault applied at the middle of the transmission line T9, total system load of 1.325 pu and considering two motor impact.

Case	**41**	**42**	**43**	**44**
Fault duration time, s	0.0800	0.0900	0.0910	0.1000
Area (A_1), pu-s	0.0598	0.0628	0.0694	0.0693
Area (A_2), pu-s	-0.0598	-0.0628	-0.0460	-0.0469
Area A_1+A_2, pu-s	0	0	0.0234	0.0224
Decision time, s	0.9270	0.9694	0.9894	0.9998
Decision	Stable	Stable	Out-of-step	Out-of-step

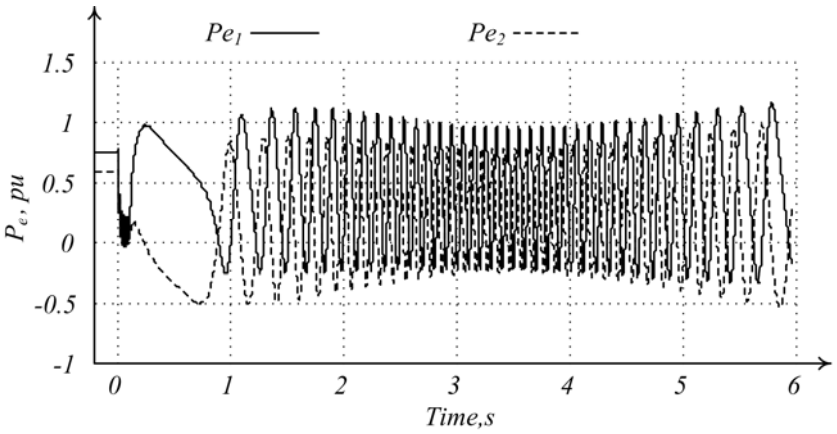

Figure 4.47 P-t curves for fault applied at the middle of T9 and cleared after 0.1 s

The Cases 9 thorough 44 listed for 17-bus multimachine depict the simulations when out-of-step relay is installed for Gen1. Simulations are also carried out with the out-of-step relay installed for Gen2. The Gen2's output power curve (Pe_2) is determined from its local current and voltage measurements and the proposed algorithm is applied. The summary of the results obtained are given in Table 4.12 through 4.14.

Table 4.12 Summary of simulation results considering no motor impact.

Case	**45**	**46**	**47**	**48**	**49**	**50**
Pre-fault load, pu	1.437	1.437	1.3992	1.3992	1.2436	1.2436
Fault duration time, s	0.1060	0.1200	0.1320	0.1400	0.1480	0.1600
Fault location	Mid. of T5	Mid. of T5	Mid. of T7a	Mid. of T7a	Mid. of T9	Mid. of T9
Area (A_1), pu-s	0.7671	0.4192	0.6110	0.4476	0.5487	0.4225
Area (A_2), pu-s	-0.0387	-0.0242	-0.0339	-0.0269	-0.0377	-0.0315
Area A_1+A_2, pu-s	0.7284	0.3590	0.5771	0.4207	0.5110	0.3190
Decision time, s	1.5904	1.2143	1.4401	1.2574	1.4005	1.2513
Decision	Out-of-step	Out-of-step	Out-of-step	Out-of-step	Out-of-step	Out-of-step

Table 4.13 Summary of simulation results considering one-motor impact.

Case	51	52	53	54	55	56
Pre-fault load	1.3199	1.3199	1.13	1.13	1.5221	1.5221
Fault duration time, s	0.1010	0.1100	0.1750	0.1800	0.0820	0.0850
Fault location	Mid. of T5	Mid. of T5	Mid. of T7a	Mid. of T7a	Mid. of T9	Mid. of T9
Area (A_1), pu-s	0.9960	0.6300	0.6592	0.6528	0.8949	0.6122
Area (A_2), pu-s	-0.0302	-0.0223	-0.0308	-0.0305	-0.0264	-0.0173
Area A_1+A_2, pu-s	0.9658	0.6077	0.6284	0.6223	0.8685	0.5949
Decision time, s	1.8075	1.4479	1.5311	1.5229	1.6668	1.3867
Decision	Out-of-step	Out-of-step	Out-of-step	Out-of-step	Out-of-step	Out-of-step

Table 4.14 Summary of simulation results considering two-motor impact.

Case	57	58	59	60	61	62
Pre-fault load	1.2162	1.2162	1.4289	1.4289	1.325	1.325
Fault duration time, s	0.1150	0.1160	0.0990	0.1100	0.0910	0.1000
Fault location	Mid. of T5	Mid. of T5	Mid. of T7a	Mid. of T7a	Mid. of T9	Mid. of T9
Area (A_1), pu-s	0.9881	0.8291	1.1411	0.6339	0.6981	0.7091
Area (A_2), pu-s	-0.2501	-0.0215	-0.0273	-0.0111	-0.0146	-0.0149
Area A_1+A_2, pu-s	0.7380	0.8076	1.1138	0.6228	0.6835	0.6942
Decision time, s	2.4819	1.6901	1.9695	1.4467	1.5256	1.5373
Decision	Out-of-step	Out-of-step	Out-of-step	Out-of-step	Out-of-step	Out-of-step

4.7. Results Discussion

4.7.1. Comment on the Motor Impacts

Different simulations considering no motor, one motor and two motor impacts were carried out to analyze their impacts on the decision making. Physically addition of a machine adds more complexity as the machine introduces more nonlinear dynamics in the system. Thus, considering no motor, one motor and two motor impacts; the algorithm was tested for different complexity levels of the power system. It was found that additional machines did not compromise the effectiveness of the proposed algorithm.

4.7.2. Marginal Cases

By increasing the fault duration for a pre-fault power, the marginally stable and out-of-step conditions were obtained as in previously listed Cases 10, 11, 14, 15, 18, 19, 22, 23, 30, 31, 42 and 43. For example, in the Cases 10 and 11, the pre-fault load was set at 1.437 pu and the fault

duration time was increased from 0.105 to 0.106 s. The system was stable for fault duration of 0.105 s and became out-of-step when the fault duration was increased to 0.106 s. Increasing the fault duration time by small amount of 0.001 s caused the system go to an out-of-step from a stable condition. When the fault duration time was increased by less than 0.001 s, the simulation results did not show significant differences in calculated area, thus the above cases were listed as marginal cases.

4.7.3. Comment on the Decision Time

As discussed for SMIB simulation in Chapter 3, when the fault duration time is increased, the severity of the swing increases. A severer swing has larger area A_1. This needs larger area A_2 to make the total area zero. For example, in Cases 9 and 10 listed before, when the fault duration time was increased from 0.06 s to 0.105 s, the area A_1 was increased from 0.0581 pu-s to 0.0941 pu-s. So in the $P_m \leq P_e$ region, the algorithm waited more for Case 10 than Case 9 to obtain the total area equal to zero. Therefore, it required more time to make the decision in Case 10. But when the swing is out-of-step, the area A_2 goes on decreasing as severity of the swing increases. Therefore less and less time is required to evaluate the area A_2 in $P_m \leq P_e$ region, so the decision time goes on decreasing. For example, when the fault duration time was increased from 0.106 s 0.12 s in the Cases 11 and 12, the area A_2 in the Case 12 dropped to 0.0438 pu-s as compared to 0.0827 pu-s in the Case 11. Case 12 needed lesser time to calculate area A_2 and therefore the decision was made faster in Case 12 compared to Case 11. The proposed algorithm required maximum decision time when the cases were marginally stable or out-of-step because the two areas were about the same.

4.8. Summary

In addition to the SMIB simulations described in Chapter 3, the proposed EAC in time domain was also tested for the detection of out-of-step condition in two machine, three machine and multimachine systems. The simulation results showed that the algorithm was effective to discriminate clear-cut stable and out-of-step conditions in a complex power system and was independent of the number of machines connected to the system. The measurement inaccuracies may sometime cause a marginally stable case appear like out-of-step case and cause the relay to trip. However, for a marginally out-of-step case, it may happen that P_e appears greater than P_m even though it is the opposite. In such a situation, the decision time may be delayed by few samples because P_e will become eventually less than P_m. So, still a correct decision will be made.

The simulation results and discussions presented in this chapter demonstrate the ease of use and the validity of the proposed algorithm for a multimachine system. This was not the case for conventional blinder scheme or traditional EAC which required complex network reduction techniques such as Lyapanov Criteria [24, 25] to reduce to a two area system for obtaining the out-of-step relay settings.

CHAPTER 5
HARDWARE IMPLEMENTATION AND TESTING USING THE REAL TIME DIGITAL SIMULATOR

5.1. Introduction

In Chapters 3 and 4, the proposed algorithm was tested on a SMIB and multimachine system using software simulation tool. This chapter describes the implementation and testing using a hardware simulation tool called the Real Time Digital Simulator (RTDS™)[4] available in the Power Research Laboratory and the other necessary hardwares to test the algorithm in a closed loop. The power system model is developed using software (RSCAD™) which can be simulated in real time by using the RTDS™ hardware. A relay model is developed using a Digital Signal Processing (DSP) board using the algorithm proposed in Chapter 3. Closed loop testing of the proposed relay model is done using the RTDS™ on a power system configuration. The results obtained from the closed loop testing are also explained.

5.2. Hardware/ Software

The main hardwares used are the RTDS™ and (ADSP-BF533™)[5] EZ LITE-KIT board. The RTDS™ is a digital simulator capable of performing the electromagnetic transient simulations in real time. The real time simulation gives an advantage of testing in a closed loop environment. This has a great advantage in terms of testing the proposed protection function accurately. The simulator is a combination of advanced hardware (it consists of Triple Processor Card (3PC) and

[4] RSCAD™ is the registered trade mark of RTDS Technologies Inc., Winnipeg, Canada
[5] ADSP-BF533™ is the registered trade mark of Analog Devices, Inc.

a Giga Processor Card (GPC)) and user friendly software RSCAD™. The simulator hardwares are assembled in modular units and are called as racks on the system. Each rack is equipped with processing and communication modules [26, 27].

Each 3PC card consists of,

- Three Analog Device's ADSP−21062 digital signal processors
- Instruction cycle time: 25 ns (= 40 MIPS)
- Floating Point computation rate: 40 − 120 MFLOPs
- Floating Point Numeric Format: IEEE 40 bit (8 bit exponent, 32 bit mantissa)
- Link Port communication channels: 6
- Link Port communication rate: 40 Megabytes/sec
- On−chip Memory: 2 Megabit static Ram

Each GPC card consists of,

- Two IBM PPC750GX PowerPC processors
- Core Frequency: 1.0 GHz
- Floating Point computation rate: 1.0 GFLOPs
- Floating Point Numeric Format: IEEE−754 64 bit
- L1 Cache: 32 Kilobyte instructions, 32 Kilobyte data
- L2 Cache: 1.0 Megabyte

Data exchange between each of the processing modules above is carried by high speed communication backplane equipped with each rack. The RSCAD™ software suite is the user's main interface to the RTDS™ hardware. All aspects of the power system such as construction circuits, recording simulation results etc are controlled through the RSCAD™. The RSCAD™ mainly has two modules: Draft and Runtime. Draft module handles construction of circuits,

power system blocks and entering of the parameters, while the Runtime module controls the operation of the hardware. Through the Runtime module users can control actions such as starting and stopping the simulation, initiating disturbance, triggering data acquisition system etc. A Workstation Interface Card (WIF) is equipped in the RTDS™ simulator which connects the RSCAD™ console to the RTDS™ hardware through ethernet [28].

Besides RTDS™, another hardware used for my research is the ADSP-BF533™ EZ LITE-KIT board. The board has the following main features,

- One ADSP-BF533™ Blackfin® Processor
- 32 MB (16M x 16-bit) SDRAM
- 2 MB (512K x 16-bit x 2) FLASH memory
- AD1836 96 kHz audio codec with input and output RCA jacks
- Three 90-pin connectors for analyzing with the processor's peripheral interfaces

The DSP board is controlled by software called the Visual DSP++ [29].

5.3. Modeling Power system and the Out-of-step Relay

A SMIB system as shown in Figure 5.1 is considered for modeling a power system in RTDS™ . The power system parameters are given in Appendix A [1].

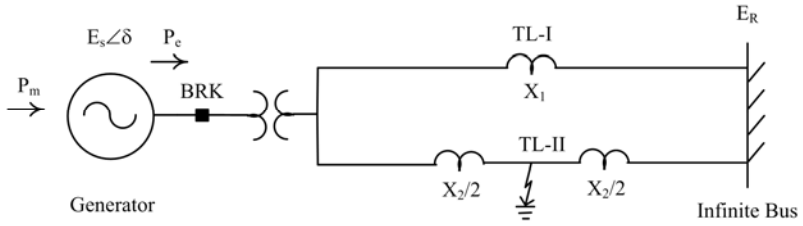

Figure 5.1 Power system model used for closed loop testing

The proposed out-of-step algorithm developed in Section 3.4 is implemented on the ADSP-BF533™ EZ LITE-KIT board. The block diagram for the closed loop testing is shown in Figure 5.2. The modeling details are described in the following sections.

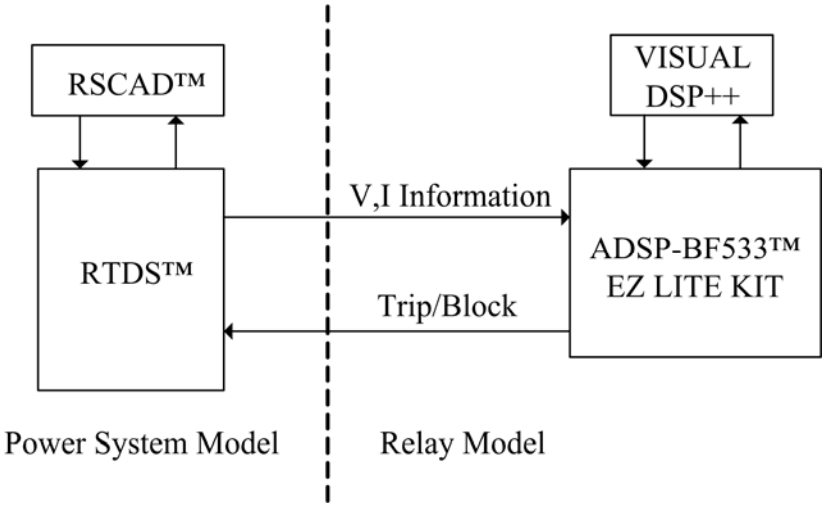

Figure 5.2 Block diagram for closed loop testing

5.3.1. Power System Model

Power system model is developed in RTDS™ using its software RSCAD™. Figure 5.3 shows the RSCAD™ model of the power system shown in Figure 5.1. A power system stabilizer is used only for suppressing the transient during the start up of the machine; it is later on disconnected from the model. A fault is applied at the BUS2 and the fault clearing time is controlled by the control system blocks as shown in Figure 5.4. Pressing the push button PB generates a pulse signal whose rising edge triggers the square wave generator SQW. The width of the square wave is controlled by multi-selector switch DIAL. The setting of DIAL determines the width of the square wave. The output of SQW is the logic signal FAULT which controls the duration of the fault applied in the power system model shown in Figure 5.3.

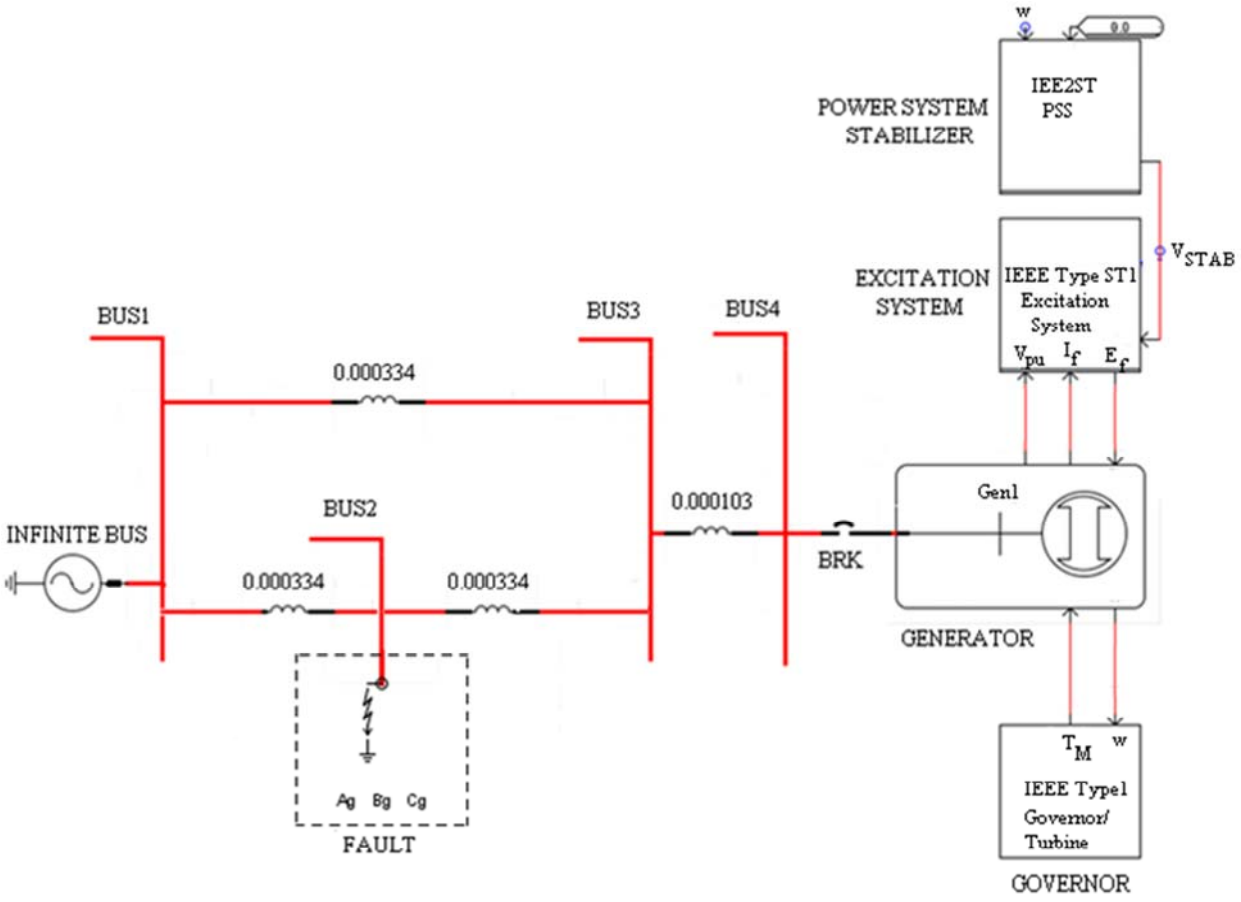

Figure 5.3 Power system model developed in RSCAD™ for closed loop testing

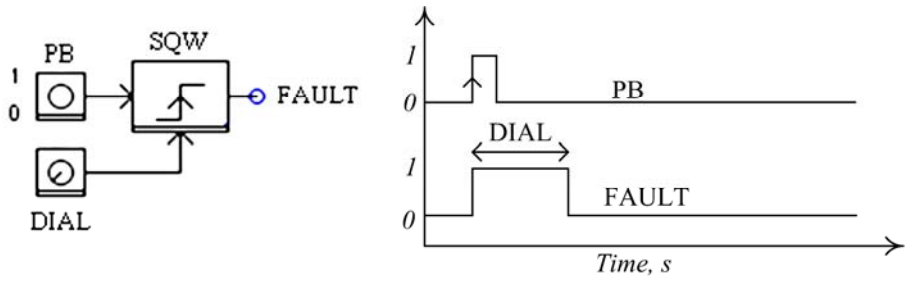

Figure 5.4 Control blocks and signals to control the fault duration time

The necessary current and voltage signals from the power system model are sent out through RTDS™'s analog output ports.

5.3.2. Out-of-Step Relay Model

The proposed out-of-step relay is modeled on the ADSP-BF533™ EZ-KIT board using its software Visual DSP++. The three phase terminal voltages and currents of the generator are fed to the DSP board through the analog output ports of the RTDS™ . The relay model developed in the DSP board has four blocks: Filtering, Down-sampling, Phasor Estimation and the Out-of-step Algorithm as shown in Figure 5.5. Each input voltage and current signals are passed through all the blocks of the relay model.

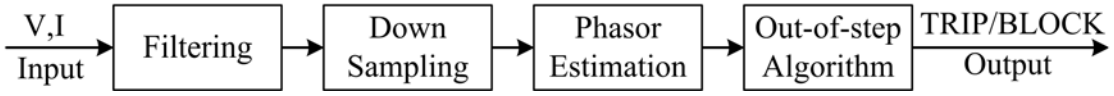

Figure 5.5 Blocks of the relay model

5.3.2.1 Filtering

A fifth order infinite impulse response (IIR) Butterworth filter is used to filter out the frequencies other than the power frequency (i.e. 60 Hz). The transfer function of the filter is given by Equation 5.1.

$$H(Z) = \frac{b_0 + b_1 z^{-1} + b_2 z^{-2} + b_3 z^{-3} + b_4 z^{-4} + b_5 z^{-5}}{a_0 + a_1 z^{-1} + a_2 z^{-2} + a_3 z^{-3} + a_4 z^{-4} + a_5 z^{-5}} \tag{5.1}$$

The filter coefficients are listed in Table 5.1. The cutoff frequency of the filter is 65 Hz (408.4 rad/s). The frequency response of the filter is shown in Figure 5.6.

Table 5.1 Filter coefficients of low pass Butterworth filter

Coefficients	Value	Coefficients	Value
a_0	1	b_0	0.01374456104486e-10
a_1	-4.97246600423435	b_1	0.06872280522430e-10
a_2	9.89024269671581	b_2	0.13744561044859e-10
a_3	-9.83592884998049	b_3	0.13744561044859e-10
a_4	4.89099364358940	b_4	0.06872280522430e-10
a_5	-0.97284148604639	b_5	0.01374456104486e-10

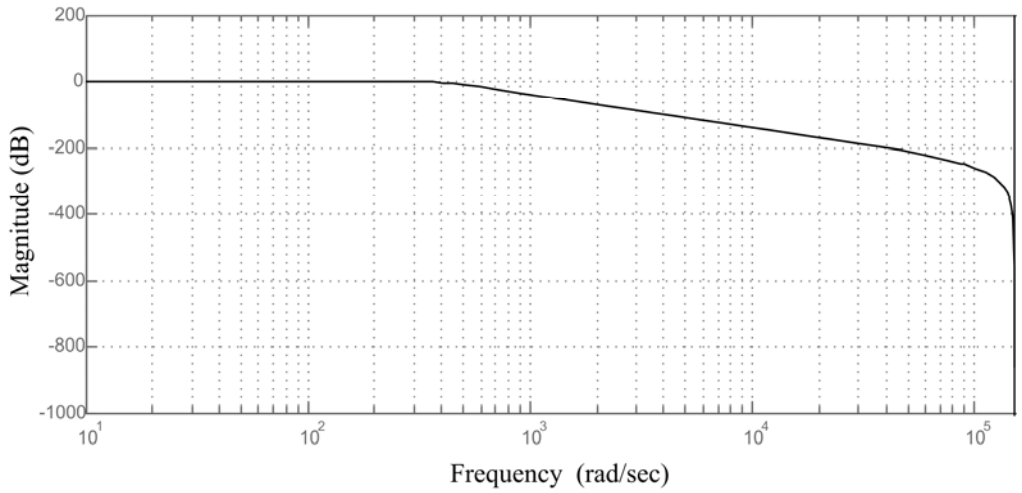

Figure 5.6 Frequency response of the low-pass Butterworth filter

5.3.2.2 Down-sampling

The DSP board samples at 48000 samples per second but for this research only 16 samples per cycle is used. As the input signals are at 60Hz, the input signals should be sampled at 960 samples per second. Thus this block downsamples the input signals by,

48000 / 960 = 50 times

5.3.2.3 Phasor Estimation

Discrete Fourier Transform (DFT) is used for the phasor estimation of voltage and current signals. A periodic signal consists of two orthogonal signals. The DFT technique employs the orthogonal signals sine and cosine to estimate the phasor of sinusoidal waveform. Consider the input signal is,

$$v(\omega t) = V_p \sin(\omega t + \theta) \tag{5.2}$$

The DFT technique gives the real and imaginary parts of the phasor as given by the following equations,

$$\mathrm{Re}(v) = V_p \cos(\theta) = \frac{2}{N}\sum_{i=0}^{N-1} v_i \sin(i\omega\Delta T) \tag{5.3}$$

$$\mathrm{Im}(v) = V_p \sin(\theta) = \frac{2}{N}\sum_{i=0}^{N-1} v_i \cos(i\omega\Delta T) \tag{5.4}$$

Where *i* represents sample number, N represents the total number of samples in a cycle and ΔT represents sampling time. The expressions $\sin(i\omega\Delta T)$ and $\cos(i\omega\Delta T)$ in Equations 5.3 and 5.4 are the two orthogonal signals (also referred as reference signals) and the frequency of these signals (i.e. ω) is same as the frequency of the input signal. The two orthogonal signals must be sampled at the same rate ΔT as the input signal. The *i*th sample of the orthogonal signal is multiplied with the corresponding *i*th sample of the input signal [30].

As calculated in Section 5.3.2, the number of samples per cycle used in this research is 16 (i.e. N=16). For a power frequency signal of 60 Hz, the sampling time becomes,

$$\Delta T = \frac{1}{60 \times 16} = 0.00104 \text{ s}$$

For 60 Hz signal and 16 samples/ cycle, the value of 16 samples of the two reference signals are listed in the Table 5.2.

Table 5.2 Coefficients of two orthogonal reference signals

i	$\sin(i\omega\Delta T)$	$\cos(i\omega\Delta T)$	i	$\sin(i\omega\Delta T)$	$\cos(i\omega\Delta T)$
0	0	1.0000000000	**8**	0	-1.0000000000
1	0.3826834323	0.9238795325	**9**	-0.3826834323	-0.9238795325
2	0.7071067811	0.7071067811	**10**	-0.7071067811	-0.7071067811
3	0.9238795325	0.3826834323	**11**	-0.9238795325	-0.3826834323
4	1.0000000000	0	**12**	-1.0000000000	0
5	0.9238795325	-0.3826834323	**13**	-0.9238795325	0.3826834323
6	0.7071067811	-0.7071067811	**14**	-0.7071067811	0.7071067811
7	0.3826834323	-0.9238795325	**15**	-0.3826834323	0.9238795325

5.3.2.4 Out-of-step Detection Algorithm

Based on Equations (5.3) and (5.4) the phasors of voltages and currents of three phases are determined and the three phase power output of the generator is calculated as,

$$P_e = \frac{1}{2}\sum_{i=1}^{3} V_p^i I_p^i \cos(\theta_1^i - \theta_2^i) \tag{5.5}$$

where, V_p^i represents peak voltage, I_p^i represents peak current, θ_1^i represents phase angle of voltage, θ_2^i represents phase angle of current of the i^{th} phase.

Rewriting the Equations (3.20) and (3.21),

For stable condition,

$$\sum_{t_0}^{t_c}(P_e\big|_{t_0-\Delta t} - P_e(t))\Delta t + \sum_{t_c}^{t_{\max}}(P_e\big|_{t_0-\Delta t} - P_e(t))\Delta t = 0 \tag{5.6}$$

For out-of-step condition,

$$\sum_{t_0}^{t_c}(P_e\big|_{t_0-\Delta t} - P_e(t))\Delta t + \sum_{t_c}^{t_{\max}}(P_e\big|_{t_0-\Delta t} - P_e(t))\Delta t > 0 \tag{5.7}$$

The Equations 5.6 and 5.7 are the basics of the out-of-step detection. While implementing using a digital hardware, for a stable system, the calculated area $\left(\sum_{t_0}^{t_c}(P_e\big|_{t_0-\Delta t} - P_e(t))\Delta t\right)$ does not

become exactly equal to the area $\left(\sum_{t_c}^{t_{\max}} (P_e\big|_{t_0-\Delta t} - P_e(t))\Delta t \right)$. Thus the condition in Equation 5.6 is modified for a stable system as,

$$\sum_{t_0}^{t_c} (P_e\big|_{t_0-\Delta t} - P_e(t))\Delta t + \sum_{t_c}^{t_{\max}} (P_e\big|_{t_0-\Delta t} - P_e(t))\Delta t \le 0 \tag{5.8}$$

The modification made in the expression may results in error in the decision time. For this research, the maximum error possible is ΔT i.e. 0.00104 s.

Based on the decision made, a digital signal is sent to the RTDS™ through its digital input port as shown in Figure 5.2. This signal is used to either trip or not the breaker BRK of Figure 5.3. If the decision made is stable, the relay sends BLOCK signal i.e. logic 0 to the breaker which does not trip the breaker. For an out-of-step condition, the relay sends TRIP signal i.e. logic 1 to the RTDS™ which trips the breaker BRK disconnecting the machine from the infinite bus. The Figure 5.7 shows the digital bit sent to the RTDS™ by relay based on the decision made.

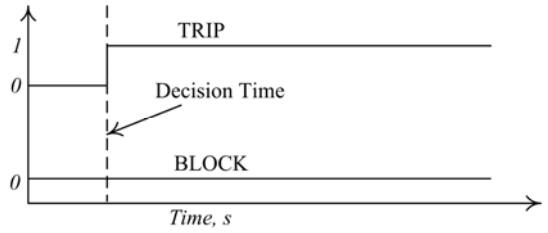

Figure 5.7 TRIP/BLOCK signal from the out-of-step relay to control the breaker BRK

5.4. Closed Loop Testing- A Single Machine Infinite Bus System

The DSP board and RTDS™ are connected as shown in Figure 5.2. Various swing conditions are generated by setting the pre-fault power angle (δ) of the generator at different values (25°, 30°, 35°, 40° and 45°); by applying various types of fault (three phase, line-ground and line-line) at the middle of the transmission line (TL2) and by varying the fault duration time.

5.4.1. Pre-fault power angle (δ) set at 25° and Three Phase Fault Applied

The pre-fault power angle of the generator is set at 25°, which results in 0.7905 pu power output from the generator. A three phase fault is applied at the middle of transmission line (TL2). Fault duration time is set at 0.52 s (i.e. 500 samples). At 500th sample, the fault is cleared by making the signal FAULT logic 0. The P-t curve for this case is shown in Figure 5.8. The area A_1 calculated is 7.6527×10^9. The area A_2 becomes 7.6565×10^9 at 734th sample. Here, the values listed for area A_1 and A_2 are scaled from DSP board. Thus this case is decided as a stable swing at 734 samples i.e. 0.7633 s. The relay model sends logic 0 (i.e. BLOCK) signal to BRK at 734th sample. Figure 5.9 shows area A_1, A_2 and the associated logical signals based on the decision made.

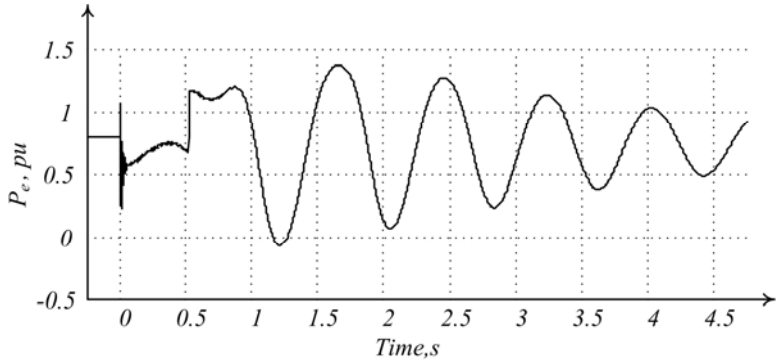

Figure 5.8 P-t curve for pre-fault δ=25° and cleared after 0.52 s

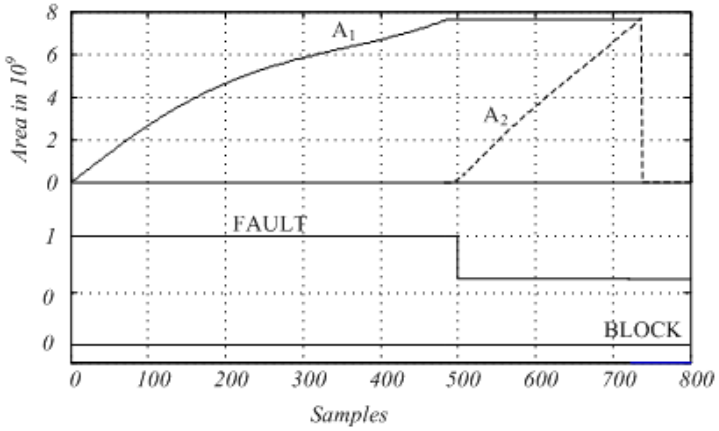

Figure 5.9 Area A_1, A_2 and the decision made for pre-fault δ=25° and cleared after 0.52 s

Next the fault duration time is increased to 0.54 s (i.e. 519 samples). The P-t curve is shown in Figure 5.10. The area A_1 and A_2 are respectively 7.2248×10^9 and 7.2441×10^9. The decision made is stable and a BLOCK signal is sent to BRK at 0.8486 s (i.e. 816th sample). Figure 5.11 shows calculated areas A_1, A_2 and the logic signals generated.

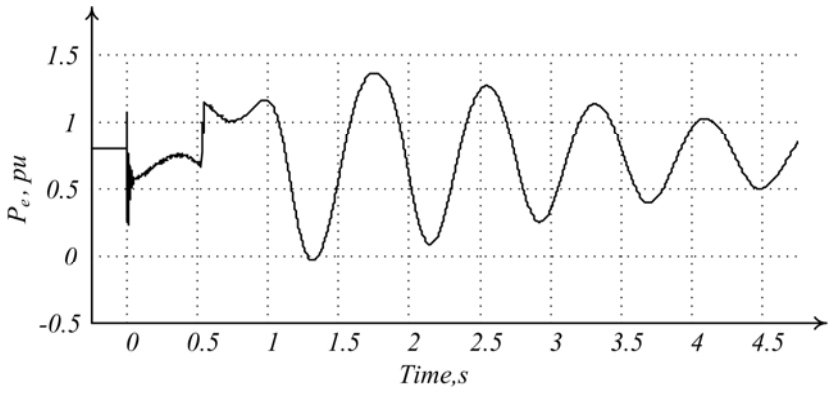

Figure 5.10 P-t curve for pre-fault δ=25° and cleared after 0.54 s

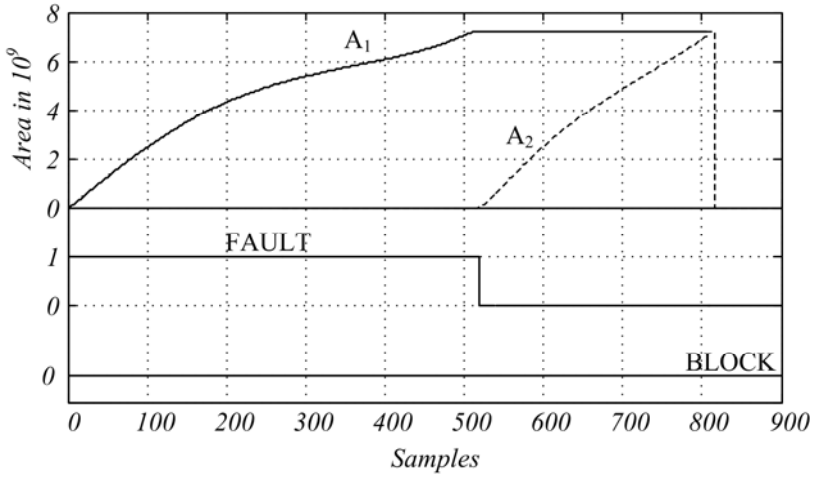

Figure 5.11 Area A_1, A_2 and the decision made for pre-fault δ=25° and cleared after 0.54 s

The fault duration time is increased to 0.555 s (i.e. 533 samples). The P-t curve is shown in Figure 5.12. The area A_1 and A_2 are respectively 7.7344×10^9 and 7.7374×10^9. The decision is made as stable and a BLOCK signal is sent to BRK at 1.0015 s (i.e. 963rd sample). Figure 5.13 shows the calculated areas A_1, A_2 and the logic signals generated.

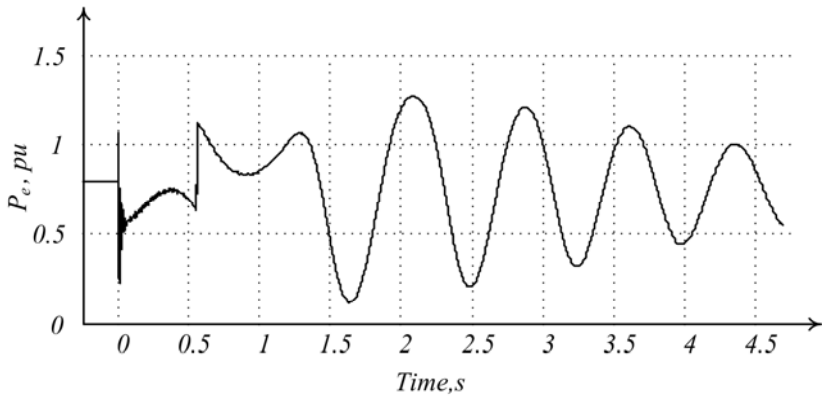

Figure 5.12 P-t curve for pre-fault δ=25° and cleared after 0.555 s

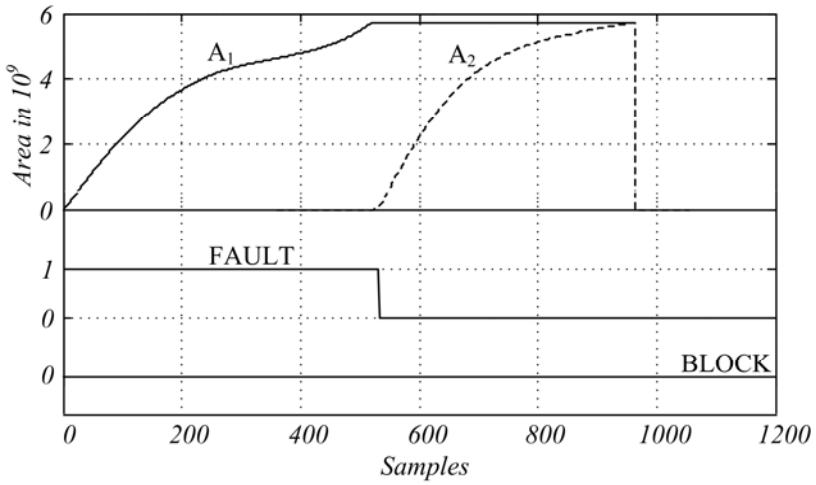

Figure 5.13 Area A_1, A_2 and the decision made for pre-fault δ=25° and cleared after 0.555 s

When the fault duration time is increased to 0.556 s (i.e. 534 samples) from 0.555, the system goes to an out-of-step condition. The P-t curve is shown in Figure 5.14. The area A_1 and A_2 are respectively 6.7229×10^9 and 4.4719×10^9. The decision is made as out-of-step and a TRIP signal (i.e. logic 1) is sent to BRK at 0.8788 s (i.e. 845th sample). Figure 5.15 shows the calculated areas A_1, A_2 and the logic signals generated.

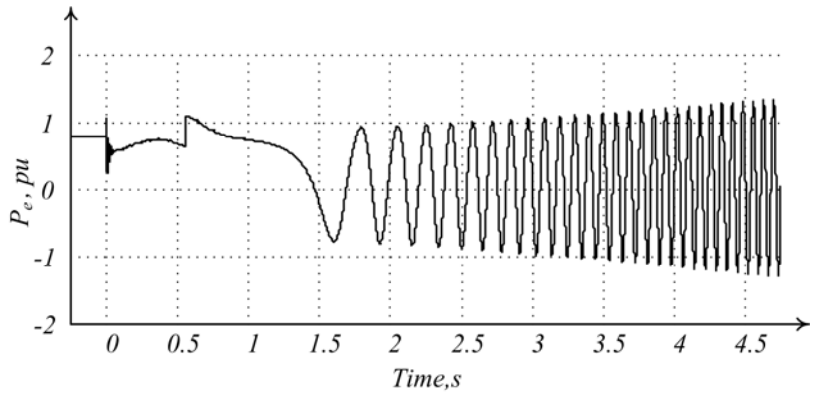

Figure 5.14 P-t curve for pre-fault δ=25° and cleared after 0.556 s

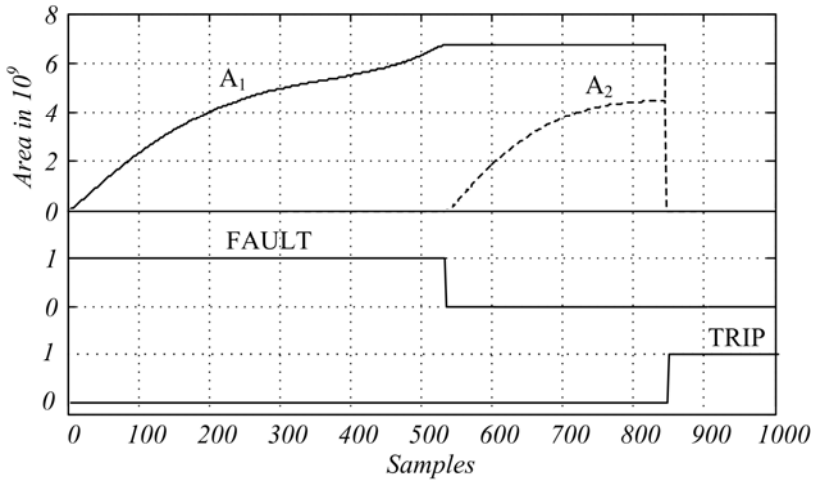

Figure 5.15 Area A_1, A_2 and the decision made for pre-fault δ=25° and cleared after 0.556 s

The fault duration time is increased further to 0.56 s (i.e. 538 samples). The P-t curve for this case is shown in Figure 5.16. The area A_1 is found to be 9.9036×10^9 where as the area A_2 is calculated 2.5761×10^9 at 729^{th} sample. Thus this case is decided as an out-of-step case at 0.7582 s and the TRIP signal is sent to BRK. The areas calculated and the logic signals generated are shown in Figure 5.17.

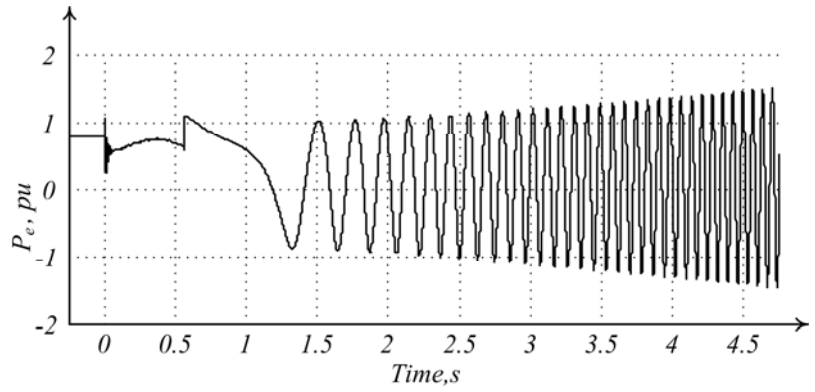

Figure 5.16 P-t curve for pre-fault δ=25° and cleared after 0.56 s

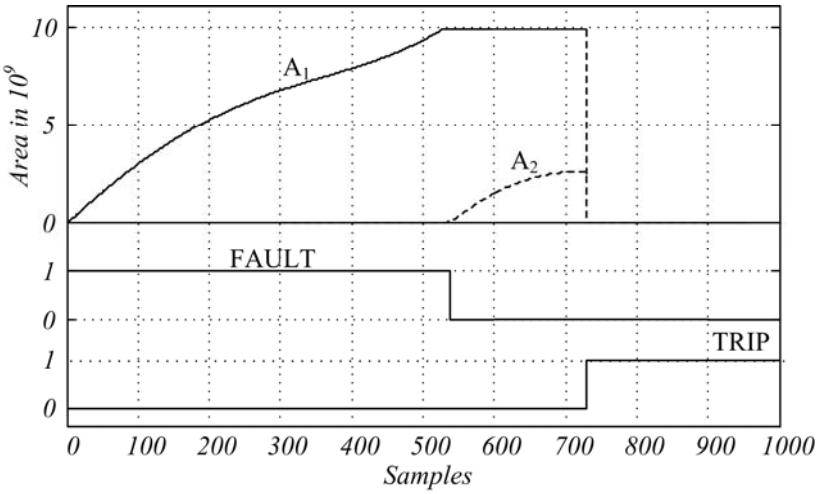

Figure 5.17 Area A_1, A_2 and the decision made for pre-fault δ=25° and cleared after 0.56 s

The fault duration time is increased further to 0.58 s (i.e. 557 samples). The P-t curve for this case is shown in Figure 5.18. The area A_1 is found to be 9.9371×10^9 where as the area A_2 is calculated 1.2183×10^9 at 669^{th} sample. Thus this case is decided as an out-of-step case at 0.6957 s and the TRIP signal is sent to BRK. The areas calculated and the logic signals generated are shown in Figure 5.19. The summary of the above six simulation cases are listed in Table 5.3.

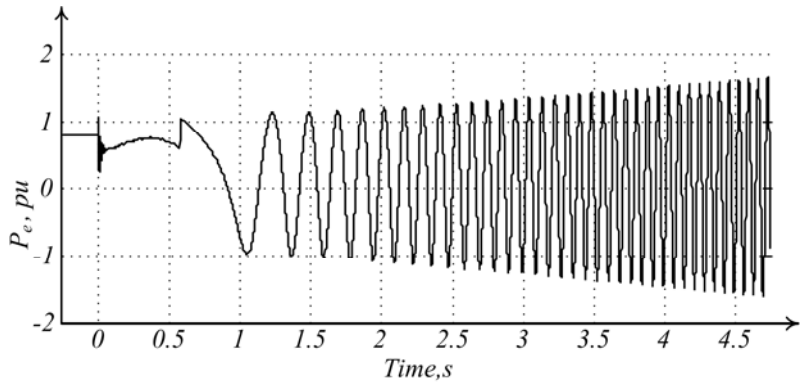

Figure 5.18 P-t curve for pre-fault δ=25° and cleared after 0.58 s

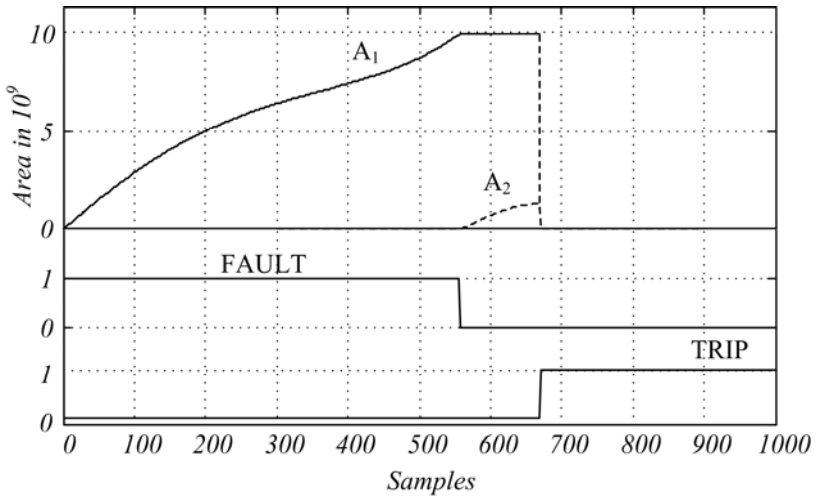

Figure 5.19 Area A_1, A_2 and the decision made for pre-fault δ=25° and cleared after 0.58 s

Table 5.3 Closed loop testing results for pre-fault δ=25° and the three phase fault applied

Case	**1**	**2**	**3**	**4**	**5**	**6**
Fault Duration Time, s	0.52	0.54	0.555	0.556	0.56	0.58
Fault Duration Samples	500	519	533	534	538	557
Area (A_1)*, in 10^9	7.6527	7.2248	7.7344	6.7229	9.9036	9.9371
Area (A_2)*, in 10^9	7.6565	7.2441	7.7374	4.4719	2.5761	1.2183
Decision	Stable	Stable	Stable	OS	OS	OS
Decision Made at Sample	734	816	963	845	729	669
Decision Time, s	0.7633	0.8486	1.0015	0.8788	0.7582	0.6957

* scaled value from DSP OS :Out-of-step

5.4.2. Pre-fault power angle (δ) set at 30° and Three Phase Fault Applied

The pre-fault δ of the generator is set at 30° which results in 0.9355 pu of power output from the generator. Six different simulations are carried with the fault duration times of 0.26, 0.30, 0.333, 0.334, and 0.36 and 0.38 s respectively. The first three simulation cases give stable swing whereas the rest of the three give out-of-step swing. The P-t curves corresponding to the stable swings are shown in Figure 5.20 through 5.22 and the out-of-step P-t curves are shown in Figure 5.23 through 5.25. The areas A_1, A_2, decision made and the decision times are summarized in Table 5.4.

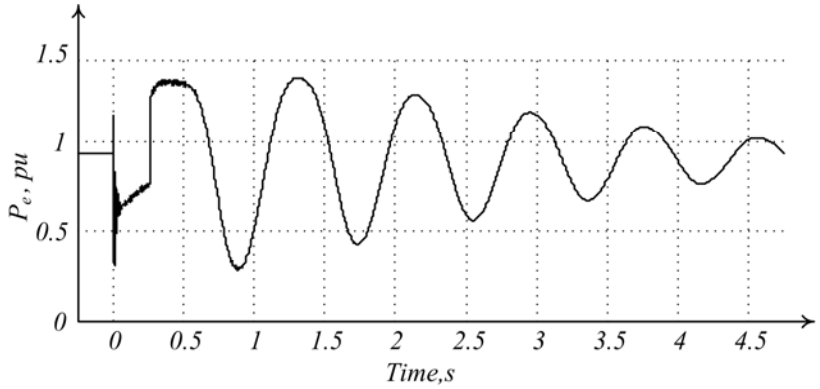

Figure 5.20 P-t curve for pre-fault δ=30° and cleared after 0.26 s

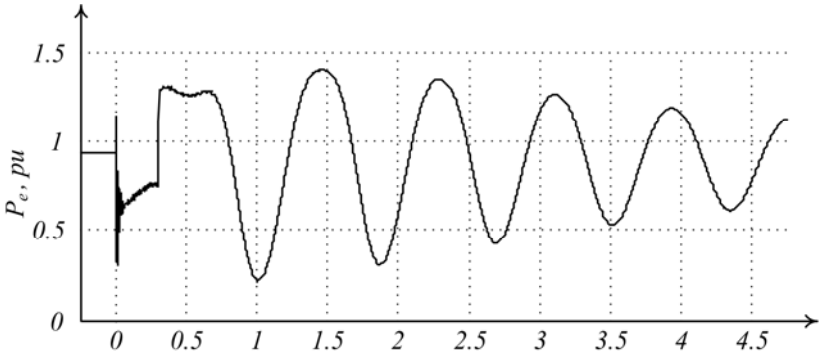

Figure 5.21 P-t curve for pre-fault δ=30° and cleared after 0.30 s

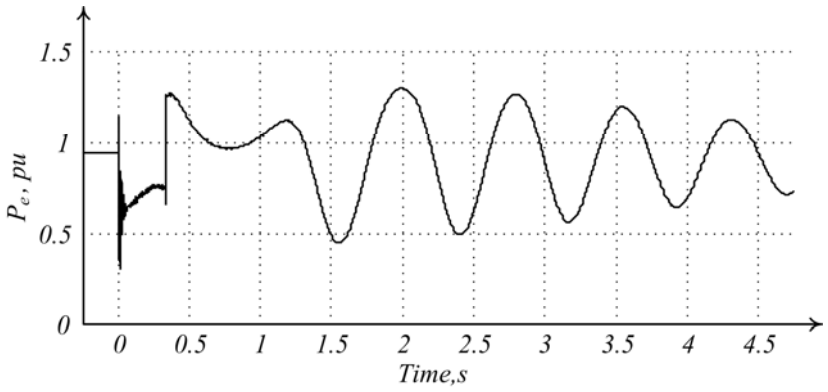

Figure 5.22 P-t curve for pre-fault δ=30° and cleared after 0.333 s

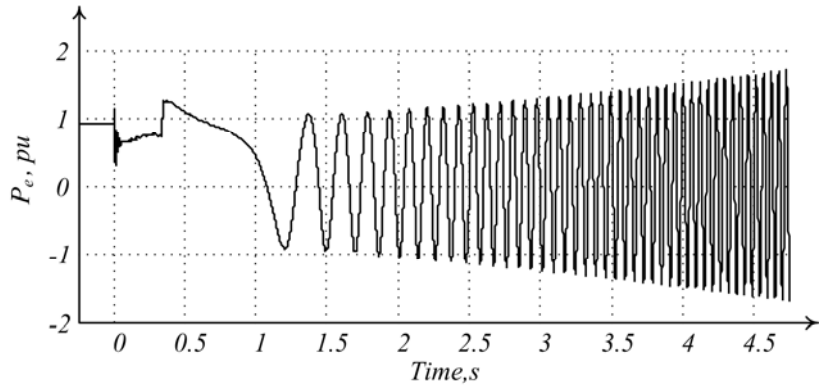

Figure 5.23 P-t curve for pre-fault δ=30° and cleared after 0.334 s

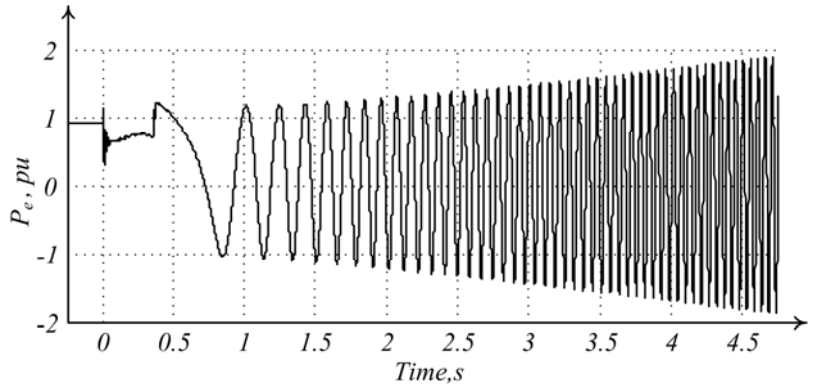

Figure 5.24 P-t curve for pre-fault δ=30° and cleared after 0.36 s

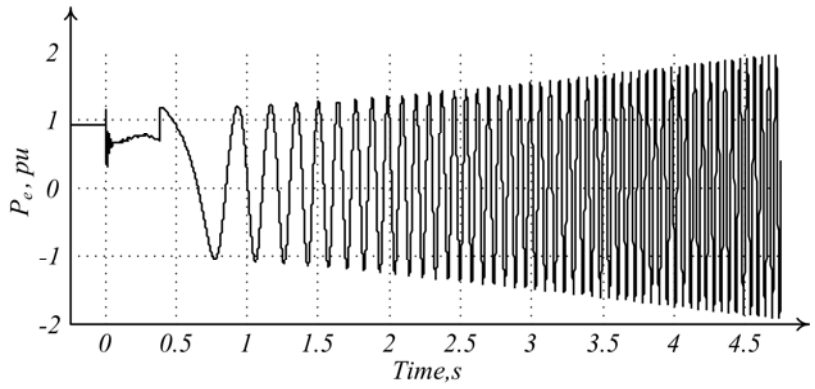

Figure 5.25 P-t curve for pre-fault δ=30° and cleared after 0.38 s

Table 5.4 Closed loop testing results for pre-fault δ=30° and the three phase fault applied

Case	**7**	**8**	**9**	**10**	**11**	**12**
Fault Duration Time, s	0.26	0.30	0.333	0.334	0.36	0.38
Fault Duration Samples	250	288	320	321	346	365
Area (A_1)*, in 10^9	7.1089	7.6791	7.0331	9.5168	9.9106	10.5240
Area(A_2)*, in 10^9	7.1142	7.6882	7.0348	4.0461	2.2082	1.0063
Decision	Stable	Stable	Stable	OS	OS	OS
Decision Made at Sample	443	518	648	572	486	458
Decision Time, s	0.4607	0.5387	0.6739	0.5948	0.5054	0.4763

* scaled value from DSP OS :Out-of-step

5.4.3. Pre-fault power angle (δ) set at 35° and Three Phase Fault Applied

The pre-fault δ of the generator is set at 35° which results in 1.0707 pu of power output from the generator. Three phase fault is applied at the middle of transmission line (TL2) and six different simulations are carried with the fault duration times of 0.22, 0.26, 0.271, 0.272, and 0.28 and 0.30 respectively. The first three simulation cases give stable swing whereas rest of the three gives out-of-step swing. The P-t curve of stable swings are shown in Figure 5.26 through 5.28 and the out-of-step P-t curves are shown in Figure 5.29 through 5.31. The areas A_1, A_2, decision made and the decision times are summarized in the Table 5.5.

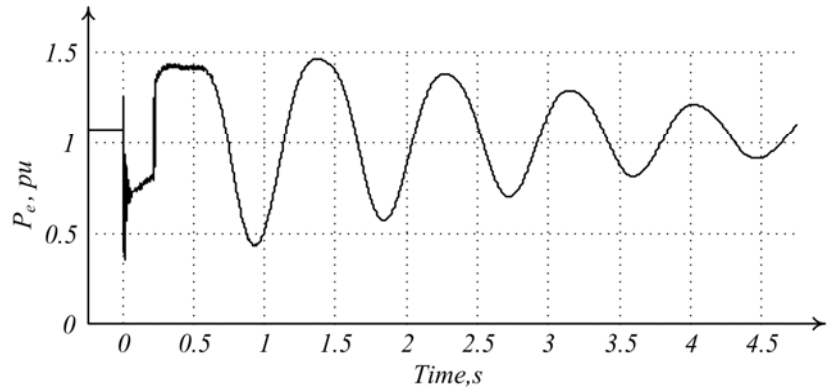

Figure 5.26 P-t curve for pre-fault δ=35° and cleared after 0.22 s

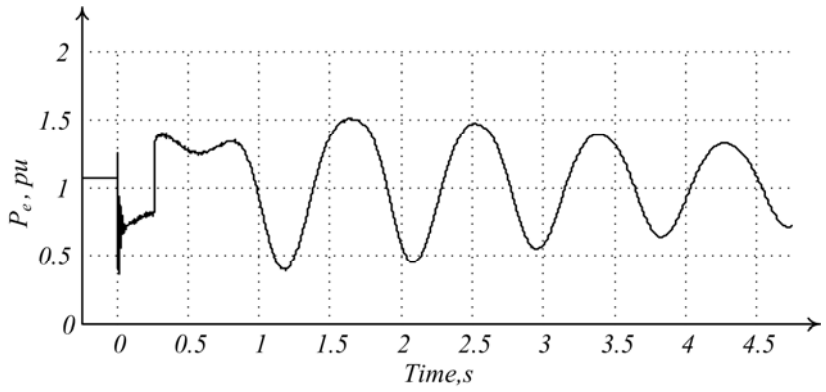

Figure 5.27 P-t curve for pre-fault δ=35° and cleared after 0.26 s

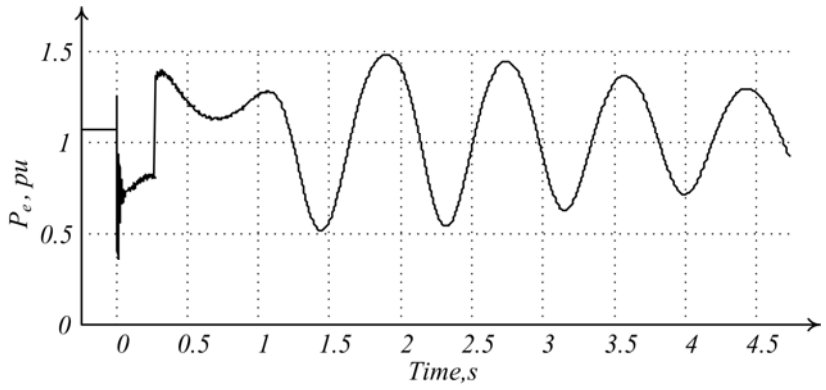

Figure 5.28 P-t curve for pre-fault δ=35° and cleared after 0.271 s

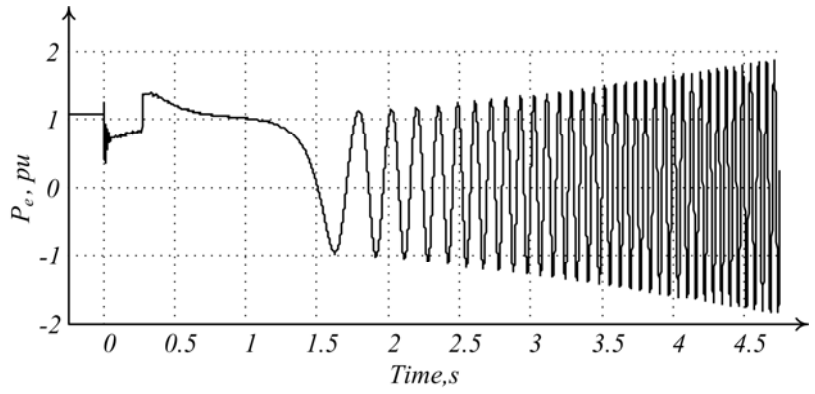

Figure 5.29 P-t curve for pre-fault δ=35° and cleared after 0.272 s

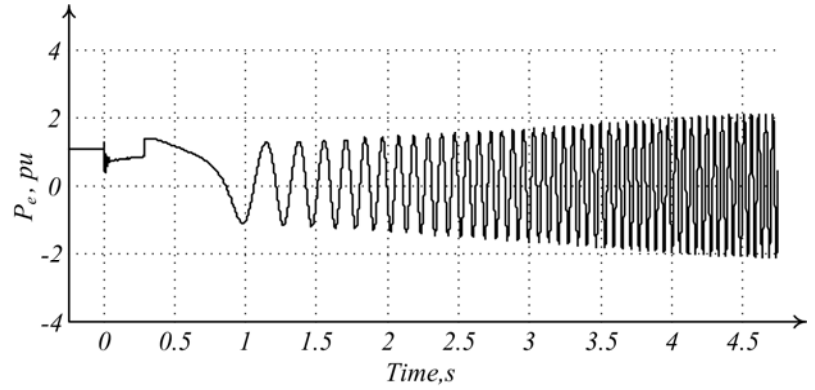

Figure 5.30 P-t curve for pre-fault δ=35° and cleared after 0.28 s

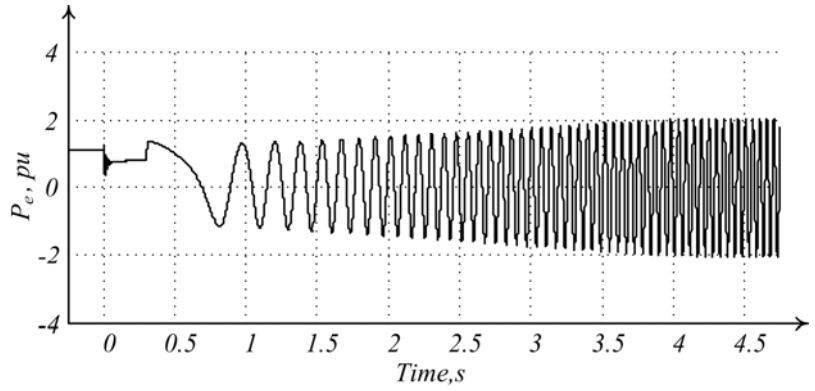

Figure 5.31 P-t curve for pre-fault δ=35° and cleared after 0.30 s

Table 5.5 Closed loop testing results for pre-fault δ=35° and the three phase fault applied

Case	**13**	**14**	**15**	**16**	**17**	**18**
Fault Duration Time, s	0.22	0.26	0.271	0.272	0.28	0.30
Fault Duration Samples	211	250	260	261	269	288
Area (A_1)*, in 10^9	7.6745	9.0839	8.9949	8.5856	10.0076	10.7481
Area (A_2)*, in 10^9	7.6769	9.0983	8.9953	6.4518	0.3553	0.21703
Decision	Stable	Stable	Stable	OS	OS	OS
Decision Made at Sample	461	707	944	669	495	437
Decision Time, s	0.4794	0.7353	0.9817	0.6957	0.5148	0.4544

* scaled value from DSP OS :Out-of-step

5.4.4. Pre-fault power angle (δ) set at 45° and Line-Ground Fault Applied

The pre-fault δ of the generator is set at 45° which results in 1.3196 pu of power output from the generator. A line-ground (Phase 'a'- ground) fault is applied at the middle of the transmission line (TL2) and six different simulations are carried with the fault duration times of 0.6, 0.68, 0.683, 0.684, and 0.70 and 0.72 respectively. The first three simulation cases give stable swing whereas rest of the three gives out-of-step swing. The P-t curve of stable swings are shown in Figure 5.32 through 5.34 and the out-of-step P-t curves are shown in Figure 5.25 through 5.37. The areas A_1, A_2, decision made and the decision times are summarized in the Table 5.6.

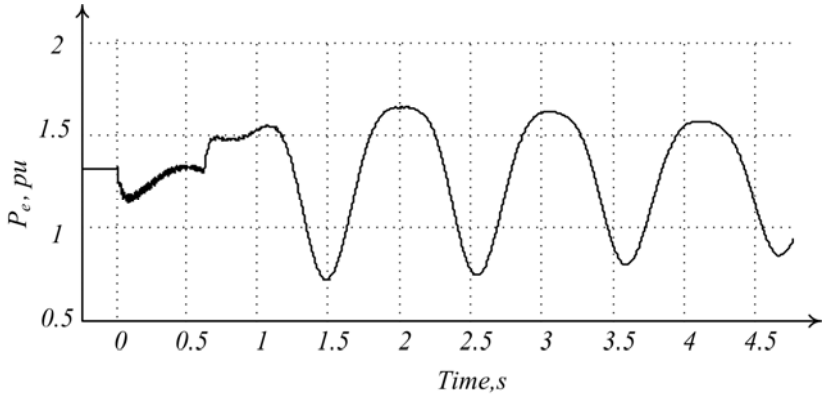

Figure 5.32 P-t curve for pre-fault δ=45° and cleared after 0.60 s

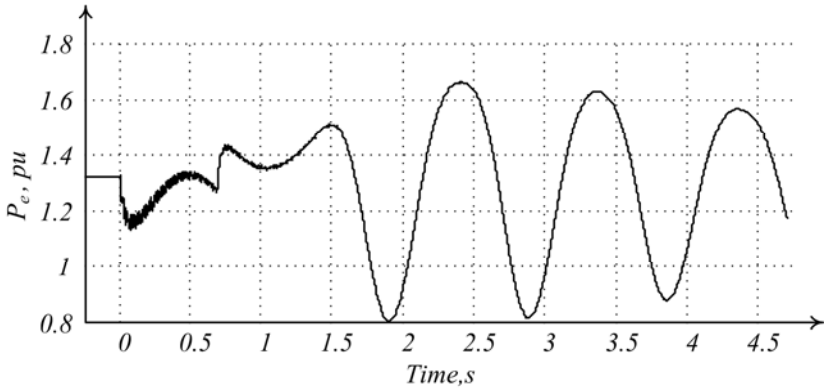

Figure 5.33 P-t curve for pre-fault δ=45° and cleared after 0.68 s

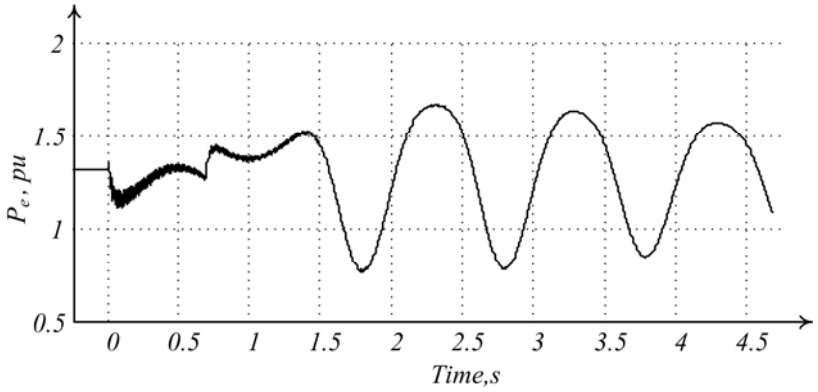

Figure 5.34 P-t curve for pre-fault δ=45° and cleared after 0.683 s

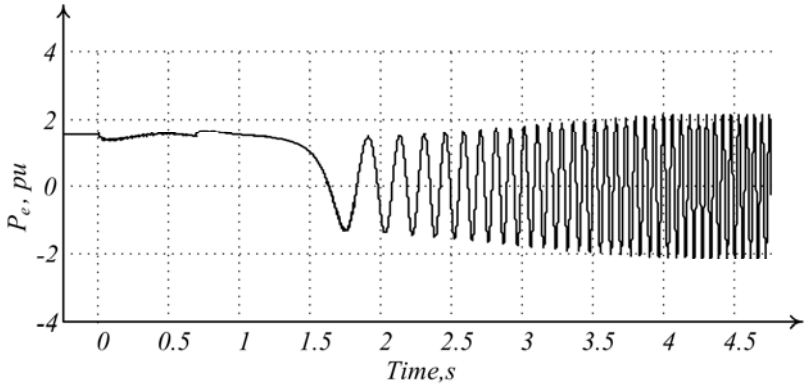

Figure 5.35 P-t curve for pre-fault δ=45° and cleared after 0.684 s

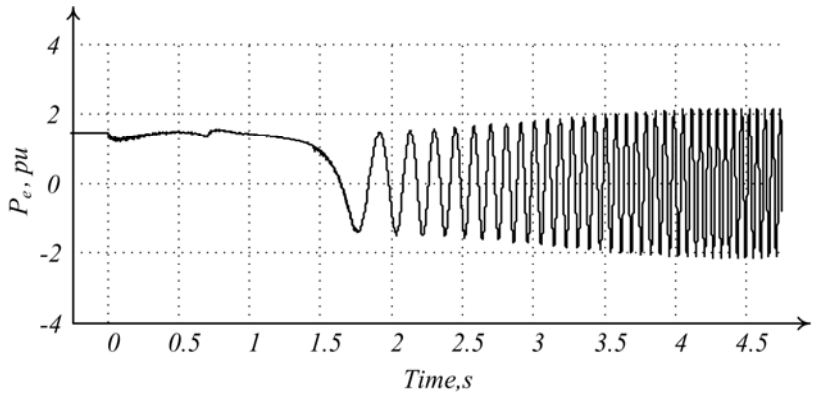

Figure 5.36 P-t curve for pre-fault δ=45° and cleared after 0.7 s

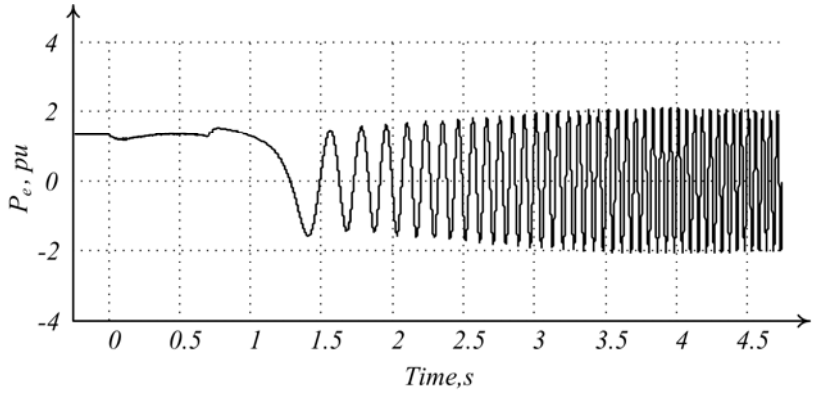

Figure 5.37 P-t curve for pre-fault δ=45° and cleared after 0.72 s

Table 5.6 Closed loop testing results for pre-fault δ=45° and line-ground fault applied

Case	**19**	**20**	**21**	**22**	**23**	**24**
Fault Duration Time, s	0.6	0.68	0.683	0.684	0.7	0.72
Fault Duration Samples	577	653	656	657	673	692
Area (A_1)*, in 10^9	4.3854	4.6673	4.6710	4.7559	4.7721	5.0413
Area (A_2)*, in 10^9	4.3919	4.6690	4.6716	1.8060	1.7778	0.6536
Decision	Stable	Stable	Stable	OS	OS	OS
Decision Made at Sample	821	1129	1246	957	937	843
Decision Time, s	0.8538	1.1741	1.2958	0.9953	0.9745	0.8767

* scaled value from DSP OS :Out-of-step

5.4.5. Pre-fault power angle (δ) set at 40° and Line-Line Fault Applied

The pre-fault δ of the generator is set at 40° which results in 1.1991 pu of power output from the generator. A line-line (Phase 'a'- phase 'b') fault is applied at the middle of the transmission line (TL2) and six different simulations are carried with the fault duration times of 0.4, 0.42, 0.435, 0.436, and 0.437 and 0.438 respectively. The first three simulation cases give stable swing whereas rest of the three gives out-of-step swing. The P-t curve of stable swings are shown in Figure 5.38 through 5.40 and the out-of-step P-t curves are shown in Figure 5.41 through 5.42. The areas A_1, A_2, decision made and the decision times are summarized in the Table 5.7.

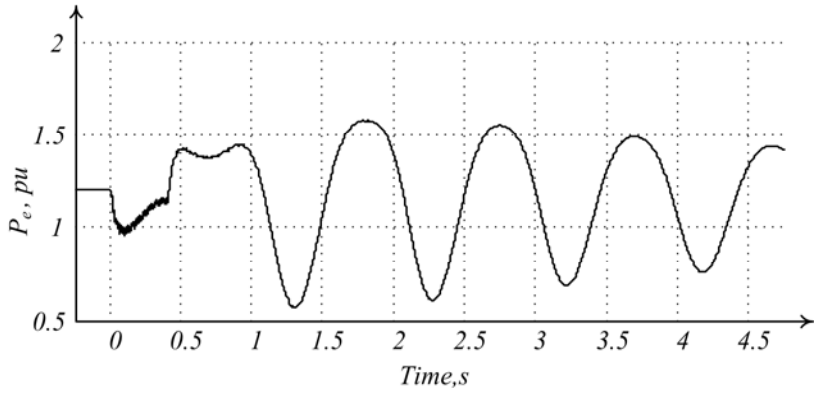

Figure 5.38 P-t curve for pre-fault δ=40° and cleared after 0.4 s

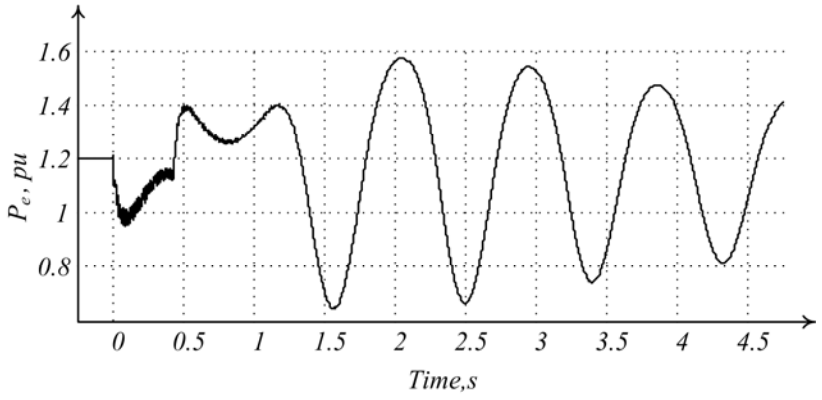

Figure 5.39 P-t curve for pre-fault δ=40° and cleared after 0.42 s

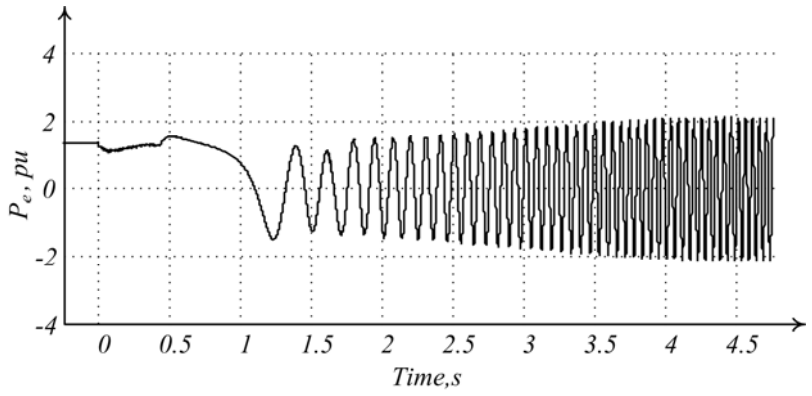

Figure 5.40 P-t curve for pre-fault δ=40° and cleared after 0.435 s

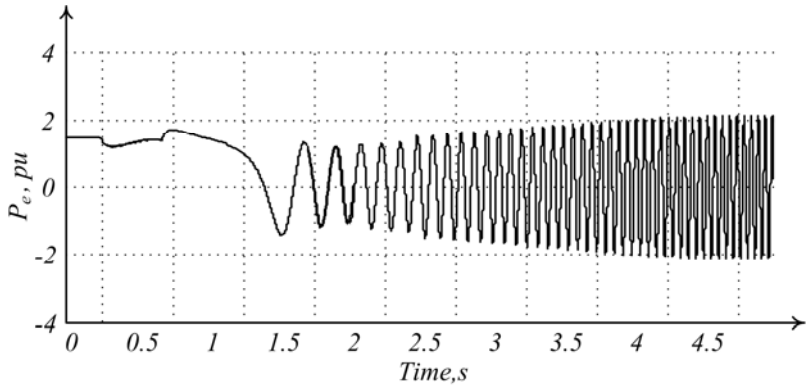

Figure 5.41 P-t curve for pre-fault δ=40° and cleared after 0.436 s

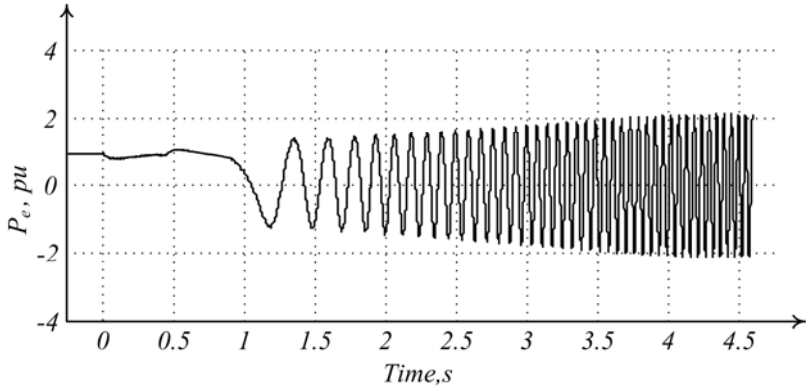

Figure 5.42 P-t curve for pre-fault δ=40° and cleared after 0.437 s

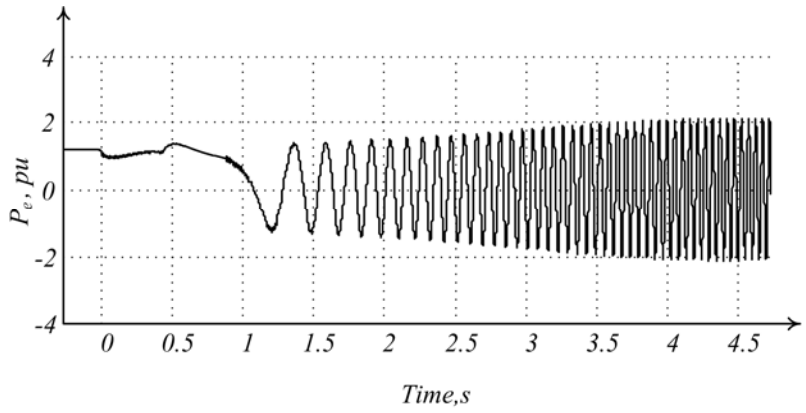

Figure 5.43 P-t curve for pre-fault δ=40° and cleared after 0.438 s

Table 5.7 Closed loop testing results for pre-fault δ=40° and line-ground fault applied

Case	**25**	**26**	**27**	**28**	**29**	**30**
Fault Duration Time, s	0.4	0.42	0.435	0.436	0.437	0.438
Fault Duration Samples	384	403	418	419	420	421
Area (A_1)*, in 10^9	6.6304	6.8467	6.9131	6.9618	6.9816	7.0148
Area (A_2)*, in 10^9	6.6318	6.8512	3.5476	3.3032	3.2839	3.1944
Decision	Stable	Stable	OS	OS	OS	OS
Decision Made at Sample	682	921	712	695	692	682
Decision Time, s	0.7093	0.9578	0.7404	0.7228	0.7196	0.7092

* scaled value from DSP OS :Out-of-step

5.5. Summary

Using the proposed EAC in the P-t domain, a relay model was developed on the DSP board. The relay used current and voltage information at the relay location and calculated the power output of the generator. The calculated power output was then used to evaluate the areas A_1 and A_2 to make the decision. The test signals for the relay i.e. the transient voltage and current signals were generated using the RTDS™ hardware. A closed loop configuration was thus developed using the DSP board (relay model) and the RTDS™ hardware (power system model). Various transient simulations were carried out in the closed loop. The simulation results showed

that the relay discriminated the stable and out-of-step conditions well. In case of the out-of-step condition, relay sent a signal to the breaker to disconnect the generator from the infinite bus.

The results obtained from the closed loop testing were in good agreement with the SMIB simulations carried out in Chapter 3. This corroborates the effectiveness of the proposed relay model for out-of-step detection. The successful real time testing using RTDS™ implies that the proposed relay can be applied to a real power system in the field for out-of-step protection. The decision times obtained from the hardware simulation was in accordance with that obtained from the software simulation in Chapter 3. However, note that the decision times can be delayed by one sampling interval (i.e. 0.00104 s) or more due to measurement inaccuracies but a correct decision will always be obtained using the proposed algorithm.

CHAPTER 6
CONCLUSIONS

6.1. Summary

The out-of-step condition and its impacts on different protection systems were discussed in Chapter 1. Literature reviews of the different techniques that have been proposed for out-of-step detection in a power system were also given in Chapter 1. The details about the methodologies used in these techniques and the shortcomings associated with them were described in Chapter 2.

Since the technique proposed in this thesis is derived from the EAC in δ domain, therefore, the δ domain EAC basics were explained first in Chapter 2. The traditional EAC has a simple concept and avoids the need of complex numerical solution of swing equation and is very helpful for stability studies. But its use as an out-of-step protection algorithm is not as effective as the theoretical concept. The complexities associated with EAC in δ domain to detect out-of-step conditions were given in Chapter 3.

In Chapter 3, it was found that the transformation of EAC from δ domain to time domain also revealed the information about the power system stability. Making the proposed modification to time domain makes the EAC concept useful for out-of-step protection by overcoming the difficulties associated with EAC in the δ domain. The proposed out-of-step relay used the area under the P-t curve. The power was calculated using the voltage and current signals at the point of installation of out-of-step relay. The proposed algorithm was tested in a SMIB configuration and the results were given in Chapter 3. From the analysis and simulations done in Chapter 3, it

was clear that the proposed algorithm is simple, can be applied to multimachine systems without any increase in complexity (EAC in δ domain is simple to apply only for a SMIB system or a two-machine system). It does not need any offline calculations/studies and is based on the information available locally i.e. at the point of installation.

In this thesis, the proposed algorithm was tested on a two-machine, three-machine and a 17-bus multimachine system in Chapter 4 to validate the ease of use and also verify the results. The simulation results showed that the proposed algorithm accurately detects the out-of-step condition in a large power system avoiding any system reductions that were done in the previous techniques.

A prototype of the relay was also built using the ADSP-BF533™ board and the associated software. The digital relay developed was then tested in closed loop and in real time using the RTDS™ hardware simulator mimicking an actual SMIB power system. The voltage and current signals were filtered and processed and fed into the ADSP-BF533™ board. The results using the RTDS were given in Chapter 5. The results showed that the proposed time domain EAC relay using the RTDS gave similar results as the software simulation results obtained in Chapter 3.

6.2. Thesis Contributions

Followings are the contributions of this thesis,

- *Studying the EAC in time domain:* Reference [22] had provided the concept of EAC in time domain by modifying the EAC in δ domain. Also an out-of-step algorithm was provided based on the EAC in time domain but it did not show the improvement of the proposed method over the EAC in δ domain and other techniques (i.e. faster decision time and fewer measurements).

In this thesis, based on the findings in [22], the natures of P-t curves for different swing scenarios have been studied. Three unique natures of P-t curve are found for SMIB system, based on which the stability of a SMIB system is discussed. Various simulations are carried out to show the advantages of the proposed algorithm (EAC in time domain) over the EAC in δ domain and other techniques. It is shown in Chapter 3 and 4 that the proposed algorithm is beneficial as it uses only local measurements and avoids offline calculation. In Chapter 4, it is also shown that the proposed algorithm avoids the network reduction techniques when applied to a multimachine configuration.

- *Verification of the proposed out-of-step algorithm:* Reference [22] tested the proposed algorithm on a SMIB in a limited manner. Only a few simulations were reported and the simulations did not include the marginal stable and out-of-step cases. The swing frequencies encountered during the simulation were not reported. Reference [22] had reported multimachine simulation studies but the studies were inconclusive; only partial simulations were carried out and the algorithm seemed to have been applied to a multimachine system by reducing it to an equivalent SMIB system which defeats the very basic purpose of this algorithm. The actual locations of relay and measurement devices were not either shown or explained for multimachine system.

  In the thesis, simulations first show the application of the proposed algorithm in a SMIB system and then the results are compared with an existing Blinder Technique. Simulations are carried in a broad manner to show the various power swings frequencies possible. In the verge of system stability, the fault duration time is

increased by a small value to depict the scenarios of marginally stable and out-of-step cases. Why a larger decision time is required for the marginal cases is discussed. Simulations for multimachine are done systematically, starting from two-machine and then for a three-machine and a 17-bus multimachine power system [33, 34]. The locations of relay in multimachine system are explained clearly. The impact of motors is investigated in 17-bus multimachine system and numerous simulations are done for various load levels, different fault location etc.

- *Digital relay modeling and closed loop testing:* Reference [22] did not implement an out-of-step relay on hardware based on the proposed algorithm.

  In this research, a prototype of digital relay has been built which uses the proposed algorithm and is based on local voltage/current information. For hardware implementation, number of issues like down sampling, filtering and phasor estimation have to be tackled and are discussed in Chapter 5. To test the prototype relay, real time electrical signals (during power swings) are required. A hardware simulator RTDS™ is used which can simulate a power system in real time and voltage/current signals can be tapped as if coming from a real power system. The closed loop testing of the prototype relay show the results are in close agreement with the results obtained from the software simulation.

6.3. Future Study

References [31, 32] listed out some of the common shortcoming of out-of-step relay i.e. they are unable to detect during high swing frequency, are unable to detect with large earth fault resistance, are unable to detect for a system with heavily loaded long transmission line and fail to incorporate the frequency deviation during the transient. As a further study, the effectiveness of

the proposed EAC algorithm in time domain can be tested for the following different scenarios: (i) various swing frequencies, which can be simulated with generators of various inertia constants. (ii) high earth fault resistance, which can be simulated if a large resistance is included in the fault branch. (iii) Heavily loaded long transmission line, which can be simulated by increasing the transmission line length and increasing the generator loading (iv) incorporating the frequency deviation, which can be implemented using a frequency tracking algorithm and finding the phasors relating to the new changed frequency.

6.4. Conclusion

The proposed EAC in time domain was applied for out-of-step detection. The simulation results showed that the proposed out-of-step algorithm is simple (based only on the local measurements) and avoids the need for any extra communication devices. The simulation results using a SMIB, two-machine, three-machine and the 17-bus system showed that the proposed algorithm can be directly used for a multimachine system without any need for system reduction.

REFERENCES

[1] P. Kundur, *Power System Stability and Control.* New York: McGraw-Hill, c1994.

[2] H. Saadat, *Power System Analysis.* Boston: WCB/McGraw-Hill, c1999.

[3] W. A. Elmore, *Protective Relaying Theory and Applications* ,2nd ed., rev. and expanded. ed.New York: Marcel Dekker, c2004.

[4] C. R. Mason, *The Art and Science of Protective Relaying.* New York: Wiley, 1956.

[5] P. M. Anderson, *Power System Control and Stability.* ,1st ed. ed.Ames: Iowa State University Press, 1977.

[6] E. W. Kimbark, *Power System Stability.* New York: Wiley, 1948-56.

[7] M.S.Sachdev, *Electric Protective Devices.* New York: McGraw-Hill Book Co. Inc., 1997.

[8] D. A. Tziouvaras, "Out-of-step protection fundamentals and advancements," Protective *Relay Engineers, 2004 57th Annual Conference for,* pp. 282-307, 2004.

[9] C. W. Taylor, "A New Out-of-Step Relay with Rate of Change of Apparent Resistance Augmentation," IEEE *Transactions on Power Apparatus and Systems,* vol. PAS-102, pp. 631-639, 1983.

[10] Lin Teng, "Study on power system separation based on the local electrical quantities," *Power System Technology, 2002. Proceedings. PowerCon 2002. International Conference on,* vol. 1, pp. 349-354 vol.1, 2002.

[11] Liancheng Wang, "A new method for power system transient instability detection," *Power Delivery, IEEE Transactions on,* vol. 12, pp. 1082-1089, 1997.

[12] V. Centeno, "An adaptive out-of-step relay [for power system protection]," *Power Delivery, IEEE Transactions on,* vol. 12, pp. 61-71, 1997.

[13] W. Rebizant, "Fuzzy logic application to out-of-step protection of generators," *Power Engineering Society Summer Meeting, 2001. IEEE,* vol. 2, pp. 927-932 vol.2, 2001.

[14] A. Y. Abdelaziz, "Adaptive protection strategies for detecting power system out-of-step conditions using neural networks," *Generation, Transmission and Distribution, IEE Proceedings,* vol. 145, pp. 387-394, 1998.

[15] "Power swing and out-of-step considerations on transmission line," *IEEE PSRC WG D6, June 2005.*

[16] J. Holbach, "New Out of Step Blocking Algorithm for Detecting Fast Power Swing Frequencies," *Power Systems Conference: Advanced Metering, Protection, Control, Communication, and Distributed Resources, 2006. PS '06,* pp. 182-199, 2006.

[17] S. M. Brahma, "Distance Relay With Out-of-Step Blocking Function Using Wavelet Transform," *Power Delivery, IEEE Transactions on,* vol. 22, pp. 1360-1366, 2007.

[18] K. H. So, "Out-of-step detection algorithm using frequency deviation of voltage," *Generation, Transmission & Distribution, IET,* vol. 1, pp. 119-126, 2007.

[19] Yuanqi Liu, "Aspects on Power System Islanding for Preventing Widespread Blackout," *Networking, Sensing and Control, 2006. ICNSC '06. Proceedings of the 2006 IEEE International Conference on,* pp. 1090-1095, 2006.

[20] John J. Grainger, W. D. Stevenson, JR., *Power System Analysis*, 4th ed. New York; McGraw-Hill, c1994.

[21] Shengli Cheng, M.S. Sachdev, "Out-of-step protection using the equal area criterion," *Electrical and Computer Engineering, Proceedings of the Canadian Conference on Electrical & Computer Engineering,* pp. 1488-1491, 2005.

[22] Shengli Cheng, "Real-time power swing detection using equal area criterion," *M.Sc. Thesis, University of Saskatchewan, April 2006.*

[23] "PSCAD User Manuals," *Manitoba HVDC Research Centre, Winnipeg, Canada.*

[24] M. A. Pai, *Energy Function Analysis for Power System Stability.* Boston: Kluwer Academic Publishers, c1989.

[25] M. A. Pai, *Power System Stability :Analysis by the Direct Method of Lyapunov.* Amsterdam ; North-Holland Pub. Co. ; c1981.

[26] D. X. Du, "An Advanced Real Time Digital Simulator Based Test System for Protection Relays," *Universities Power Engineering Conference, 2006. UPEC '06. Proceedings of the 41st International,* vol. 3, pp. 851-855, 2006.

[27] P. Forsyth, "Real time digital simulation for control and protection system testing," Power *Electronics Specialists Conference, 2004. PESC 04. 2004 IEEE 35th Annual,* vol. 1, pp. 329-335 Vol.1, 2004.

[28] "RTDS Manuals," *RTDS Technologies Inc., Winnipeg, Canada.*

[29] "ADSP-BF533 EZ-KIT lite evaluation system manual," *Analog Devices Inc.,*

[30] M.S.Sachdev, "Lecture Notes: Digital Techniques in Power System Measurement." *University of Saskatchewan, Saskatoon ,Canada, 2004.*

[31] D. Tziouvaras, "Relay Performance During Major System Disturbances," Protective *Relay Engineers, 2007. 60th Annual Conference for,* pp. 251-270, 2007.

[32] A. Mechraoui, "A new principle for high resistance earth fault detection during fast power swings for distance protection," *Power Delivery, IEEE Transactions on,* vol. 12, pp. 1452-1457, 1997.

[33] S. Paudyal, R.Gokaraju, M.S.Sachdev, S.Cheng, "Out-of-Step Detection using Energy Equilibrium Criterion in Time Domain," *Electric Power Components and Systems*, Submitted March 2008.

[34] S. Paudyal, R.Gokaraju, M.S.Sachdev, "Out-of-Step Protection Using Energy Equilibrium Criterion in Time Domain-SMIB and 3-Machine Case Studies," *TENCON 2008*, Submitted May 2008.

APPENDIX A
SMIB PARAMETERS

Base MVA=2220MVA, Base kV=24kV

Generator MVA rating=2220MVA,

Generator Voltage=24kV

Direct Axis Transient Reactance (X_d') =0.3

Inertia Constant (H) =3.5 MW-s/MVA,

Frequency=60Hz, Infinite Bus Voltage=0.9 pu

Transformer=j0.15 pu, TL-I=j0.5 pu,TL-II=j0.93 pu

APPENDIX B
PSCAD MODEL OF SMIB SYSTEM AND EAC ALGORITHM BLOCK

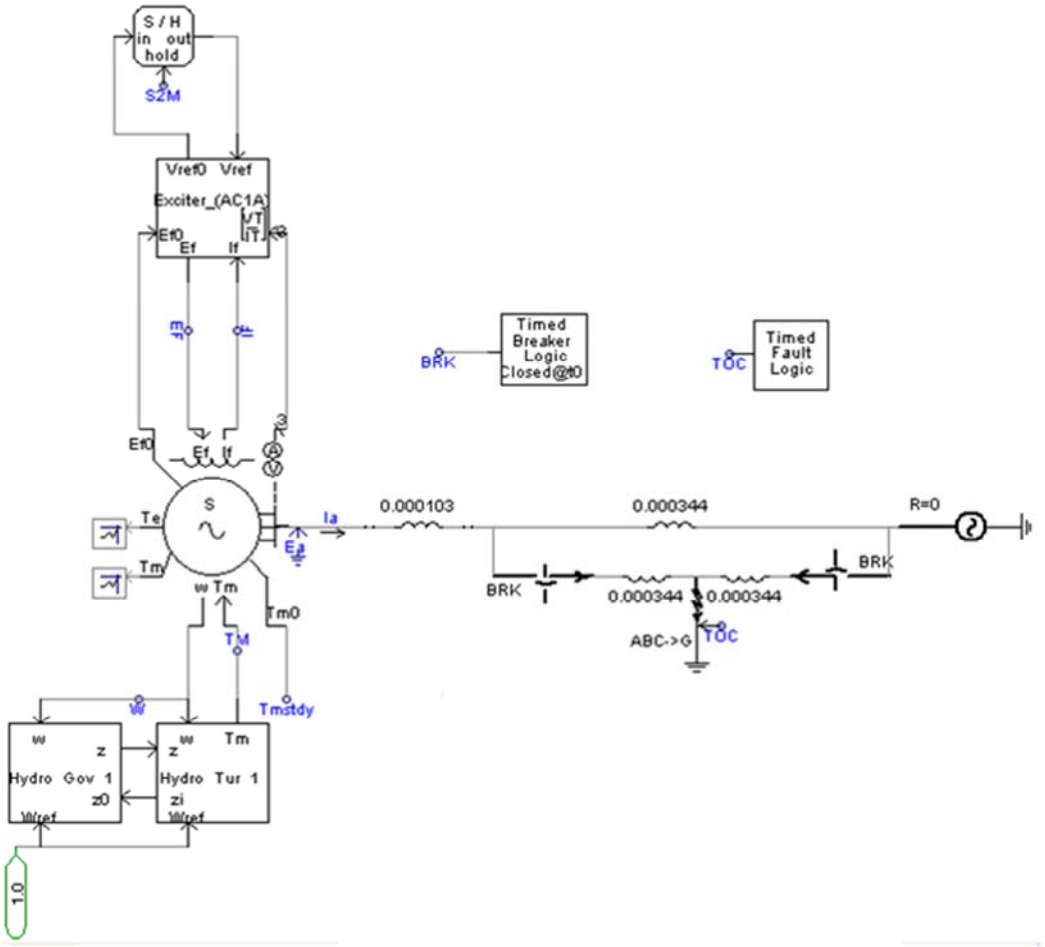

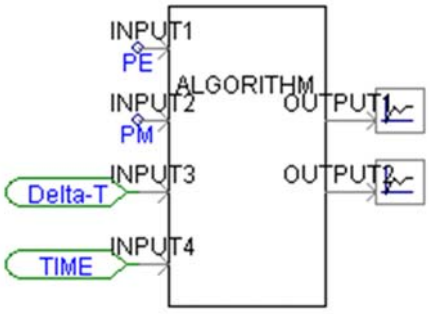

APPENDIX C
GUIDLEINES FOR BLINDER SETTINGS

RRI= Right Resistance-Inner is set so that the impedance locus during most severe stable swing does not cross inner rectangle. The most sever case is assumed to occur when the generator is fully loaded.

RRO=Right Resistance-Outer is set so that it is far away from full load impedance and is less than the impedance at fault removal of the most sever fault.

LRI =Same as RRI but in negative direction.

LRO = Same as RRO but in negative direction.

TXI = Set to cover 40% of transmission line.

TXO = Set to cover 60% of transmission line.

BX =Set to detect swing center passing anywhere in generator and transformer.

APPENDIX D
TWO MACHINES INFINITE BUS AND THREE MACHINE INFINITE BUS PARAMETERS

Two Machine Infinite Bus Parameters:

Base MVA=1000MVA

Generator-1 rating=1000 MVA

Generator-2 rating=1000 MVA

Bus Voltage=500kV

Z=0.6142+ j11.529 Ω

Three Machine Infinite Bus Parameters

Base MVA=635MVA

Generator-1 rating=555 MVA

Generator-2 rating=635 MVA

Generator-2 rating=66 MVA

Bus Voltage=24kV

Z_1=0.048+ j0.48Ω, Z_2=0.00576+ j0.573Ω, Z_3=0.0288+ j0.288 Ω

Z_4=0.0576+ j0.576Ω, Z_5=0.0142+ j0.142 Ω, Z_6=0.0192+ j0.192Ω,

Z_7=j0.0957Ω

APPENDIX E
17-BUS MULTIMAHCINE PARAMETERS

Table D.1 Generator Parameters

Generator	**S1**	**S2**
Rated Power (MW)	1500	2000
Rated L-L Voltage (kV)	15	15
X_d (pu)	0.866	0.866
Angular Frequency (rad/sec)	376.992	376.992
Inertia Constant (sec)	1.7	1.7

Table D.2 Transformer Parameters

Name	**MVA Rating**	**Voltage Ratio(kV)**	**X_d(pu)**
Tr1	1500	15/500	0.1
Tr2	3000	15/500	0.1
Tr3	800	15/500	0.1
Tr4	900	15/500	0.1
Tr5	1000	500/735	0.1
Tr6	1000	735/500	0.1
Tr7	1000	500/735	0.1
Tr8	1000	735/500	0.1

Table D.3 Motor Parameters

Motor	**M1**	**M2**
Rated Power(MW)	600	500
Rated L-L Voltage(kV)	15	15
Angular Frequency(rad/sec)	376.992	376.992

Table D.4 Transmission Line Parameters

Transmission Line	**Length(km)**	**Reactance(pu)**
TL1	120	0.1343
TL2	50	0.07
TL3	45	0.05603
TL4	160	0.0716
TL5	100	0.1166
TL6	60	0.0706
TL7a	130	0.0709
TL7b	130	0.0709
TL8	50	0.05431
TL9	45	0.04888
TL10	50	0.04888
TL11	50	0.05974
TL12	45	0.03258
TL13	45	0.04888

APPENDIX F
PSCAD MODEL OF 17-BUS MULTIMACHINE SYSTEM

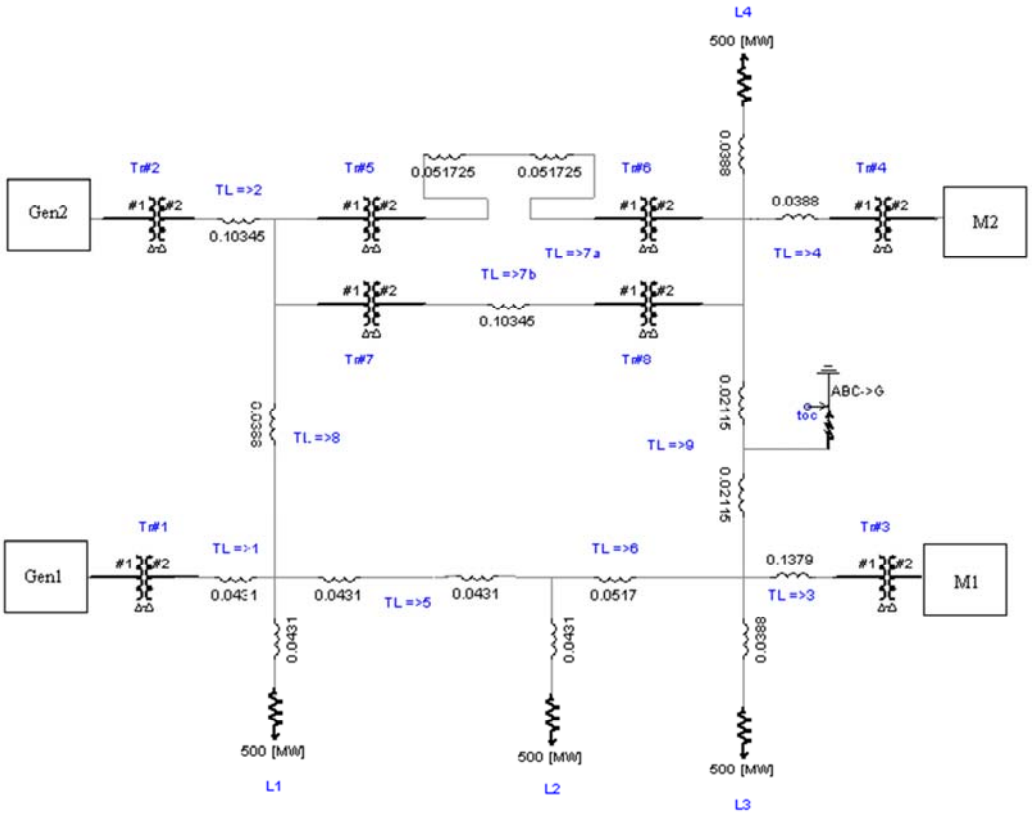

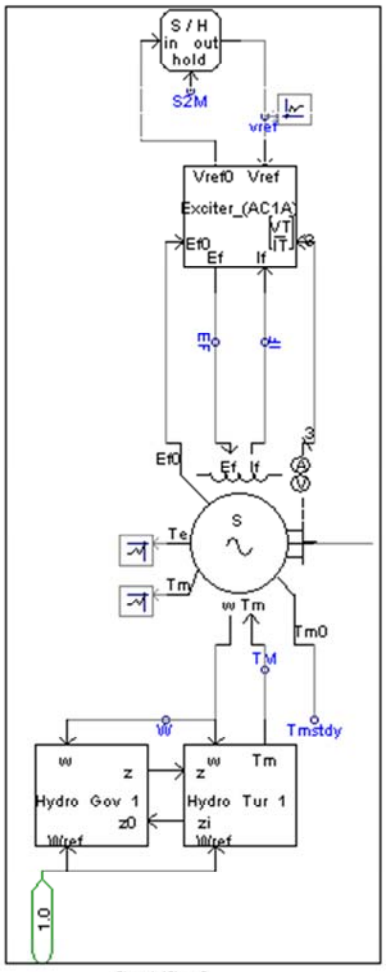

Gen1/Gen2

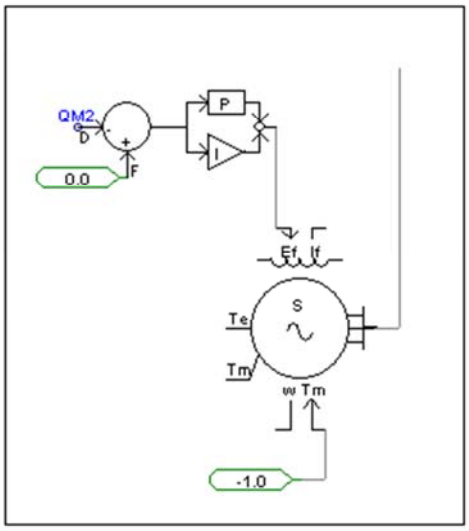

M1/M2